

EUROPEAN ORGANISATION FOR NUCLEAR RESEARCH (CERN)



Submitted to: JHEP



CERN-EP-2026-052  
13th March 2026

# Search for displaced decays of long-lived particles in events with missing transverse momentum in $\sqrt{s} = 13$ TeV $pp$ collisions with the ATLAS detector

The ATLAS Collaboration

A search for long-lived particles in events with significant missing transverse momentum and at least one displaced vertex is presented. This analysis is performed using  $137 \text{ fb}^{-1}$  of  $pp$  collision data collected between 2016–2018 during Run 2 of the Large Hadron Collider by the ATLAS detector. Displaced vertices are identified using two different secondary vertexing algorithms, including a novel "fuzzy" vertexing algorithm optimized for identifying displaced decays of heavy quarks. Separate searches are performed using each algorithm, and the expected Standard Model background is independently estimated for each search using a data-driven procedure. No significant excess is observed over the background in either case. The results are used to set 95% confidence-level limits on potential beyond-the-Standard Model physics that could produce this final state. Results are interpreted in the context of four models: long-lived gluinos that form  $R$ -hadrons before decaying, neutralinos decaying via Higgs-mediated channels in the Bino-Wino coannihilation model, long-lived Higgsinos decaying to axinos, and an exotic Higgs portal model predicting displaced decays of light pseudoscalars.

© 2026 CERN for the benefit of the ATLAS Collaboration.

Reproduction of this article or parts of it is allowed as specified in the CC-BY-4.0 license.

arXiv:2603.12051v1 [hep-ex] 12 Mar 2026

# Contents

<b>1</b>	<b>Introduction</b>	<b>2</b>
<b>2</b>	<b>Signal models and Monte Carlo simulation</b>	<b>3</b>
2.1	Gluino $R$ -hadron	4
2.2	Bino-Wino coannihilation	4
2.3	DFSZ axino	6
2.4	Higgs portal to long-lived particles	6
2.5	Monte Carlo simulations and event generation	6
<b>3</b>	<b>ATLAS detector and data acquisition</b>	<b>9</b>
<b>4</b>	<b>Event reconstruction and displaced vertexing</b>	<b>10</b>
4.1	Tracks and primary vertices	11
4.2	Standard secondary vertices	11
4.3	Fuzzy secondary vertices	12
4.4	Detector material map	14
4.5	Physics object definitions	15
<b>5</b>	<b>Signal regions and background estimation</b>	<b>16</b>
5.1	Common event-level selections	17
5.2	Signal region definitions	17
5.3	Background estimates and validation regions	20
<b>6</b>	<b>Systematic uncertainties</b>	<b>25</b>
6.1	Background estimate uncertainties	25
6.2	Reconstruction uncertainties	26
6.3	Theory uncertainties	27
<b>7</b>	<b>Results and interpretation</b>	<b>28</b>
7.1	Statistical model	28
7.2	Model-independent limits	29
7.3	Interpretations	30
<b>8</b>	<b>Conclusion</b>	<b>33</b>

## 1 Introduction

As the search continues for new physical processes that go beyond what is described by the Standard Model (SM) of particle physics – so-called *BSM physics* – the range of hypothesized BSM models and their observable signatures has also continued to widen. The classes of models that predict the presence of long-lived particles (LLPs) are particularly interesting both theoretically and experimentally. Theoretically, long lifetimes are generated through the presence of heavy, off-shell particles in the decay, through phase space suppression factors or suppression from approximate symmetries that introduce very small effective coupling constants [1]. Experimentally, such particles may have proper lifetimes ranging from

a few picoseconds to several nanoseconds, resulting in decay lengths from fractions of a millimeter to several meters or more, thus leading to diverse signatures involving multiple types of sensors and detector apparatus.

LLP decays can yield a variety of characteristic experimental signatures depending on the production mechanisms involved, the particle kinematics, and the properties of the decay process. One of the most striking signatures at a collider experiment is the presence of a massive, identifiable displaced vertex (DV). This remarkable signature can be produced by decays that involve multiple outgoing charged particles and occur within the fiducial volume of the detector, but at a significant distance from the interaction point (IP) of the incoming beams. While such displaced signatures of BSM processes have long been sought after at both colliders and beam dump experiments, the energy, intensity, and data volume of the Large Hadron Collider (LHC) [2], along with the sophistication and sensitivity of detectors like those of the ATLAS experiment [3], provide unprecedented sensitivity in searches for these rare yet distinctive processes.

The results presented here use data recorded by the ATLAS detector to conduct a broad search for evidence of BSM processes that yield DVs produced within the inner detector (ID) in conjunction with significant missing transverse momentum  $\vec{p}_T^{\text{miss}}$ , with magnitude  $E_T^{\text{miss}}$ , indicating the production of particles that subsequently escape the ATLAS detector unobserved. Using the 2016-2018 (Run 2) dataset of  $137 \text{ fb}^{-1}$  proton-proton ( $pp$ ) collisions collected by the ATLAS experiment at a center-of-mass energy of  $\sqrt{s} = 13 \text{ TeV}$  [4], this analysis searches for events with one or more DVs with a large reconstructed mass and a high track multiplicity. The relatively inclusive set of selection criteria implements two different DV reconstruction algorithms, one of which is specifically optimized for cases in which LLP decays yield heavy-flavor hadrons. The resulting low-background search results are interpretable in the context of several BSM models that predict displaced signatures, including models never-before confronted with data such as a full supersymmetric axion/axino model.

This search expands the dataset used by over a factor of four compared to previous ATLAS searches for similar signatures [5]. In addition, ATLAS has searched for DVs in events with final states involving jets or muons [6–8], and the CMS and LHCb Collaborations have also searched extensively for related signatures and models of BSM physics [9–19].

The details of the physics models used for the interpretation of the results are described in Section 2. Section 3 presents the relevant information regarding the data taking conditions and detector apparatus used in the analysis. The special reconstruction algorithms and event selection criteria are presented in Section 4. Section 5 discusses the detailed event selection criteria and methodology used to estimate the sources and levels of backgrounds relevant to the search. The sensitivity to experimental and theory uncertainties of the analysis is described in Section 6. Finally, Section 7 presents the results and their interpretations.

## 2 Signal models and Monte Carlo simulation

Supersymmetric (SUSY) extensions of the SM of particle physics provide solutions to the hierarchy problem [20, 21] by predicting new particles which are partners of SM particles [22–27] – the partners of SM fermions being bosons and those of SM bosons being fermions.  $R$ -parity-conserving SUSY models [28] are considered in this paper. In these models, the supersymmetric partners of the Higgs and electroweak gauge bosons mix to form mass eigenstates known as neutralinos ( $\tilde{\chi}_i^0$ ) and charginos ( $\tilde{\chi}_i^\pm$ ), which are linear combinations of the Bino, Wino, and Higgsino gauge eigenstates. In most of the models considered here, the lightest neutralino ( $\tilde{\chi}_1^0$ ) is the stable lightest supersymmetric particle (LSP) and a dark-matter

candidate [29, 30], though in the Dine-Fischler-Srednicki-Zhitnitsky (DFSZ) axino model the fermionic superpartner of the axion (the axino,  $\tilde{a}$ ) serves as the LSP [31] (see Section 2.3 for more details).

Four BSM LLP models are considered that involve a variety of production mechanisms and decay modes. These consist of a Gluino  $R$ -hadron model [32], long-lived neutralinos in a Bino-Wino coannihilation model [33, 34], Higgsinos decaying to axinos in the DFSZ axino model, and light pseudoscalars from an exotic Higgs portal model [35]. Despite their different theoretical motivations, these models share common experimental signatures: DVs and significant  $E_T^{\text{miss}}$ . This commonality allows a single general search strategy to be used. For optimized sensitivity, different signal regions are constructed for the different topologies across these models. Moreover, these models cover a wide range of both parameter space and physics motivation, from the pair-production of long-lived gluinos via the strong interaction, to axion-axino physics, to an exotic Higgs portal model.

To maximize sensitivity to this range of models, two classes of signal regions (SRs) are designed: one optimized for processes that typically produce one or more well-separated massive DVs per event, and a second optimized for models with LLP decays to  $b$ -quarks. The details of these standard DV (SDV) and “fuzzy” DV (FDV) SRs, respectively, are given in Section 5.

The dominant background for these DV+ $E_T^{\text{miss}}$  signatures is expected to be  $Z(\rightarrow \nu\nu)$ +jets processes in which the  $E_T^{\text{miss}}$  due to the neutrinos occurs in conjunction with anomalously massive DVs from hadronic interactions with detector materials. Consequently, these backgrounds can only be estimated using precise information regarding the position and composition of detector materials as well as the particle interaction dynamics with those materials. Modeling of these background processes faces significant challenges, such as the misreconstruction of tracks, in even the most modern Monte Carlo (MC) simulations. This leads to poor simulation-based modeling of the kinematics and number of DVs produced by SM processes, thus necessitating a data-driven approach for background estimation. Nonetheless, both  $Z$  + jets and  $\gamma$  + jets MC samples are used for preliminary studies of the analysis design and the selection requirements.

## 2.1 Gluino $R$ -hadron

The first of the models considered is a split-SUSY model [32] with pair-produced long-lived gluinos which hadronize into  $R$ -hadrons before decaying (see Figure 1(a)). Such signatures can be created in a number of similar models [28, 36]. Each  $R$ -hadron decays to two SM quarks and a stable neutralino LSP,  $\tilde{\chi}_1^0$ , via an  $R$ -parity conserving process mediated by heavy virtual squarks, thus yielding significant  $E_T^{\text{miss}}$  in the final state as the neutralinos escape the detector undetected. The decay of the gluino is suppressed by the high mass of the virtual squarks which mediate the decay, causing the gluino to become long-lived, resulting in up to two massive displaced vertices. The branching ratio of the  $R$ -hadron is assumed to be flavor democratic to the first two generations of quarks. This model is targeted by the SDV SR as the decay products are light quarks.

## 2.2 Bino-Wino coannihilation

The second benchmark model is the pair-production of the lightest chargino,  $\tilde{\chi}_1^\pm$ , and the long-lived second-lightest neutralino,  $\tilde{\chi}_2^0$ , in the Bino-Wino coannihilation model [33, 34] (see Figure 1(b)). In this model,  $\tilde{\chi}_1^\pm$  and  $\tilde{\chi}_2^0$  are Wino-like, and the neutralino LSP,  $\tilde{\chi}_1^0$ , is Bino-like. The mass difference between the  $\tilde{\chi}_2^0$  and the  $\tilde{\chi}_1^0$  is favored to be a few tens of GeV to match experimentally observed dark matter relic

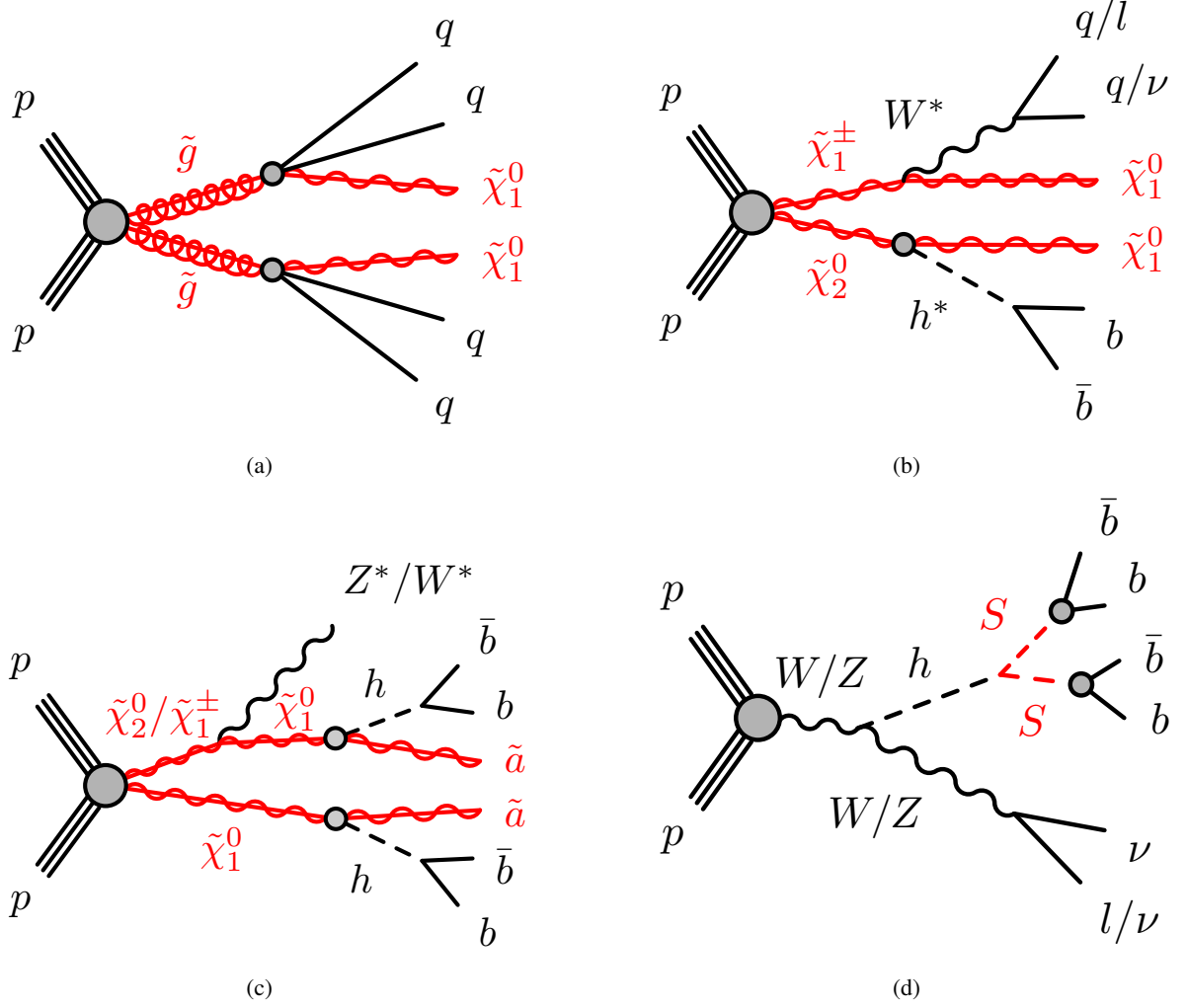


Figure 1: Illustrative diagrams for the four signal interpretations considered in this analysis; the (a) Gluino  $R$ -hadron model described in Section 2.1; (b) the Bino-Wino coannihilation model described in Section 2.2; (c) the DFSZ axino model described in Section 2.3; and (d) the Higgs portal described in Section 2.4. Red lines indicate BSM particles, and the small gray circles indicate displaced vertices.

density constraints [33]. While the  $\tilde{\chi}_1^\pm$  decays promptly to the  $\tilde{\chi}_1^0$  and a pair of leptons or quarks via an off-shell  $W$ -boson emission in most of the parameter space, the  $\tilde{\chi}_2^0$  may be long-lived depending on the parameter space.

When the Higgsino mass is large enough, and the ratio of vacuum expectation values is relatively small, which is the parameter space considered in this analysis,  $\tilde{\chi}_2^0$  is typically long-lived and decays via an off-shell Higgs boson, which subsequently decays mostly to a pair of  $b$ -hadrons. A single massive FDV is expected, due to the  $b$ -hadrons, along with  $E_T^{\text{miss}}$  from the escaping neutralino LSP.

### 2.3 DFSZ axino

Another model considered for this search is a SUSY scenario in which the minimal supersymmetric standard model (MSSM) [37] is extended with the addition of the DFSZ [38, 39] axion and associated Peccei-Quinn (PQ) symmetry [31] (see Figure 1(c) for a representative diagram). In this model, the Higgs sector carries PQ charge and so the axino has a direct coupling with both Higgsinos and SUSY fermions. The axino, as a neutral fermion, additionally has a small perturbative mixing with the up- and down-type Higgsino states, which gives rise to a fifth neutralino mass eigenstate  $\tilde{\chi}_5^0$ .

This analysis considers an  $R$ -parity conserving scenario in which the axino (or rather,  $\tilde{\chi}_5^0$ ) is both the lightest neutralino and the LSP, and so escapes the detector as a stable, undetected particle. The next two lightest supersymmetric particles are  $\tilde{\chi}_1^0$  and  $\tilde{\chi}_2^0$ , which are considered to be pure-Higgsino states with a very small mass gap. Note that while it is common for  $\tilde{\chi}_1^0$  to be reserved for the lightest neutralino state,  $\tilde{a}$  is chosen for the new, mostly-axino neutralino to avoid confusion with the standard MSSM neutralinos. The axino's couplings to other particles depend on the axion decay constant,  $f_a$ . Because the axion is only feebly coupled to the SM,  $\tilde{\chi}_1^0$  can be long-lived and its lifetime depends on both  $f_a$  and  $m_{\tilde{\chi}_1^0}$  [31]. The axino mass,  $m_{\tilde{a}}$ , strongly influences the magnitude of the observable  $E_T^{\text{miss}}$  in the final state.

Due to the neutralino mixing,  $\tilde{\chi}_1^0$  can decay to  $\tilde{\chi}_5^0$  by emitting either a Higgs or a  $Z$  boson. This analysis considers  $hh$  and  $ZZ$  channels; the diagram in Figure 1(c) is for the  $hh$  channel. Only the  $h \rightarrow b\bar{b}$  (with initially expected better sensitivity in the FDV SR) and  $Z \rightarrow q\bar{q}$  (with expected better sensitivity in the SDV SR) decays are considered due to the requirements on the presence of high track-multiplicity DVs. These modes are enforced in the MC simulation by setting their branching ratios to 1, and the resulting cross-sections are scaled by the corresponding SM branching ratios to reflect the expected physical rates.

### 2.4 Higgs portal to long-lived particles

The final model used to interpret the results of this search is a Higgs portal model [35] (see Figure 1(d)). This model introduces a new decay channel for the Higgs boson into a pair of pseudoscalar LLPs, called  $S$ , which subsequently decay into  $b\bar{b}$  pairs. One or two FDVs are thus expected.  $S$  is generated as a pseudoscalar although the analysis does not exploit its charge-parity properties. If both pseudoscalar LLPs decay within the ID, DVs can be reconstructed from their decay products. The source of  $E_T^{\text{miss}}$  for this model depends on the production mechanisms for the Higgs boson. One mechanism involves the decay of top quarks, produced in association with the Higgs boson, into  $W$  bosons that subsequently decay leptonically. This process is the dominant contribution for the majority of the lifetime range of interest due to its large  $E_T^{\text{miss}}$  from the kinematics of its escaping neutrinos. The other involves vector bosons directly produced alongside the Higgs boson, which also decay leptonically. If one of the LLPs escapes detection in the calorimeter or is not reconstructed, it can also result in  $E_T^{\text{miss}}$  and leave only a single DV in the event.

### 2.5 Monte Carlo simulations and event generation

MC simulations are used to model the expected signal processes and to study the event selection strategy (see Section 5). The signal processes described in Sections 2.1–2.4 are generated using either MADGRAPH [40] or POWHEG [41, 42], with the decays of the primary particles provided by MADSPIN [43, 44], or by PYTHIA [45]. Finally, PYTHIA is used to simulate the parton showering and hadronization for all of the

signal processes, and the subsequent decays of bottom and charm hadrons are performed by EVTGEN [46]. The LLP decays are characterized by kinematic and lifetime distributions determined by the underlying BSM models. Background processes, including  $Z$  + jets and  $\gamma$  + jets, are generated with SHERPA [47, 48]. All generated events for both signal and background processes are passed through a detailed GEANT4 [49] simulation, which models the interactions of particles with the ATLAS detector, including the propagation of  $R$ -hadrons [50] and realistic collision conditions with pileup representative of each run period [51]. The simulated events then undergo standard ATLAS digitization, reconstruction, and an additional tracking step to recover displaced tracks from the signal, with two secondary vertexing algorithms applied to identify both standard and fuzzy displaced vertices (see Section 4).

Detailed descriptions of the implementation of each model are provided in the following subsections, while Table 1 summarizes the technical details of MC event generation.

Table 1: Summary of MC generation details for signal and background samples.

Model	Generator	Decay simulation	Cross-section order (QCD)	Mass / Lifetime ranges
Glauino $R$ -hadron	MADGRAPH 2.6.2 (NNPDF2.3LO)	PYTHIA 8.24 (A14 tune)	NNLO+NNLL	$m_{\tilde{g}}$ : 400–3000 GeV $\Delta m_{\tilde{g}, \tilde{\chi}_1^0}$ : 10–2900 GeV $\tau$ : 0.01–30 ns
Bino-Wino coannihilation	MADGRAPH 2.9.5 (NNPDF23LO)	MADSPIN + PYTHIA 8.212 (A14 tune)	NLO+NLL	$m_{\tilde{\chi}_2^0}$ : 100–1100 GeV $\Delta m_{\tilde{\chi}_2^0, \tilde{\chi}_1^0}$ : 20–50 GeV $\tau$ : 0.01–3 ns
DFSZ axino	MADGRAPH 2.9.16 (NNPDF23LO)	MADSPIN + PYTHIA 8.307 (A14 tune)	NLO	$m_{\tilde{a}}$ : 0–500 GeV $m_{\tilde{\chi}_1^0}$ : 200–1000 GeV $m_a$ : 56–5690 $\mu\text{eV}$ $\tau$ : 0.00058–6.0 ns
Higgs portal	POWHEG 2 (NNPDF23LO)	PYTHIA 8.307/8.212 (A14 tune)	NLO	$m_S$ : 5–55 GeV $\tau$ : 0.0033–3.3 ns
$Z \rightarrow \nu\nu$ + jets	SHERPA 2.2.11	SHERPA 2.2.11	NLO	–
$Z \rightarrow \mu\mu$ + jets	SHERPA 2.2.11	SHERPA 2.2.11	NLO	–
$\gamma$ + jets	SHERPA 2.2.2	SHERPA 2.2.2	NLO	–

### Glauino $R$ -hadron model

The matrix element (ME) calculation for the gluino pair-production was performed with MADGRAPH 2.6.2 at leading-order (LO) precision [40]. PYTHIA 8.24 was then used to simulate the decays of the  $R$ -hadrons, the parton showering, and the underlying event [45]. The A14 set of tuned underlying event and shower parameters [52] was used with the NNPDF2.3 LO [53] parton distribution function set to generate the  $R$ -hadron samples. The gluino pair-production cross-sections and their uncertainties have been calculated

at approximate next-to-next-to-leading order (NNLO) with next-to-next-to-leading logarithmic (NNLL) accuracy in accordance with the PDF4LHC15 recommendations [54, 55]. The gluinos in the simulated samples have mass  $m_{\tilde{g}}$  between 400–3000 GeV, mean proper lifetime  $\tau$  between 0.01–30 ns, and neutralino mass  $m_{\tilde{\chi}_1^0}$  set from a range of  $\Delta m_{\tilde{g}, \tilde{\chi}_1^0}$  between 10–2900 GeV.

### Bino-Wino coannihilation model

The ME for the pair-production of Wino-like  $\tilde{\chi}_1^\pm \tilde{\chi}_2^0$  is calculated using MADGRAPH5\_AMC@NLO 2.9.5 at next-to-leading-order (NLO) precision with next-to-leading-logarithmic (NLL) order accuracy, with NLO+NLL production cross-sections calculated by the LHC SUSY cross-section working group [56, 57]. The decay of  $\tilde{\chi}_1^\pm$  and  $\tilde{\chi}_2^0$  are simulated using MADSPIN [43]. The events are then interfaced with PYTHIA 8.212 to model parton showering, hadronization, and the underlying events with A14 tune and NNPDF2.3 LO [53] parton distribution function sets. The branching ratios  $\tilde{\chi}_1^\pm \rightarrow \tilde{\chi}_1^0 W^*$  and  $\tilde{\chi}_2^0 \rightarrow \tilde{\chi}_1^0 h^*$  are set to 100%. For an off-shell Higgs boson with mass between 20–50 GeV, the branching ratio  $h^* \rightarrow b\bar{b}$  is predicted to be approximately 90% [58], and is set to 100% in this analysis for simplicity. The simulated samples have  $m_{\tilde{\chi}_2^0}$  between 100–1100 GeV,  $\tau$  between 0.01–3 ns, and  $\Delta m_{\tilde{\chi}_2^0, \tilde{\chi}_1^0}$  between 20–50 GeV.

### DFSZ axino model

MADGRAPH5\_AMC@NLO 2.9.16 is used to generate the ME for neutralino ( $\tilde{\chi}_1^0$  and  $\tilde{\chi}_2^0$ ) pair-production, with a small  $\Delta m = 2.5$  GeV between the masses of  $\tilde{\chi}_1^0$  and  $\tilde{\chi}_2^0$ . This causes a prompt  $\tilde{\chi}_2^0 \rightarrow \tilde{\chi}_1^0 Z^*$  ( $\nu\bar{\nu}$ ) decay to a very off-shell  $Z^*$ , followed by the subsequent decay of both  $\tilde{\chi}_1^0$  to axinos. Due to the small mass difference and low-momentum decay products, it is assumed that hadronic and leptonic decays of the  $Z^*$  will result in similar selection efficiencies and not otherwise impact the analysis. This process is also indistinguishable from chargino-neutralino pair production, where the charged Higgsino decays via  $\tilde{\chi}^\pm \rightarrow \tilde{\chi}_1^0, W^*$  as shown in the representative diagram in Figure 1(c). The production cross-section is reweighted to the inclusive NLO Higgsino pair production cross-section [56, 57], which also includes these processes.

The mean Higgsino lifetime is determined by the axion decay parameter  $f_a$ . This parameter is related to the *axion* and *neutralino* masses, but not the axino mass (which remains a free parameter). This is consistent as the mass difference between the axino and Higgsino is always at least 400 GeV,  $m_{\tilde{\chi}_1^0} - m_{\tilde{a}} > 400$  GeV. The primary neutralinos in the simulated samples have masses between 200–1000 GeV, whereas the axino mass ranges from massless up to 500 GeV. For the QCD axion model, the axion mass,  $m_a$ , is determined from  $f_a$ , for which two values are adopted in this analysis:  $f_a = 5 \times 10^9$  GeV and  $5 \times 10^{10}$  GeV. The corresponding axion masses are thus  $m_a = 113$   $\mu$ eV and 1138  $\mu$ eV respectively. The cases of subsequent  $\tilde{\chi}_1^0 \rightarrow \tilde{a}h$  and  $\tilde{\chi}_1^0 \rightarrow \tilde{a}Z$  decays are considered, which are performed with MADSPIN, with decay branching ratios  $h \rightarrow b\bar{b}$  and  $Z \rightarrow q\bar{q}$  respectively set to 100%. Parton showering, hadronization and underlying event generation is subsequently handled by PYTHIA 8.307 [59], using the A14 tune and NNPDF2.3 LO parton distribution function set.

## Higgs portal model

MC samples were generated for Higgs boson production associated with vector bosons ( $VH$ ), top-quark pairs ( $ttH$ ), and via gluon–gluon fusion ( $ggH$ ) to support the Higgs portal search.  $W$  and  $Z$  bosons from  $VH$  production and from top quark decays can produce neutrinos in the event, contributing to the  $E_T^{\text{miss}}$ . Due to this, the  $ttH$  mode dominates the sensitivity at most lifetimes, with the higher cross-section  $ggH$  mode only relevant at higher lifetimes when there is a higher chance of LLPs escaping detection.  $VH$  and  $ggH$  samples were produced using POWHEG 2 and PYTHIA 8.212 at NLO and  $ttH$  samples at LO using POWHEG 2. VBF production was not used due to its very low sensitivity, as the low transverse boost makes it difficult to reconstruct an LLP with high enough  $E_T^{\text{miss}}$ .

For the Higgs portal process, PYTHIA 8.307 was used to decay the Higgs bosons from these samples into a pair of pseudoscalar LLPs  $S$ , which subsequently decay to  $b\bar{b}$  with a 100% branching fraction. In both cases the NNPDF2.3 LO parton distribution function set and A14 tune are used, and samples are scaled to production cross-sections from the LHC Higgs working group [58]. Samples were generated with  $S$  masses between 5–55 GeV and  $\tau$  between 0.0033–3.3 ns. The  $ggH$  mode was only generated at  $\tau = 3.3$  ns, where it has non-negligible efficiency.

## 3 ATLAS detector and data acquisition

The ATLAS experiment [3] at the LHC is a multipurpose particle detector with a forward–backward symmetric cylindrical geometry and a near  $4\pi$  coverage in solid angle.<sup>1</sup> It consists of the ID surrounded by a thin superconducting solenoid providing a 2 T axial magnetic field, electromagnetic and hadronic calorimeters, and a muon spectrometer.

The ID covers the pseudorapidity range  $|\eta| < 2.5$ . The high-granularity silicon pixel detector covers the vertex region and typically provides four measurements per track, the first hit generally being in the insertable B-layer (IBL). It is followed by the SemiConductor Tracker (SCT), which usually provides eight measurements per track. These silicon detectors are complemented by the transition radiation tracker (TRT), which enables radially extended track reconstruction up to  $|\eta| = 2.0$ . The TRT also provides electron identification information based on the fraction of hits (typically 30 in total) above a higher energy-deposit threshold corresponding to transition radiation.

Lead/liquid-argon (LAr) sampling calorimeters provide electromagnetic (EM) energy measurements with high granularity within the region  $|\eta| < 3.2$ . A steel/scintillator-tile hadronic calorimeter covers the central pseudorapidity range ( $|\eta| < 1.7$ ). The endcap and forward regions are instrumented with LAr calorimeters for EM and hadronic energy measurements up to  $|\eta| = 4.9$ . The muon spectrometer surrounds the calorimeters and is based on three large superconducting air-core toroidal magnets with eight coils each. The field integral of the toroids ranges between 2.0 and 6.0 T m across most of the detector. The muon spectrometer includes a system of precision tracking chambers up to  $|\eta| = 2.7$  and fast detectors for

---

<sup>1</sup> ATLAS uses a right-handed coordinate system with its origin at the nominal interaction point (IP) in the center of the detector and the  $z$ -axis along the beam pipe. The  $x$ -axis points from the IP to the center of the LHC ring, and the  $y$ -axis points upwards. Polar coordinates  $(r, \phi)$  are used in the transverse plane,  $\phi$  being the azimuthal angle around the  $z$ -axis. The pseudorapidity is defined in terms of the polar angle  $\theta$  as  $\eta = -\ln \tan(\theta/2)$  and is equal to the rapidity  $y = \frac{1}{2} \ln \left( \frac{E+p_z}{E-p_z} \right)$  in the relativistic limit.

Angular distance is measured in units of  $\Delta R \equiv \sqrt{(\Delta y)^2 + (\Delta \phi)^2}$ .

triggering up to  $|\eta| = 2.4$ . The luminosity is measured mainly by the LUCID-2 [60] detector, which is located close to the beampipe.

Events of interest are selected by the two-level ATLAS trigger system [61]. The first-level trigger is implemented in hardware and uses a subset of the detector information to accept events at a rate below 100 kHz. This is followed by a software-based trigger that reduces the accepted event rate to 1.25 kHz on average depending on the data-taking conditions. A software suite [62] is used in data simulation, in the reconstruction and analysis of real and simulated data, in detector operations, and in the trigger and data acquisition systems of the experiment.

The events used in this analysis are from  $pp$  collisions at  $\sqrt{s} = 13$  TeV, recorded under stable beam conditions at the LHC during 2016–2018. The dataset corresponds to an integrated luminosity of  $137 \text{ fb}^{-1}$  with an uncertainty of 0.84%, requiring all detector systems to be recording good quality data [63]. Data from 2015 are not included due to the need for special large-radius track reconstruction (see Section 4.1) which was only available from 2016.

The primary dataset was collected by triggers targeting large  $E_T^{\text{miss}}$  [64]. During data taking, events were accepted when the trigger-level calorimeter-based  $E_T^{\text{miss}}$  exceeded thresholds ranging from 50 – 70 GeV, with the specific value adjusted according to the instantaneous luminosity in each data-taking period. The efficiency of these triggers reaches approximately 100% for events in which the high-precision  $E_T^{\text{miss}}$  calculated in the offline reconstruction exceeds 180 GeV. Because muons deposit minimal energy in the calorimeters, samples of  $Z \rightarrow \mu\mu$  events provide a mechanism to emulate the  $E_T^{\text{miss}}$  signature and to validate the MC simulation modeling of the  $E_T^{\text{miss}}$  trigger performance. A comparison of trigger efficiencies between data and simulation in  $Z \rightarrow \mu\mu$  events shows agreement at the level of 1% both in the portion of the turn-on region that is used ( $150 < E_T^{\text{miss}} < 180$  GeV) and on the efficiency plateau ( $E_T^{\text{miss}} > 180$  GeV). This procedure builds confidence that the  $E_T^{\text{miss}}$  trigger behavior is well-modeled in the simulation and hence reliable for searches for BSM signals. Additional validation was performed using signal MC samples, where the trigger efficiency was studied as a function of the high-precision offline  $E_T^{\text{miss}}$ , confirming accurate modeling for events with genuine missing transverse momentum. Further details regarding event selections based on the  $E_T^{\text{miss}}$  are discussed in Section 4.5.

Auxiliary data samples used to validate the background estimation were selected using triggers requiring one photon [65], with transverse momentum  $p_T(\gamma) > 140$  GeV, or triggers requiring multiple jets [66].

## 4 Event reconstruction and displaced vertexing

The analysis signature is one or more DVs in the presence of sufficiently large  $E_T^{\text{miss}}$ . Two different algorithms are used in this analysis in two separate signal regions for the reconstruction of DVs from tracks: standard secondary vertexing (outlined in Section 4.2) used to target general scenarios such as the Gluino  $R$ -hadron scenario, and fuzzy secondary vertexing (outlined in Section 4.3) used to target scenarios with LLPs eventually decaying into  $b$ -hadron products such as in the Bino-Wino coannihilation or Higgs portal scenarios. The material map veto, used to select against vertices that are likely created as the result of hadronic interactions of particles with detector material, is an important aspect of the control, validation, and signal region definitions of the analysis. Its design is outlined in Section 4.4. Definitions of other physics objects such as the  $E_T^{\text{miss}}$  used for the trigger defining the signal and validation regions, photons used for the trigger defining the control regions, as well as jets used for background estimation, are detailed

in Section 4.5. The specific cleaning requirements for tracks and vertices, along with the estimation of their background processes, are detailed along with analysis selections in Section 5.

## 4.1 Tracks and primary vertices

ATLAS uses two tracking algorithms to reconstruct the trajectories of charged particles in the ID. The first is the standard track reconstruction algorithm, which is optimized to efficiently reconstruct tracks originating either from the IP or from the decays of SM particles such as  $b$ -hadrons [67]. The standard tracking algorithm is performed in two passes, both of which place constraints on the track hit multiplicities and the transverse impact parameter ( $d_0$ ) and longitudinal impact parameter ( $z_0$ ) of the track candidates with respect to the primary vertex ( $|d_0| < 10$  mm and  $|z_0| < 250$  mm, respectively). The first pass forms silicon-seeded track candidates from hits in the pixel detector and SCT. Hits in the TRT that are compatible with an extrapolated track candidate are then added to the track. The second pass utilizes unused track segments in the TRT to define nearby seed regions, in which additional track seeds based on silicon hits are produced; from these, silicon-seeded tracks are produced and then extended into the TRT, much as in the first pass. The second tracking pass is used to recover reconstruction efficiency for tracks that have a slightly displaced origin and therefore a relatively small transverse impact parameter, such as tracks from  $b$ -decays.

The selections required by the standard track reconstruction algorithm result in inefficiencies for tracks with large impact parameters, which are critical for reconstructing the decays of LLPs. In order to recover efficiency for tracks originating from LLP decays, a second track reconstruction algorithm called *large-radius tracking* (LRT) is performed in a dedicated reconstruction step [68]. Hits in the ID that are not associated to a standard track are used by the LRT algorithm to reconstruct track candidates with looser requirements on the transverse ( $|d_0| < 300$  mm) and longitudinal ( $|z_0| < 1500$  mm) impact parameters. Unlike in standard tracking, LRT track candidates do not require hits in the pixel detector. No distinction between tracks reconstructed by the standard and those reconstructed by the LRT algorithms is made in the subsequent reconstruction steps.

Collision vertices (CVs) consistent with  $pp$  interactions from the beam are reconstructed using the tracks reconstructed by the standard tracking algorithms [69]. CVs are required to have at least two associated tracks. The vertex with the greatest sum of squared transverse momenta of the tracks associated with the vertex  $\Sigma p_T^2$ , is identified as the *primary vertex* (PV). Tracks are then refitted using this identified PV as a constraint to obtain the track parameters with respect to the point of closest approach in the transverse plane between a track and the beam line, or the perigee.

## 4.2 Standard secondary vertices

LLP decays in the ID resulting in two or more tracks can be reconstructed as a DV by a dedicated standard displaced vertexing algorithm [70], and the resulting DVs are denoted as SDVs. Displaced vertexing begins by forming two-track seed vertices from pairs of *selected tracks*. Selected tracks, including both standard and LRT tracks, must have  $p_T > 1$  GeV and pass several hit multiplicity requirements. To be used in SDV seeding, tracks must have at least six SCT hits or at least one pixel hit, and tracks with fewer than two pixel hits must have at least one hit in the TRT. Tracks with  $p_T < 25$  GeV are subject to additional requirements in order to suppress contributions from *fake tracks* – those erroneously produced via combinatorial reconstruction effects – which tend to have low  $p_T$ . These tracks are required to have at

least seven SCT hits, and they must additionally have at least 20 hits in the TRT if they are reconstructed with  $|\eta| < 1.7$ .

Two-track seed vertices are formed by a  $\chi^2$ -based fitting algorithm [71]. Once all two-track seed vertices of selected tracks have been formed, the seed vertices are iteratively merged to form  $n$ -track vertices. If a track is compatible with more than one vertex at this stage, it is associated to the vertex with which it has a more compatible fit. If the distance between the estimated positions of a pair of vertices is not significant enough, determined using a significance estimator based on the position uncertainty of the vertices, the pair of vertices can be merged. At this point, SDVs are composed strictly of selected tracks. In the final step of the algorithm, additional tracks are attached to SDVs to recover efficiency lost due to the strict seed track requirements. These *attached tracks* have loosened hit multiplicity requirements relative to selected tracks. Attachment is accepted only if the reduced  $\chi^2$  is less than 20.

At this point, the final vertex fit using all the selected and attached tracks is performed and track parameters with respect to the associated SDV are re-calculated. The number of tracks associated with a SDV is denoted as  $N_{\text{Tracks}}^{\text{SDV}}$ , and the visible invariant mass of the SDV, denoted  $m_{\text{SDV}}$ , is calculated from the four-momenta of its constituent tracks, under the assumption that each track was produced by a charged pion.

### 4.3 Fuzzy secondary vertices

Since the SDV algorithm relies heavily on vertex fitting, which assumes that all particles from the LLP decay originate from a single point, a significant number of tracks fail to be reconstructed as a single vertex when the LLP decay involves  $b$ -hadrons, due to their sizable decay length. *Fuzzy displaced vertexing* is a DV reconstruction algorithm targeting such LLP decays.

The fuzzy displaced vertexing algorithm begins by forming two-track seed vertices from selected track pairs. Prior to seed vertex formation, two levels of selection are applied: track-level preselection and track-pair preselection. For track-level preselection, tracks must meet the following criteria:  $p_{\text{T}} > 1$  GeV, at least two hits in the silicon detector, and no association with any CVs. All combinations of preselected tracks are then evaluated for their likelihood of originating from an LLP using a multivariable analysis. A Boosted Decision Tree (BDT) algorithm in TMVA package [72] is used to determine the scores indicating the signal-track-pair-likeness using track pairs from an LLP in the signal MC events as the signal training samples and pairs of two tracks randomly selected from the background events as the background training samples. The LLP used is  $\tilde{\chi}_2^0$  in the Bino-Wino coannihilation, with a mass of 300–500 GeV, a lifetime of 0.01–1 ns, and a mass difference from  $\tilde{\chi}_1^0$  of 30 GeV. The input variables used for signal-track-pair-likeness BDT are listed in Table 2. The importance of each input variable in determining the signal-track-pair-likeness slightly depends on the LLP lifetime, but generally, the most important input variables are the angular separations between two tracks in the  $\eta$  and  $\phi$  directions,  $\Delta\eta$  and  $\Delta\phi$ . The next important input variables are the transverse and longitudinal impact parameters of track #1/#2,  $d_0^{(1/2)}$ ,  $z_0^{(1/2)}$ , the longitudinal impact parameter with respect to the beam spot of track #1/#2,  $z_0^{\text{BS},1/2}$ , and the  $p_{\text{T}}$  asymmetry between tracks,  $p_{\text{T}}^{\text{asym}}$ . This track-pair selection step ensures that seed vertex fitting is performed only on pairs likely to originate from an LLP, reducing computational demands and minimizing the formation of fake vertices. A two-track seed vertex is created by the fitting algorithm used in the SDV algorithm if the score quantifying the signal-track-pair-likeness exceeds a defined threshold. This threshold corresponds to approximately 98% efficiency in selecting signal track pairs for the Bino-Wino coannihilation model with  $m_{\tilde{\chi}_2^0} = 300$  GeV,  $\Delta m_{\tilde{\chi}_2^0, \tilde{\chi}_1^0} = 30$  GeV, and  $\tau = 0.3$  ns.

Table 2: Input variables to the signal-track-pair-likeness BDT. The superscript indicates the index of the track (1 or 2). Since the first seven rows include the variables for both tracks #1 and #2, there are 18 variables in total.

Variables	Description
$\eta^{(1)}, \eta^{(2)}$	$\eta$ direction of tracks #1 and #2
$d_0^{(1)}, d_0^{(2)}$	Transverse impact parameter of tracks #1 and #2
$S(d_0^{(1)}), S(d_0^{(2)})$	$ d_0 /\sigma(d_0)$ of tracks #1 and #2, where $\sigma(d_0)$ is $d_0$ uncertainty of tracks #1 and #2
$z_0^{(1)}, z_0^{(2)}$	Longitudinal impact parameter of tracks #1 and #2
$z_0^{\text{BS},1}, z_0^{\text{BS},2}$	Longitudinal impact parameter with respect to the beam spot of tracks #1 and #2
$S(z_0^{(1)}), S(z_0^{(2)})$	$ z_0 /\sigma(z_0)$ , where $\sigma(z_0)$ is $z_0$ uncertainty
$\mathcal{HC}^{(1)}, \mathcal{HC}^{(2)}$	Category indicating the innermost hit layer of tracks #1 and #2 (0: First Pixel layer, 1: Second Pixel layer, 2: Third or fourth Pixel layers, 3: SCT layers)
$\Delta\eta$	Angular separation in $\eta$ direction between tracks #1 and #2
$\Delta\phi$	Angular separation in $\phi$ direction between tracks #1 and #2
$p_T^{\text{asym}}$	$p_T$ asymmetry between tracks #1 and #2 ( $= (p_T^{(1)} - p_T^{(2)}) / (p_T^{(1)} + p_T^{(2)})$ )
$\Delta\mathcal{HC}$	Difference of $\mathcal{HC}$ between tracks #1 and #2

After forming two-track seed vertices, multiple seed vertices may correspond to a single LLP decay. To address this, vertex merging is performed to combine these seed vertices into a single vertex. When the LLP decay involves  $b$ -hadrons, the seed vertices tend to be spatially distributed, so this merging step is performed independently of the fitting process. Each seed vertex is assigned a score indicating its signal-track-pair-likeness, which is initially determined during the two-track seed-forming step. The merging process is carried out in descending order of this score.

Seed vertices with particularly high scores are designated as ‘‘primary seeds.’’ Approximately 85% of the reconstructed seed vertices meet the primary seed criteria for the Bino-Wino coannihilation model with  $\tau = 0.3$  ns. The seed vertices are referred to as ‘‘substitute seeds’’ of a primary seed if the differences in their positions  $x$ ,  $y$ , and  $z$  from the primary seed ( $\Delta x^{\text{prim}}$ ,  $\Delta y^{\text{prim}}$ , and  $\Delta z^{\text{prim}}$ ) are all within a threshold. The threshold is defined as  $\Delta x^{\text{prim}}, \Delta y^{\text{prim}}, \Delta z^{\text{prim}} < 1$  mm for  $r_{\text{seed}} < 23.5$  mm,  $\Delta x^{\text{prim}}, \Delta y^{\text{prim}}, \Delta z^{\text{prim}} < 3$  mm for  $23.5 \text{ mm} \leq r_{\text{seed}} < 33.5$  mm, and  $\Delta x^{\text{prim}}, \Delta y^{\text{prim}}, \Delta z^{\text{prim}} < 5$  mm for  $r_{\text{seed}} \geq 33.5$  mm, where  $r_{\text{seed}}$  is the radial position of the primary seed. If the primary and substitute seeds satisfy the criterion in Eq. (1), the substitute seed is merged with the primary seed:

$$\sum p_T^{\text{prim}} + \sum p_T^{\text{sub}} > 3.0 \text{ GeV} \times (\phi_{\text{max}} - \pi/2) + 4.0 \text{ GeV}, \quad (1)$$

where  $\sum p_T^{\text{prim}}$  and  $\sum p_T^{\text{sub}}$  represent the sum of the  $p_T$  of the two tracks included in the primary and substitute seeds, respectively, and  $\phi_{\text{max}}$  is the maximum angle between the tracks from the primary and substitute seeds. This merging procedure is performed in descending order of the primary seeds’ scores. This criterion is designed to prevent the merging of large numbers of fake seed vertices formed from unrelated random track pairs. As a final step, seed groups are iteratively merged until no two groups share any common seeds. The resulting seed groups are then defined as FDVs. For FDVs, the vertex position is defined as the average of the position of the two-track seed vertices associated with the FDV, and track parameters with respect to this point are obtained. The uncertainty of the vertex position is also defined as the standard deviation of the associated two-track seed vertices. The number of tracks associated with an FDV and the visible invariant mass of an FDV, denoted as  $N_{\text{Tracks}}^{\text{FDV}}$  and  $m_{\text{FDV}}$ , are defined in the same way as the SDV. The number of two-track seed vertices associated with the FDV is denoted as  $N_{\text{Seeds}}^{\text{FDV}}$ .

The primary advantage of FDVs is their ability to include more tracks compared to SDVs, particularly when the signal LLP decay involves  $b$ -hadrons. This results in significantly higher signal selection efficiency. On the other hand, the rate of fake FDVs with high track multiplicity is also higher than that of SDVs. Figure 2 illustrates the efficiency of reconstructing an LLP decay as a vertex with at least five tracks and an invariant mass greater than 10 GeV, using both standard and fuzzy displaced vertexing methods as a function of the truth radial displacement of the LLP decay from the beamline axis ( $L_{xy}$ ). Only tracks matched to the truth particles originating from the LLP decay are counted. The fuzzy vertexing method demonstrates significantly higher efficiency than the standard method for the Bino-Wino coannihilation model, e.g., 2.6 times at  $L_{xy} = 50$  mm and 3.2 times at  $L_{xy} = 100$  mm, whereas the increase in efficiency in the Gluino  $R$ -hadron model is limited.

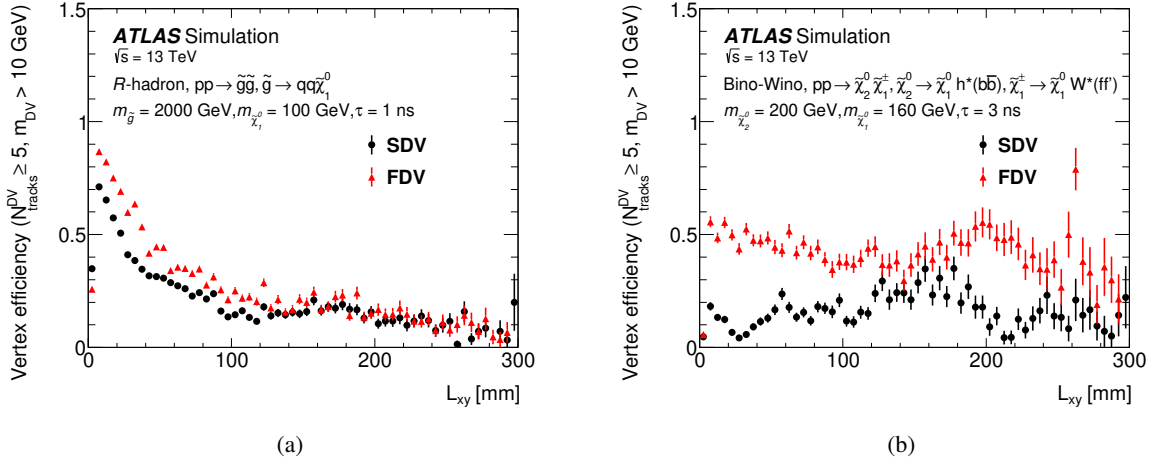


Figure 2: Vertex reconstruction efficiency for the standard and fuzzy vertexing methods for (a) Gluino  $R$ -hadron and (b) Bino-Wino coannihilation models.  $L_{xy}$  is the radial displacement of the truth position of the DV from the beamline axis. The spike around  $L_{xy} = 260$  mm is due to statistical fluctuations, as confirmed by looking at other signal models.

#### 4.4 Detector material map

Hadronic interactions with detector material are a significant source of background in DV searches. To mitigate this, a veto is employed to exclude vertices reconstructed at positions consistent with being inside detector material, as identified by a material map [7]. DVs must pass this veto to be included in the signal regions, ensuring the search remains focused on genuine LLP decay signals rather than material-related background.

In addition to its role in defining the signal regions, the material map veto is also used to create a background-dominated validation region (VR) for background estimates by reversing the veto. DVs identified as originating inside detector material are dominated by background from hadronic interactions and have negligible signal contamination. This region provides a crucial sample for validating background estimate performance, as detailed in Sections 5.3.4 and 5.3.6.

The material map itself is constructed by analyzing the positions of low-mass vertices in data to identify regions of high vertex density. These regions are compared with the known locations of detector components to map the material distribution. The material map is represented as a cylindrical histogram, where each

bin (sub-mm) is classified as either inside or outside material, as shown in Figure 3. This map defines slightly less than 50% of the ID's fiducial volume (radius < 300 mm) as subject to the veto criteria.

Two versions of the material map veto are implemented to provide flexibility. The loose veto checks whether the position of a DV falls within a bin identified as containing material and vetoes it accordingly. The strict veto excludes DVs not only based on their position but also by considering neighboring bins to account for potential mismatches between bin boundaries and actual material boundaries. Additionally, the strict veto incorporates reconstruction uncertainties in the DV position by excluding DVs whose uncertainty ellipsoid intersects any material-containing bins. This ensures a more robust rejection of material-related backgrounds for the FDV case as the vertex position is less precisely defined. A cross-check is also performed against the simulation geometry to validate the veto. The strict veto is used for any SR requirements, whereas the loose veto is used in some CRs or VRs when required to reduce signal contamination. In MC simulations, the same material map and veto algorithm are applied. However, in real data, the layers of the pixel detector are slightly offset in the  $x - y$  plane due to their attachment to the beam pipe, the position of which can vary relative to the rest of the ATLAS detector. Such relative shifts are corrected for in the simulation to align with the real detector geometry.

By combining the material map veto for signal regions with the reversed veto for background validation, this approach ensures both an effective background suppression for LLP searches and reliable validation of background estimates.

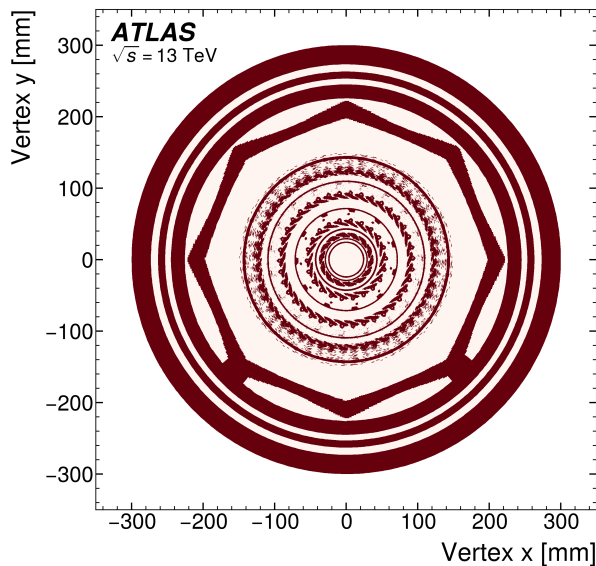


Figure 3: Map showing a cross-section at  $z = 0$  of the physical material comprising the ATLAS detector's beam pipe and tracking detector, used to define the "material map veto" [7].

#### 4.5 Physics object definitions

Tracks and PVs are reconstructed as described in Section 4.1. Events are required to have the PV associated with at least two standard tracks with transverse momentum  $p_T > 500$  MeV. Tracks reconstructed by the standard track reconstruction algorithm (standard tracks) must have transverse momentum  $p_T > 500$  MeV and pseudorapidity range  $|\eta| < 2.7$ . Tracks reconstructed by the LRT (LRT tracks) must have transverse momentum  $p_T > 1$  GeV and pseudorapidity range  $|\eta| < 5.0$  [68].

Muon candidates are reconstructed within the pseudorapidity range  $|\eta| < 2.5$  from tracks in the muon spectrometer that are matched to ID tracks. These candidates must have transverse momentum  $p_T > 10$  GeV and satisfy the *medium* identification criteria detailed in Ref. [73].

Electron candidates are reconstructed from isolated energy deposits in the EM calorimeter matched to ID tracks [74, 75]. They are required to satisfy  $|\eta| < 2.47$ ,  $p_T > 10$  GeV, and the *LooseAndBLayer* identification requirement described in Ref. [76].

Photons are used in the baseline vertex selections to remove displaced vertices arising from photon conversion, and are also used to define the control region. Photon candidates are reconstructed from energy deposits in the EM calorimeter. Both unconverted photon candidates without matching ID tracks and converted photon candidates with a two-track conversion vertex or with a single track are used. They are required to satisfy  $|\eta| < 2.37$ ,  $p_T > 25$  GeV, and the *Tight* identification requirement described in Ref. [74].

Jets are reconstructed from three-dimensional topological energy clusters in the calorimeters [77] using the anti- $k_t$  clustering algorithm [78, 79] with radius parameter  $R = 0.4$ . Only jets with  $p_T > 20$  GeV and  $|\eta| < 2.8$  are retained. Events are rejected if they contain any jet with  $p_T > 20$  GeV that fails basic quality requirements designed to suppress detector noise and non-collision backgrounds [80]. To avoid double-counting of energy depositions in the calorimeter, jets within a distance  $\Delta R = 0.2$  of an electron candidate are discarded. Jets containing  $b$ -hadrons ( $b$ -jets) are used for background estimation. They are identified using the *DLI*  $b$ -tagging algorithm [81]. It is a multivariate classification algorithm that combines information from the impact parameters of the tracks and the secondary and tertiary decay vertices in the jet. The  $b$ -tagging working point with a 77% efficiency is used in this analysis.

The  $E_T^{\text{miss}}$  is defined as the magnitude of the negative vector sum of the transverse momenta of all identified physics objects (electrons, photons, muons, jets) and an additional soft term accounting for energy not associated with hard objects. For an overview of how  $E_T^{\text{miss}}$  is computed, see Ref. [82]. In order to reduce the effects of jets from pileup collisions on  $E_T^{\text{miss}}$  resolution, a jet vertex tagger [83] and a forward jet vertex tagger [84] are applied to the jets with  $|\eta| < 2.4$  and  $p_T < 60$  GeV and those with  $2.5 < |\eta| < 4.5$  and  $p_T < 60$  GeV, respectively, in the  $E_T^{\text{miss}}$  calculation. These jet vertex tagger requirements are not applied to the jets used in the analysis. The soft term is constructed from all tracks that are not associated with any physics object and are linked to the PV. This approach ensures that the  $E_T^{\text{miss}}$  reflects the best available calibration of the high- $p_T$  objects while preserving pileup independence in the soft term. Unless otherwise noted,  $E_T^{\text{miss}}$  selections are based on this definition in the offline analysis. An additional related quantity, referred to as hadronic  $E_T^{\text{miss}}$ , is calculated similarly as the magnitude of the negative vector sum of the transverse momenta of all calorimeter energy clusters, which are assumed to originate from hadronic objects [82]. This effectively reduces contributions from identified leptons and photons.

## 5 Signal regions and background estimation

SRs are defined by a set of selection criteria intended to enrich the fraction of signal events and minimize the fraction of background events retained. These criteria are optimized for sensitivity to the signal models introduced in Section 2, while limiting contamination from background processes. To identify these DVs, the two different vertexing algorithms introduced in Section 4 are used. This search is implemented as a counting experiment in two distinct SRs defined by the vertexing algorithm used. Events containing vertices reconstructed with the SDV algorithm are categorized in the SDV SR, while events reconstructed

with the FDV algorithm are placed in the FDV SR. The expected number of background events in each SR and VR is estimated using signal depleted photon-triggered control regions (CRs), which have the same SR or VR selection criteria, except the events are photon-triggered instead of  $E_T^{\text{miss}}$  triggered and the  $E_T^{\text{miss}}$  selection criteria are dropped. This is because the mechanisms behind the origin of DVs are linked to jets and overall event track activity, and are therefore independent to whether or not a photon or  $E_T^{\text{miss}}$  is present in the event. The estimate is validated in VRs, where the events must be  $E_T^{\text{miss}}$  triggered, however some other SR selection criteria related to vertex requirements are inverted to ensure a signal depleted but kinematically similar region to the SR. This section describes the details of the SR, VR, and CR definitions, as well the background estimation methods. The uncertainties involved in the background estimation, as well as other systematic uncertainties, are detailed in Section 6. An independent validation for the SDV SR is also done via a component-based background estimate which uses different CRs and VRs. The SDV and FDV regions are designed to be sensitive to different signal topologies, so orthogonality is not enforced between the two vertexing regions. However, while the SDV SR searches for at least one DV, the FDV SR is divided into two orthogonal SRs that require exactly one FDV and at least two FDVs. A common set of event-level selections determines the events considered in both SRs.

## 5.1 Common event-level selections

As detailed in Section 3, events in the SRs are required to pass  $E_T^{\text{miss}}$  triggers and have an offline reconstructed  $E_T^{\text{miss}} > 150$  GeV and hadronic  $E_T^{\text{miss}} > 180$  GeV. Events are vetoed if affected by detector issues such as calorimeter noise or data corruption. To ensure the event originates from a  $pp$  collision in the detector's IP, a PV with  $|z_{\text{PV}}| < 200$  mm is required. Non-collision background (NCB) contamination, such as beam halo [85–87], is suppressed by requiring that the leading jet in the event deposits no more than 80% of its energy in a single calorimeter layer and no more than 96% of its energy in the EM calorimeter. Events containing any jets with  $p_T > 50$  GeV overlapping dead tile modules are rejected if the azimuthal angular separation between the  $E_T^{\text{miss}}$  and the jet,  $\Delta\phi(E_T^{\text{miss}}, \text{jet})$ , is less than 0.3. All SR events must meet these common event-level selection criteria.

A CR is populated by events triggered by a single photon with  $p_T(\gamma) > 140$  GeV. These events must pass the same common selection criteria as above, *except* that they must fail the combined  $E_T^{\text{miss}}$  trigger and offline  $E_T^{\text{miss}}$  selections, so that the CR is orthogonal to the SRs. This region was chosen as the CR because the events triggered by a single photon ( $\gamma$  + jets) and  $E_T^{\text{miss}}$  ( $Z$  + jets) have a similar topology except for the difference between photon and  $E_T^{\text{miss}}$ , and they have large statistics and negligible signal contamination from models of interest.

## 5.2 Signal region definitions

This section defines the two SRs for this search: SDV SR and FDV SR, based on the vertexing algorithm. The FDV SR is further divided into two mutually exclusive sub-regions: the single fuzzy vertex sub-region (1FDV) for models with exactly one LLP decay, and the two fuzzy vertices sub-region (2FDV) for models involving pair production of LLPs decaying to two or more distinct FDVs. These sub-regions are analyzed independently, and their results are statistically combined for the final FDV SR result. For FDV SR and its associated CR, an additional event-level selection called *strict NCB veto* is applied to reject the NCB processes more strictly. It rejects the events if the fraction of the charged component of the leading jet is lower than 10% of the fraction of energy that is found in its single most energetic calorimeter layer. The strict NCB veto filters out NCB processes to a negligible level, but also removes signal events where a jet

from an LLP becomes the leading jet. Therefore, it is only used for FDV SR, which targets models where the leading jet generally comes from initial-state radiation.

After common event-level selections, candidate DVs must pass baseline criteria (Table 3) to ensure they are well-measured and reduce background. The reconstructed vertex position must be in the fiducial region, which is defined as a radial displacement from the beamline axis  $r_{\text{DV}} = \sqrt{x_{\text{DV}}^2 + y_{\text{DV}}^2} < 300$  mm and axial displacement from the origin  $|z_{\text{DV}}| < 300$  mm, where  $x_{\text{DV}}$ ,  $y_{\text{DV}}$ , and  $z_{\text{DV}}$  are the cartesian coordinates of the DV. The requirement that the vertex is separated in the transverse plane from all reconstructed CVs,  $\Delta r_{xy}(\text{DV}, \text{CV})$ , is to avoid mislabeling CVs as secondary vertices and suppress the background from the decay of heavy-flavor hadrons. It is also required that the vertex is not reconstructed near an energetic photon,  $\Delta R(\text{DV}, \gamma)$ , to remove DVs arising from photon conversions. The selection on the maximum track transverse momentum ( $\max(p_{\text{T}}^{\text{track}})$ ) with respect to the scalar sum of the transverse momentum of all tracks in the vertex is in place to suppress background from vertices that contain mismeasured tracks. SDVs must have a reduced  $\chi^2$  in the vertex fitting,  $\chi^2/N_{\text{DoF}}$ , of less than 5 to remove the misreconstructed vertices.

Table 3: Baseline vertex selection criteria for SDV SR and FDV SR (including the 1FDV and 2FDV subregions).

Baseline vertex selections	SDV SR	FDV SR
Vertexing algorithm	Standard DV algorithm (SDV)	Fuzzy DV algorithm (FDV)
Vertex position	$r_{\text{DV}} < 300$ mm, $ z_{\text{DV}}  < 300$ mm	
$\Delta r_{xy}(\text{DV}, \text{CV})$	$> 4$ mm for any CV	
Material map veto	Strict veto required (Section 4.4)	
$\Delta R(\text{DV}, \gamma)$	$> 0.1$ , for photons with $p_{\text{T}}(\gamma) > 60$ GeV	
$\max(p_{\text{T}}^{\text{track}})/(\text{scalar sum } p_{\text{T}}^{\text{track}})$	$< 0.95$	$< 0.9$
$\chi^2/N_{\text{DoF}}$	$< 5$	–

Vertices passing the baseline vertex selections are used to develop and validate the background estimation methods for the SRs. Additional quality selections are applied to tracks associated with the DVs in order to remove tracks that appear to originate from background processes from DVs. These selections are placed on track variables including  $|d_0|/\sigma(d_0)$ , the track  $d_0$ -significance, the azimuthal angle between the track and the PV-SDV vector  $\Delta\phi_{\text{PV-SDV}}$  and the PV-FDV vector  $\Delta\phi_{\text{PV-FDV}}$ , and the three-dimensional angle between the track and the PV-DV vector  $\alpha$ . The DV properties, including  $N_{\text{Tracks}}^{\text{DV}}$ ,  $m_{\text{DV}}$ , and  $N_{\text{Seeds}}^{\text{DV}}$ , are recalculated after removing tracks failing the quality selections, while the vertex refitting is not performed and the vertex position is not redefined. The *signal vertex selections* are then applied to generate the SRs, summarized in Table 4. The signal vertex selections are applied to the following values: the track multiplicity  $N_{\text{Tracks}}^{\text{DV}}$ , the invariant mass of the DV  $m_{\text{DV}}$ , the number of selected tracks  $N_{\text{Sel. Tracks}}^{\text{DV}}$ , the separation between the DV and closest jet  $\Delta R_{\text{DV,jet}}$ , the number of two-track seed vertices associated with the FDV  $N_{\text{Seeds}}^{\text{DV}}$ , the angular separation in  $\eta$  direction from the PV to the DV  $|\eta_{\text{PV-DV}}|$ , and the maximal  $\Delta\eta$  between a single track and the sum of the four-vector of the other tracks ( $\max_i [\Delta\eta(\vec{p}_{\text{track},i}, \sum_j \vec{p}_{\text{track},j} - \vec{p}_{\text{track},i})]$ ). It is required that the number of vertices satisfying these criteria,  $N_{\text{DV}^{\text{sat}}}$ , for the SDV and 1FDV region is at least one, whereas the 2FDV region requires two or more. For the 1FDV sub-region it is also required that there is no additional FDV that satisfies the full SR selections for the 2FDV sub-region in order to keep the 1FDV and 2FDV sub-regions mutually exclusive.

The signal efficiencies are key metrics used in optimizing selection criteria and validating this analysis. Table 5 summarizes the signal efficiency values for a range of representative sample signal points,

Table 4: Full vertex selection criteria for SDV SR and FDV SR (including the 1FDV and 2FDV subregions).

Full SR vertex selection	SDV SR	FDV SR	
		1FDV	2FDV
Vertices	SDV	FDV	
$N_{\text{Tracks}}^{\text{DV}}$	$\geq 5$	$\geq 5$	$\geq 4$
$m_{\text{DV}}$ [GeV]	$> 10$	$> 10$	$> 1.5$
$N_{\text{Sel. Tracks}}^{\text{DV}}$	$\geq 2$	–	–
$N_{\text{Seeds}}^{\text{DV}}$	–	$\geq \binom{N_{\text{Tracks}}^{\text{DV}}}{2} - 1$	$\geq N_{\text{Tracks}}^{\text{DV}}$
$\Delta R_{\text{DV}, \text{jet}}$	–	–	$< 0.4$
$ \eta_{\text{PV-DV}} $	–	–	$< 2.5$
$\max_i [\Delta\eta(\vec{p}_{\text{track}, i}, \sum_j \vec{p}_{\text{track}, j} - \vec{p}_{\text{track}, i})]$	–	$< 3.5$	–
$N_{\text{DV sat}}$	$\geq 1$	$\geq 1^\dagger$	$\geq 2$

<sup>†</sup> The event must not have any additional FDVs satisfying the 2FDV selections.

highlighting the spread of efficiency values across samples in their respective SRs. Note that for the Higgs portal model, efficiency is defined relative to the signal samples used at a given lifetime. The lower efficiency at  $\tau = 3.3$  ns is because  $ggH$  production is only included at that lifetime.

Table 5: Summary of signal efficiencies in each signal region for models with fixed mass parameters and varied lifetimes.

Model	Lifetime $\tau$ [ns]	Efficiency [%]		
		SDV SR	1FDV SR	2FDV SR
Gluino $R$ -hadron $m_{\tilde{g}} = 1600$ GeV $m_{\tilde{\chi}_1^0} = 100$ GeV	0.01	6.4	0.29	0.084
	0.1	41	1.1	0.36
	3.0	6.9	0.09	0.0029
DFSZ axino ( $ZZ$ ) $m_{\tilde{a}} = 400$ GeV $m_{\tilde{\chi}_1^0} = 800$ GeV	0.0045	9.26	0.48	0.012
	0.097	40.19	0.1	0.30
	1.5	5.15	0.99	0.11
Bino-Wino coannihilation $m_{\tilde{\chi}_1^0} = 650$ GeV $m_{\tilde{\chi}_2^0} = 700$ GeV	0.03	0.13	0.37	0.055
	0.3	0.10	0.20	0.024
	3.0	0.014	0.037	0.006
Higgs portal $m_S = 55$ GeV	0.0033	0.007	0.007	0.022
	0.033	0.026	0.023	0.057
	3.3	0.0003	0.0003	0.0002

For an accurate estimate of the background contributions to each SR, a data-driven approach is employed. The background estimates for each SR are independently derived and optimized accordingly. The following sections detail the background estimation methods and their validation per SR.

### 5.3 Background estimates and validation regions

Due to the origin and composition of the expected background contributions, multiple VRs are defined for each SR. These VRs are chosen to be kinematically similar to the SRs while being statistically independent, allowing us to test the background prediction techniques in adjacent phase spaces. The VRs are constructed by modifying key selection criteria such as  $N_{\text{Tracks}}^{\text{DV}}$ ,  $m_{\text{DV}}$ ,  $N_{\text{Seeds}}^{\text{DV}}$ , and whether the material map veto flags them as being positioned either inside or outside of detector material. For the SDV SR and 1FDV SR, VRs are defined by selecting vertices with exactly four tracks in the middle mass range (10–20 GeV), or by selecting vertices in the lower mass ranges (5–10 GeV) with more than four tracks. The photon-triggered CRs are defined with similar boundaries. The VR definition for the 2FDV SR is discussed in Section 5.3.6. The background estimation methods are tested in each of these VRs to ensure reliable predictions in the corresponding SRs. These VRs are built so that the amount of possible signal contamination is not significant.

#### 5.3.1 SDV background estimate

Searches for SDVs with high invariant mass and multiple tracks face minimal background due to the rarity of SM processes producing such signatures. Background SDVs in general primarily arise from:

- **Hadronic interactions (HI)**, where particles interact with detector material, producing collimated tracks and low-mass vertices.
- **Accidental crossings (AX)**, where unrelated tracks from the primary vertex or pileup attach to a SDV, increasing its apparent mass and track count.
- **Merged vertices (MV)**, where separate SDVs are mistakenly combined into a single vertex with higher mass and multiplicity.

All three sources of background are estimated inclusively with a data-driven technique that exploits the relationship between SDVs and the track density of the event to predict the number of background vertices. The estimated number of background events in the SR,  $N_{\text{bkg}}$ , is computed using an event-DV probability (EDP)  $P(\text{vertex} | N_{\text{Tracks}}^{\text{Event}}, N_{b\text{-tag}})$ , where  $N_{\text{Tracks}}^{\text{Event}}$  is the total number of tracks associated with any CV and  $N_{b\text{-tag}}$  is the number of  $b$ -tagged jet count per event. Defined in Eq. (2), the EDP represents the probability of reconstructing an SR-like vertex satisfying the baseline vertex selections with the additional requirement:  $m_{\text{DV}} > 5$  GeV and  $N_{\text{Tracks}}^{\text{DV}} \geq 4$ , which is measured in the CR. To correct for the effects of differences in the distributions of the number of pileup collisions, the events in the CR are weighted such that the distributions of the number of pileup collisions match those of the events passing the common selections (Section 5.1) when calculating the EDP. This selection on  $m_{\text{DV}}$  and  $N_{\text{Tracks}}^{\text{DV}}$  is intentionally less stringent than the SDV SR requirement, as the stricter criteria result in too few events to generate a non-trivial estimate. The extrapolation factor  $f$ , obtained from the CR events according to Eq. (3), corrects for this by extrapolating to the SR selection values. The dependency of  $f$  on  $N_{\text{Tracks}}^{\text{Event}}$  and  $N_{b\text{-tag}}$  is confirmed to be negligible compared to the other uncertainties in the background estimate. The EDP is applied to all events passing the common event-level selections described in Section 5.1 for the SR region, and the background

estimate is then computed as in Eq. (4), where the sum is taken over the SR. This SDV background estimate method (also used for 1FDV) counts number of DVs instead of events with DVs. Since events with more than one DV with  $N_{\text{Tracks}}^{\text{DV}} \geq 4$  and  $m_{\text{DV}} > 5$  GeV are very rare, the uncertainty from using this approximation is small compared to other uncertainties in the background estimate.

$$P(\text{vertex} | N_{\text{Tracks}}^{\text{Event}}, N_{b\text{-tag}}) = \frac{N_{\text{Vertex}}^{\text{CR}}(N_{\text{Tracks}}^{\text{Event}}, N_{b\text{-tag}})}{N_{\text{Events}}^{\text{CR}}(N_{\text{Tracks}}^{\text{Event}}, N_{b\text{-tag}})} \quad (2)$$

$$f = \frac{N_{\text{vertex}}^{\text{CR}}(m_{\text{DV}} > 10 \text{ GeV}, N_{\text{Tracks}}^{\text{DV}} \geq 5)}{N_{\text{vertex}}^{\text{CR}}(m_{\text{DV}} > 5 \text{ GeV}, N_{\text{Tracks}}^{\text{DV}} \geq 4)} \quad (3)$$

$$N_{\text{bkg}} = f \cdot \sum_{\text{events}} P(\text{vertex} | N_{\text{Tracks}}^{\text{Event}}, N_{b\text{-tag}})_i \quad (4)$$

This method predicts an expected background of  $0.6 \pm 0.4$  events in the SDV SR, with the dominant uncertainty being statistical.

### 5.3.2 SDV background estimate validation

The predictions of the background estimation method are tested in three statistically independent sideband VRs. Events in these sideband VRs are required to satisfy all the SDV SR requirements, except for the relaxed conditions of  $5 < m_{\text{SDV}} < 10$  GeV or  $m_{\text{SDV}} < 20$  GeV with  $N_{\text{Tracks}}^{\text{SDV}} = 4$ . The full background estimate procedure, including calculating an EDP and extrapolation factor  $f$  is done for each VR. The details of the VRs and a comparison of the predicted and observed number of events in each VR are shown in Figure 4. The predictions of the background estimate are found to agree with the number of observed events in data for all three of the VRs within the uncertainty.

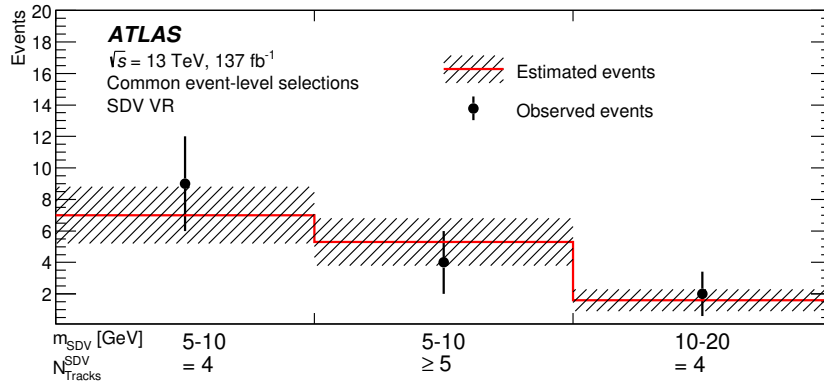


Figure 4: Estimated and observed events in the sideband VRs of the SDV SR. The gray hashed band shows the background estimate uncertainties from the CR's statistics and from the distributions of the number of pileup collisions between events in the CR and the events that pass common event-level selections.

In addition to validating the background estimate in sideband regions, a separate background estimate is performed where the contribution from each source – hadronic interactions, merged vertices and accidental crossings – is estimated independently. Each contribution is estimated using data-driven techniques

that construct mass templates describing the shape of  $m_{\text{SDV}}$  for background SDVs from the particular background source. These methods are described and validated in previous ATLAS searches for displaced vertices [5, 6], and will only be briefly detailed here:

- **HI:** The HI SDV mass distribution is modeled as

$$N_{\text{SDV}}(m_{\text{DV}}; b, C, l) = \left[ \frac{1}{C(m_{\text{DV}} - b)} + \exp\left(\frac{m_{\text{DV}} - b}{l}\right) \right]$$

where  $b$ ,  $C$ , and  $l$  are fitted constants, and the resulting fit is integrated to produce an estimate of the number of HI background SDVs created.

- **AX:** The rate of accidental crossings is estimated from data, using candidate 2- and 3-track  $K_S^0 \rightarrow \pi^+\pi^-$  decay SDVs, with the identified AX tracks' kinematics saved. Artificial accidentally-crossed SDVs are created by attaching the above AX tracks to data SDVs. Their mass distributions are scaled by the accidental crossing rate, and integrated to yield an estimated number of background SDVs.
- **MV:** Merged SDVs are created by artificially overlapping events in data and reclustering vertices. The resulting vertices are used to estimate the merging rate – by comparing distances between vertices to those in the original data – and to produce MV mass templates. The templates are rescaled by the merging rate, and integrated to yield an estimated number of background SDVs.

The total expected background obtained in each VR and the SDV SR agree within statistical uncertainty with the expected background from the inclusive method.

The estimated number of background events in SDV SR with its uncertainty is shown in Table 6.

### 5.3.3 1FDV background estimate

The background estimate for 1FDV SR uses the same approach as the data-driven SDV SR background estimate, described in Section 5.3.1, using the FDVs instead of SDVs. The expected background is predicted to be  $0.8 \pm 0.5$  events in the 1FDV SR. The dominant uncertainty comes from the statistical uncertainty in the number of FDVs in the CR. The uncertainty also includes the effect of the difference in the distributions of the number of pileup collisions between the photon-triggered CR and  $E_{\text{T}}^{\text{miss}}$  triggered regions.

### 5.3.4 1FDV background estimate validation

Events in the VR are required to meet the same criteria as the 1FDV SR, except that the  $N_{\text{Tracks}}^{\text{FDV}}$  requirements are relaxed from  $N_{\text{Tracks}}^{\text{FDV}} \geq 5$  to  $N_{\text{Tracks}}^{\text{FDV}} \geq 4$ , and the  $m_{\text{FDV}}$  requirements are changed from  $m_{\text{FDV}} > 10$  GeV to  $2 < m_{\text{FDV}} < 5$  GeV, which defines the nominal VR. Another set of sideband VRs is developed by loosening the conditions on  $N_{\text{Seeds}}^{\text{FDV}}$ . To validate the effects of background hadronic interactions (Section 4.4), a third VR is defined by requiring vertices to be located inside the material determined by the material map veto flags. The selection criteria for these VRs are summarized in Figure 5. For each VR, the full background estimation procedure described in Section 5.3.1 is applied, and the predicted and observed numbers of FDVs are compared. Figure 5 shows the estimated and observed event yields in the 1FDV VRs. This estimate procedure roughly predicts the observation well, but the observation is not statistically compatible with the prediction in all VRs, indicating potential non-closure effects. To account for these effects, a 22%

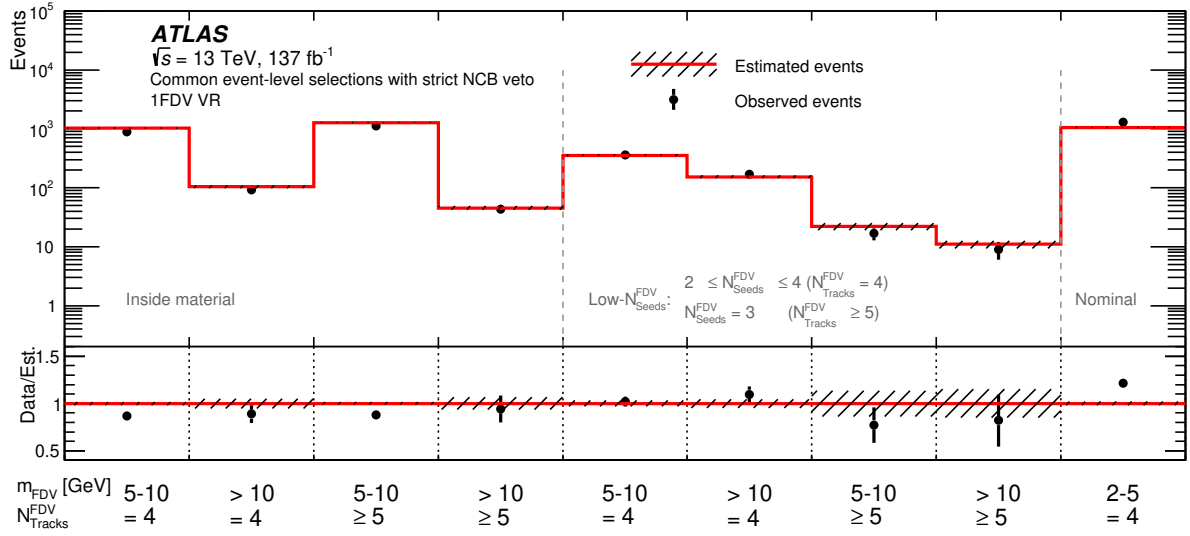


Figure 5: Estimated and observed events in the sideband VRs of the 1FDV VRs. The gray hashed band shows the background estimate uncertainties from the CR's statistics and from the distributions of the number of pileup collisions between events in the CR and the events that pass common event-level selections and the strict NCB veto. The non-closure uncertainty discussed in the text is not included here.

relative uncertainty, which corresponds to the maximum discrepancy between the estimated and observed event yields for each VR bin, is applied as a non-closure systematic uncertainty for the 1FDV background estimate. The estimated number of background events in 1FDV SR with its uncertainty is shown in Table 6.

### 5.3.5 2FDV background estimate

The background estimation strategy for the 2FDV SR follows a similar inclusive approach to the SDV and 1FDV SRs, leveraging correlations between FDVs and jet properties rather than track density. This estimate is obtained using a probability distribution over the jets in the  $E_T^{\text{miss}}$  triggered region, defined by the probability of an individual event containing a FDV near a jet. This probability is parameterized based on the jet's  $p_T$  and whether or not the jet is  $b$ -tagged. The estimates for the SDV, 1FDV, and 2FDV regions were initially all tested taking into account both the event- and jet-DV probabilities. It was found that the heavier SDV and 1FDV regions were primarily dependent on the event-DV correlations, while the less selective 2FDV region were primarily dependent on the jet-DV correlations due to differing kinematics. As the statistical uncertainty originating from having the estimate divided up into too many probability bins is larger than the contribution of the subdominant correlation, only the primary correlation is used. The individual jet probabilities, referred to as the jet-FDV probability (JFP), are calculated in the photon-triggered CR as shown in Eq. (5), where  $N_{n\text{FDVs}}^{\text{CR}}(b_{\text{tag}}, p_T)$  represents the number of instances where  $n$  FDVs are matched to jets of  $(b_{\text{tag}}, p_T)$ , and  $N_{\text{Jets}}^{\text{CR}}(b_{\text{tag}}, p_T)$  represents the total number of jets that exist with  $(b_{\text{tag}}, p_T)$ .

$$\text{JFP}_{(n)}(\text{FDV} \mid \text{jet}(b_{\text{tag}}, p_{\text{T}})) = \frac{N_{n\text{FDVs}}^{\text{CR}}(b_{\text{tag}}, p_{\text{T}})}{N_{\text{Jets}}^{\text{CR}}(b_{\text{tag}}, p_{\text{T}})} \quad (5)$$

In the CR, the JFP is determined using jets spatially matched to FDVs within  $\Delta R \leq 0.4$ . If multiple FDVs are matched to the same jet, it contributes to the estimation of  $\text{JFP}_{(\geq 2)}$ , whereas if a jet only matches a single FDV it contributes to  $\text{JFP}_{(1)}$ .

The number of background events with two or more FDVs,  $N_{\text{bkg}}^{\geq 2\text{FDV}}$  is then calculated in Eq. (6), with the number of background events with  $n$  background FDVs,  $N_{\text{bkg}}^{n\text{FDV}}$ , given by Eqs. (7) and (8) below.

$$N_{\text{bkg}}^{\geq 2\text{FDV}} = N_{\text{bkg}} - N_{\text{bkg}}^{1\text{FDV}} - N_{\text{bkg}}^{0\text{FDV}} \quad (6)$$

$$N_{\text{bkg}}^{0\text{FDV}} = \sum_{\text{events } E} \left[ \prod_{\text{jets } j \text{ in event } E} \left( 1 - \text{JFP}_{(1)} - \text{JFP}_{(\geq 2)} \right) \right] \quad (7)$$

$$N_{\text{bkg}}^{1\text{FDV}} = \sum_{\text{events } E} \left[ \prod_{\text{jets } j_E \text{ in event } E} \text{JFP}_{(1)} \left( \prod_{\text{jets } j \neq j_E \text{ in event } E} \left( 1 - \text{JFP}_{(1)} - \text{JFP}_{(\geq 2)} \right) \right) \right] \quad (8)$$

An expected background of  $1.3 \pm 0.6$  events is predicted in the 2FDV SR, with the dominant uncertainty being statistical.

### 5.3.6 2FDV background estimate validation

Events in the 2FDV VR are required to satisfy the 2FDV SR conditions, except for the relaxed requirement of  $N_{\text{Tracks}}^{\text{FDV}} = 3$  or  $2 \leq N_{\text{Seeds}}^{\text{FDV}} < N_{\text{Tracks}}^{\text{FDV}}$ , creating sideband VRs.

In addition to the  $N_{\text{Tracks}}^{\text{FDV}}$  and  $N_{\text{Seeds}}^{\text{FDV}}$  - sideband VRs, the estimate is validated using both the strict inside material and strict outside material map vetoes defined in Section 4.4. Exceptionally, the outside-material, greater-than-three-tracks, and low-seed validation regions were loosened to increase statistics by relaxing the material map veto and including the entire mass range ( $m_{\text{FDV}} > 0$  GeV). The selection criteria for these two VRs are shown in Figure 6. The  $N_{\text{bkg events}}^{\geq 2\text{FDV}}$  is calculated for each VR using the background estimation method outlined in Section 5.3.5. Figure 6 compares each VR's predicted and observed number of events with two or more FDVs. As with 1FDV, the estimated and observed number of events are roughly consistent, but the discrepancy between them could not be explained by statistical fluctuation alone, indicating potential non-closure effects. Better closure is more important for VRs that differ from the SR by only one selection criterion (the 3rd, 5th, and 7th bins in Figure 6) than those that differ by two (1st, 4th, and 6th bins) or more (2nd) selection criteria. To account for potential non-closure effects, a 20% relative uncertainty is applied as a non-closure systematic for the 2FDV background estimate.

The estimated number of background events in 2FDV SR with its uncertainty is shown in Table 6.

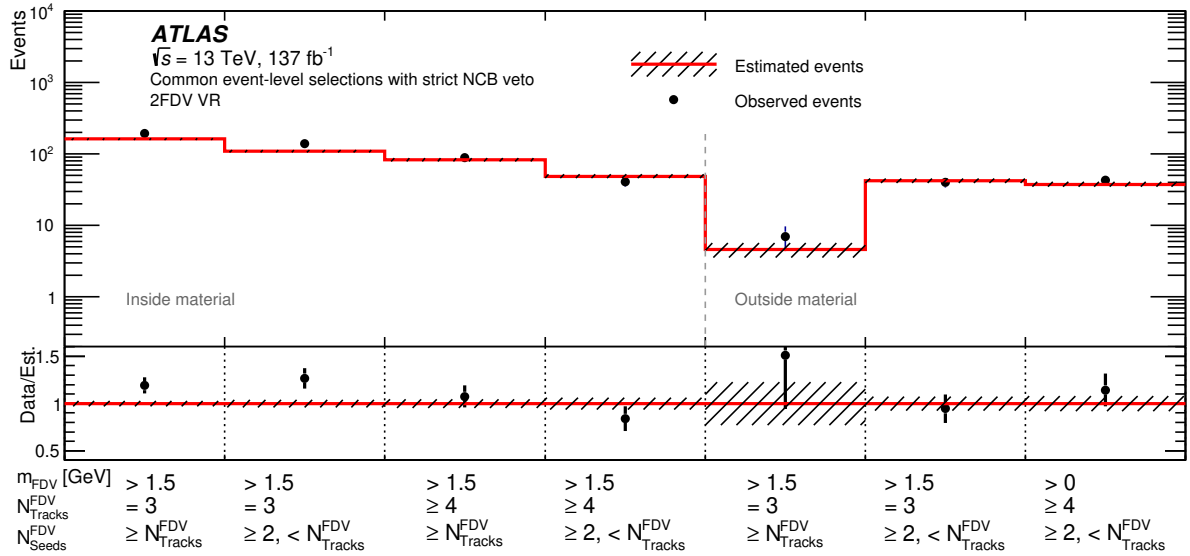


Figure 6: Estimated and observed number of events in the sideband VRs of the 2FDV SR. The gray hashed band shows the relative background estimate uncertainties from the CR’s statistics and distributions of the number of pileup collisions between events in the CR and the events that pass common event-level selections and the strict NCB veto. The non-closure uncertainty discussed in the text is not included here.

## 6 Systematic uncertainties

The uncertainties considered in this analysis can be divided into three categories. The first are uncertainties arising from the background estimation methods, which are detailed in Section 6.1. The second are uncertainties from object reconstruction in the detector, which are detailed in Section 6.2. Finally, theory uncertainties from the signal models must also be considered in the interpretation of results, which are detailed in Section 6.3.

### 6.1 Background estimate uncertainties

Multiple sources contribute to background estimate uncertainties and are evaluated for each SR. The dominant source in each region is statistical, which is propagated to the final estimate using a pseudo-experiment approach (similar to how the final fit is performed in Section 7.1). The standard deviation of the estimated background from 10,000 pseudo-experiments is then assigned as an uncertainty on the final background estimate. In the FDV regions, an additional non-closure uncertainty of 22% for the 1FDV SR and 20% for the 2FDV SR is assigned to cover discrepancies between this estimate and observed data in some of the VRs.

A further uncertainty is assigned to account for differences in the distributions of the number of pileup collisions between events in the CRs (where the event- or jet-DV probabilities are calculated) and the SRs (where the event- or jet-DV probabilities are applied). The estimated background using the pileup weighted events is taken as the central value of the background estimate, as described in Section 5.3.1. To assess this uncertainty, the estimated background is re-evaluated using unweighted events. The difference between the weighted and unweighted estimates is assigned as an uncertainty on the background estimate. Like the

Table 6: A summary of the breakdown of background estimate uncertainties per signal region.

Region	Estimated background	Uncertainties			Total uncertainty
		Statistical	Pileup	Non-closure	
SDV SR	$0.6 \pm 0.4$	$\pm 70\%$	$\pm 5\%$	–	$\pm 71\%$
1FDV SR	$0.8 \pm 0.5$	$\pm 57\%$	$\pm 2\%$	$\pm 22\%$	$\pm 61\%$
2FDV SR	$1.3 \pm 0.6$	$\pm 45\%$	$\pm 4\%$	$\pm 20\%$	$\pm 50\%$

statistical uncertainty, the pileup uncertainty is evaluated for the background estimate in each region. A maximum pileup uncertainty of 5% is assessed in the SDV SR. Each of these uncertainties is summarized in Table 6.

## 6.2 Reconstruction uncertainties

Potential sources of reconstruction uncertainty – those stemming from how physics objects are reconstructed – are the mismeasurement of offline and online  $E_T^{\text{miss}}$ , as well as track reconstruction. Their effects are estimated and propagated to the predicted MC signal yields. Offline  $E_T^{\text{miss}}$  uncertainties are estimated by rescaling the different contributions to the measured  $E_T^{\text{miss}}$  (e.g. the soft term, see Section 4.5), via their associated systematic uncertainties [82]. Sources include the jet energy scale (JES) and resolution (JER) [88] (up to 1.9%) and uncertainties in the scale and resolution of the soft term (up to 0.4%) [82]. For online  $E_T^{\text{miss}}$ , uncertainties are estimated by deriving scale factors to account for inefficiency in data not modeled in MC, in the 150 – 180 GeV range.

For estimating the uncertainties related to tracking inefficiencies, an MC-data comparison is performed using 2-track  $K_S^0$  candidate DVs. The  $K_S^0$  candidate DV yield is measured as a function of  $r_{\text{DV}}$ . This  $r_{\text{DV}}$ -dependent yield profile is then compared between data and MC simulation and interpreted as a proxy for tracking inefficiencies that are imperfectly modeled in the simulation. These are combined in quadrature with a baseline 1.8% tracking inefficiency, determined from performance studies of standard tracking. Track reconstruction uncertainties estimated via this method for SDVs are shown in Figure 7. The same process is also performed for FDVs. The obtained FDV associated tracking uncertainties are similar to those of SDV in terms of both the magnitude of the uncertainty and its year or  $r_{\text{DV}}$  dependency. This combined tracking inefficiency estimate is then used to perform a “track-killing” study, where tracks are removed from DVs (separately for SDVs and FDVs) based on the estimated inefficiencies and the signal yields recomputed. The track reconstruction uncertainty for some representative signal samples is shown in Figure 8. The uncertainty in the signal yields from the track reconstruction uncertainty is one of the dominant sources of systematic uncertainty for most samples, being particularly pronounced for those corresponding to longer LLP lifetimes, where DVs increasingly include LRT tracks, which are expected to have larger reconstruction uncertainty [68]. It contributes up to 18% in the Higgs portal model.

The signal samples considered are normalized to the recorded luminosity of the 2016-2018 dataset. The uncertainty in this recorded luminosity, discussed in Section 3, is propagated as an additional experimental systematic uncertainty on each signal.

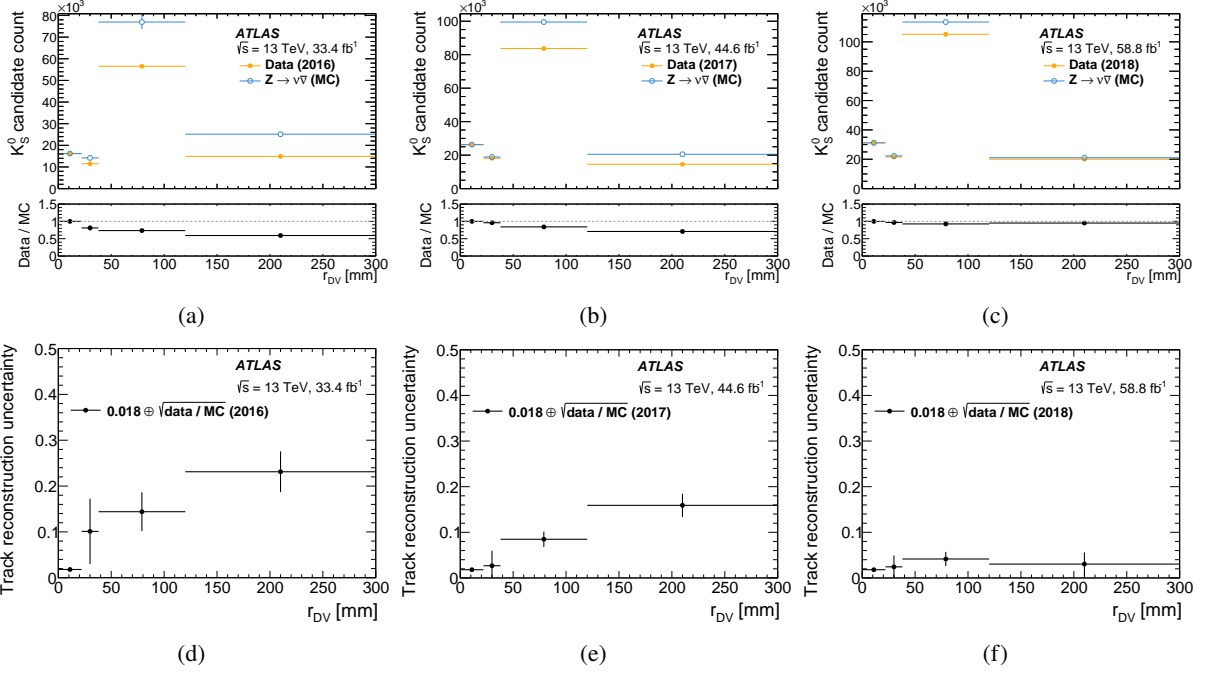


Figure 7: Example counts of 2-track  $K_S^0 \rightarrow \pi^+ \pi^-$  candidate decay SDV in MC and data and their MC/data ratios, for years (a) 2016, (b) 2017 and (c) 2018. The error bars include statistical uncertainty only. The MC counts are normalized to match the data in the innermost bin. The resulting track reconstruction uncertainties are shown in (d)–(f), where a (standard) baseline 1.8% uncertainty has been added in quadrature.

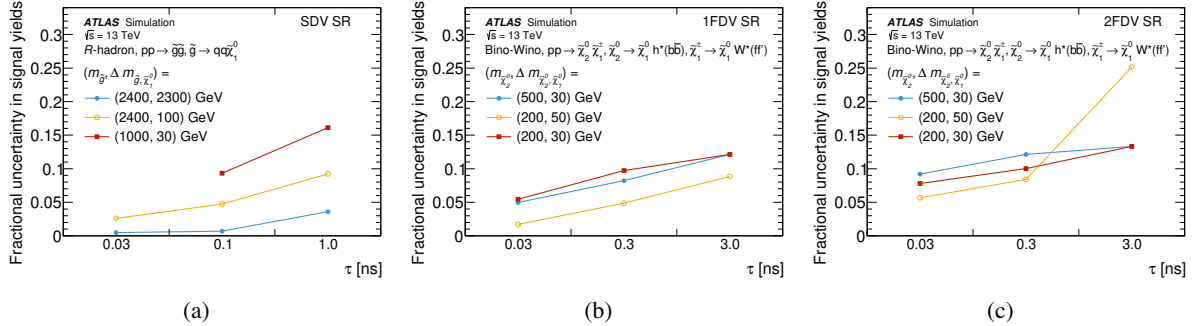


Figure 8: Example of fractional uncertainties on the signal yields from track reconstruction uncertainties, for (a) the SDV SR for the Gluino  $R$ -hadron, and (b) the 1FDV and (c) the 2FDV SRs for the Bino-Wino coannihilation model.

### 6.3 Theory uncertainties

Theory uncertainties are calculated during the generation of the MC signal samples described in Section 2 by varying the choice of renormalization and factorization scales by a factor of two; this approach generates six variations, two in which the scales are varied together and four in which the scales are varied independently. A seven-point envelope is then taken around the nominal value to evaluate an uncertainty.

The choices of parton distribution function (PDF) set and strong coupling constant  $\alpha_s$  are also varied during MC event generation. These uncertainties are then evaluated for each physics signal process and the signal yields in the relevant SRs are then recomputed for each variation. The standard deviation of those

yields is taken as the systematic uncertainty for that sample.

Theory uncertainties contribute approximately 0.6–14% depending on the signal model. For the Gluino  $R$ -hadron model, the full set of MC event-level theory uncertainties could not be evaluated for each sample, due to complexities in simulating  $R$ -hadrons. A conservative theory uncertainty calculated for a representative subset of samples is instead applied.

Table 7: Ranges of relative systematic uncertainties (16th–84th percentile, equivalent to a  $\pm 1$  standard deviation if the distributions were Gaussian) for each signal model and associated signal region.

Systematic uncertainty	Gluino $R$ -hadron (SDV SR) (%)	DFSZ axino, $ZZ$ (SDV SR) (%)	Higgs portal (2 FDV SR) (%)	Bino-Wino coannihilation (1 FDV SR) (%)
JES and JER	0.16–0.56	0.13–0.90	0.94–1.9	0.27–0.59
MET soft term	0.022–0.33	0.018–0.12	0.16–0.39	0.053–0.14
Theory	12	0.52–1.5	5.0–13	3.0–7.5
Tracking	2.1–13	0.89–7.2	6.4–18	2.3–9.6

Table 7 presents the ranges of systematic uncertainties for each signal model, grouped by signal region. The values reflect the spread of uncertainties observed across all tested parameter combinations of each signal model, using the 16th to 84th percentile interval to approximate one standard deviation while retaining asymmetric variation where present.

There are additional theory uncertainties in the production cross-sections, determined by the LHC SUSY [54, 56, 57] and Higgs working groups [58]. These uncertainties only impact the normalization of the overall yield, not the selection efficiency, and so are treated separately and not included in Table 7.

## 7 Results and interpretation

One event is observed in SDV SR and five events are observed in FDV SR. Of those five, three pass the 1FDV SR criteria and two pass the 2FDV SR criteria. A small local excess is seen over the background prediction in the 1FDV SR reported in Table 6, but in the 2FDV and SDV SRs there is good agreement between data and background.

A series of statistical tests on the observed events are then performed; the statistical model is described in Section 7.1 below, with results in Section 7.2 and 7.3.

### 7.1 Statistical model

To determine the compatibility of each signal model with the observed data, a series of profile likelihood fits [89] are performed, with a profile negative-log-likelihood ratio test statistic [90]. A  $CL_s$  frequentist approach [91] is used to set 95% confidence-level limits.

Fits are performed by comparing  $\mu S + B$  to the observed data in each signal region. The signal and background yields  $S$  and  $B$  are modelled by the product of Poissonian distributions, with the background yield in the signal region evaluated as described in Section 5. The signal strength parameter  $\mu$  is a free parameter that scales the number of predicted signal events. The discovery  $p$ -value, which gives

the consistency of the background-only hypothesis with the data, can be determined by setting  $\mu = 0$ . As the low signal region counts invalidate the asymptotic approximation [90], fits are performed using 10,000 pseudo-experiments to numerically determine the distribution of the test statistic for a given signal hypothesis. The software packages `pyhf` 0.7.6 [92, 93] and `cabinetry` 0.6.0 [94, 95] are used to carry out these steps.

The SDV and FDV signal regions are fit independently. A single-bin fit is performed for the SDV region. The two FDV regions can also be fit independently as single bins, as is done in Section 7.2 below, or combined into one two-bin fit with the 1FDV and 2FDV sub-regions treated as separate bins, as is done in Section 7.3. Systematic uncertainties on the signal or background are represented by a series of uncorrelated Gaussian nuisance parameters, although in the combined FDV fit, each signal systematic is treated as fully correlated across the two FDV bins. The definitions of all systematics can be found in Section 6 above. The background estimate systematics are consistently the dominant source of uncertainty in the fit.

Discovery  $p$ -values are calculated and quoted in Table 8. Since no significant excess was seen in any of the signal regions, limits are set on both a generic (model-independent) BSM signal and on the specific signal models introduced in Section 2. Limits are set by testing different signal hypotheses, varying the signal strength to find the value of  $\mu$  corresponding to a 95% confidence level. Separate fits were performed for each signal model in both the SDV and combined FDV regions. Although the optimization of selection criteria was guided by the signal region efficiency of each model, as summarized in Table 5, the region which provides the strictest expected limits on a given model is ultimately used to set the limits reported in Section 7.3 below.

The theory uncertainties in the production cross-sections for the different signal models are not treated as nuisance parameters. Instead, fits are performed to the signal yield scaled up or down by this uncertainty in order to set limits on a  $\pm 1\sigma$  variation of the production cross-section.

## 7.2 Model-independent limits

Model-independent constraints are first determined on the presence of excess signal above the estimated backgrounds. The methods of maximal likelihood fitting described above are used to set constraints on the *visible cross-section* of any non-SM process in any of the signal regions, provided such a signal does not contaminate any of the control regions used for background estimation. To avoid assumptions about how a generic signal would be correlated between the 1FDV and 2FDV regions, separate 1FDV and 2FDV fits are performed. As these fits are performed with a signal, there are no signal systematic uncertainties; the only nuisance parameters included in these fits are for the systematic uncertainties in the background estimates.

The product of the signal strength and 1 fb test signal,  $\mu S$ , is interpreted as the visible cross-section  $\langle A\epsilon\sigma \rangle$ , which is the product of acceptance, detection efficiency and process cross-section. Table 8 provides the model-independent limits for the SDV and FDV signal regions.  $S_{\text{obs}}^{95}$  and  $S_{\text{exp}}^{95}$  are the 95% CL upper limits on the observed and expected number of signal events under the background-only hypothesis. The observed limit was found to be within  $1\sigma$  of the expected limit for the SDV signal region, and within  $2\sigma$  for the FDV signal regions.

Table 8: Model-independent limits for the SDV and combined FDV signal regions. The observed number of events, compared to expected background, is also shown for comparison.  $\langle A\epsilon\sigma \rangle_{\text{obs}}^{95}$  is the 95 CL upper limit on the visible cross-section,  $S_{\text{obs}}^{95}$  and  $S_{\text{exp}}^{95}$  is the 95% CL upper limits on the observed and expected number of signal events (the latter given the expected number of background events),  $p(s=0)$  is the discovery  $p$ -value and  $Z$  is the corresponding Gaussian significance.

Region	Observed (Expected)	$\langle A\epsilon\sigma \rangle_{\text{obs}}^{95}$ [fb]	$S_{\text{obs}}^{95}$	$S_{\text{exp}}^{95}$	$p(s=0)$	$Z$
SDV SR	1 ( $0.6 \pm 0.4$ )	0.0280	3.84	$3.20^{+1.17}_{-0.05}$	0.32	0.46
1FDV SR	3 ( $0.8 \pm 0.5$ )	0.0469	6.42	$3.62^{+1.53}_{-0.18}$	0.06	1.59
2FDV SR	2 ( $1.3 \pm 0.6$ )	0.0353	4.83	$3.98^{+1.59}_{-0.63}$	0.31	0.50

### 7.3 Interpretations

The methods described above are also used to set model-dependent limits on each of the four signal models in either the SDV or the combined FDV region.

The strongest limits on the Gluino  $R$ -hadron come from the SDV signal region, as expected given the absence of  $b$ -jets in the final state. The observed and expected limits are shown in Figure 9 as a function of both mass and lifetime, showing that the gluino mass is constrained to be greater than approximately 1.8–2.5 TeV for a wide range of neutralino masses and gluino lifetimes. These results extend constraints across a lifetime range of 0.01–0.1 ns by more than 200 GeV in  $m_{\tilde{g}}$  compared to the 2016-only result from ATLAS [5].

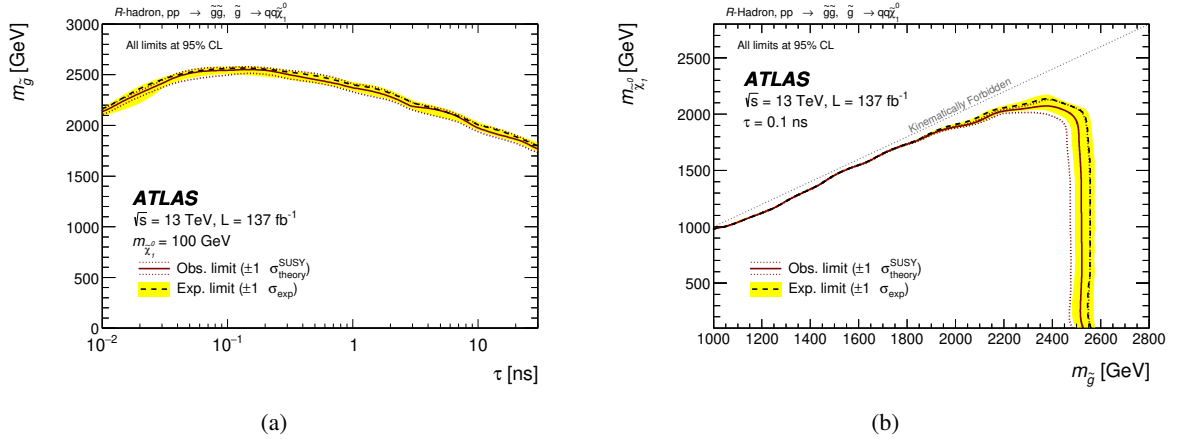


Figure 9: Observed and expected 95% confidence-level upper limits on the  $R$ -hadron model as a function of (a) the gluino lifetime and  $R$ -hadron mass with the lightest neutralino mass  $m_{\tilde{\chi}_1^0} = 100$  GeV, and (b) the gluino and neutralino masses for a gluino lifetime  $\tau = 0.1$  ns. The area below the contour is excluded.

The Bino-Wino coannihilation model described in Section 2.2 performs best in the FDV signal region, as expected due to the  $b$ -jets in the final state. Figure 10 shows the observed and expected limits, which constrain the lightest neutralino masses to be greater than approximately 350–650 GeV for a wide range of lifetimes and mass splittings. The observed limit is lower than the expected limit because of the small excess in 1FDV SR. The largest observed  $p$ -value under the Bino-Wino coannihilation model is obtained as 0.52 when  $m_{\tilde{\chi}_2^0} = 700$  GeV,  $\Delta m_{\tilde{\chi}_2^0, \tilde{\chi}_1^0} = 40$  GeV, and  $\tau = 0.3$  ns.

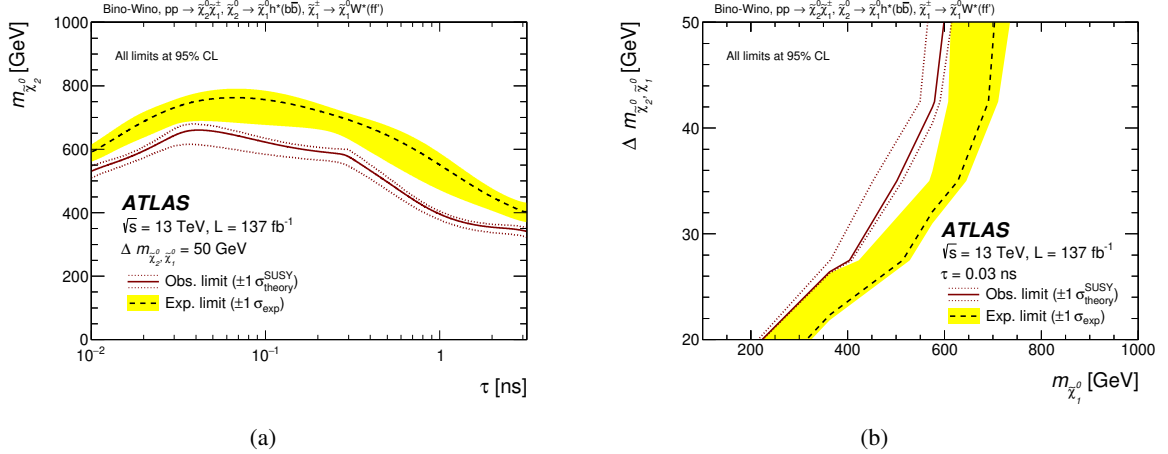


Figure 10: 95% confidence level observed and expected upper limits on the masses and lifetimes of the Bino-Wino coannihilation model, with exclusion contours as described in Figure 9. The exclusion as a function (a) of  $\tilde{\chi}_2^0$  lifetime and mass with a mass splitting between  $\tilde{\chi}_2^0$  and  $\tilde{\chi}_1^0$   $\Delta m_{\tilde{\chi}_2^0, \tilde{\chi}_1^0} = 50$  GeV and (b) of mass splitting and  $\tilde{\chi}_1^0$  mass with a lifetime  $\tau = 0.03$  ns. The weaker constraint on the observed limit compared to the expected limit is due to a small excess in FDV SR. The area below the contour is excluded for the left plot, and the area to the left of the contour is excluded for the right plot.

In the DFSZ axino model described in Section 2.3, the final state can include either four displaced  $b$ -jets (in the case of a Higgs boson final state) or four displaced light-quark jets (in the case of a  $Z$  boson final state). In principle, the presence of  $b$ -jets in the final state should lead to stronger sensitivity in the FDV SR for the Higgs boson scenario, while the SDV SR should perform better for the  $Z$  boson final state. However, stronger expected limits were seen for both final states in the SDV SR than in the FDV SR<sup>2</sup>, with the  $Z$  boson final state providing more stringent constraints as expected. As shown in Figure 11, the observed cross-section limits for the  $Z$  boson final state are 2–3 times better than those for the Higgs boson final state, consistent with the better performance of the SDV algorithm in reconstructing the light-quark jets from  $Z$  decays. The constraints exclude significant portions of the studied parameter space at 95% confidence level for both production mechanisms, particularly for axion masses ( $m_a$ ) between 100 and 2500  $\mu\text{eV}$  when the neutralino mass is fixed at 800 GeV (a), and for neutralino masses ( $m_{\tilde{\chi}_1^0}$ ) below approximately 400 GeV when the axion mass parameters are held constant (b). This is the first time limits have been set explicitly on this model; while a past search has probed a similar DFSZ axino scenario [96], it was previously assumed that the axino would be promptly produced and did not directly constrain  $f_a$ .

The Higgs portal model introduced in Section 2.4 is best constrained in the FDV SR. Observed and expected limits are set on the branching ratio of  $h \rightarrow SS \rightarrow 4b$  and shown in Figure 12. These exclusions are compared to a target 12% branching ratio, above which exotic undetected Higgs boson decays have been excluded [97]. For pseudoscalar masses  $m_S = 25$  GeV and above, this analysis excludes a significant region of phase space below this target, down to a branching ratio of 2.6–12.9% for pseudoscalar lifetimes  $\tau_S \leq 0.03$  ns. Complementary searches for LLPs place stronger constraints on the Higgs portal model for lifetimes of 0.03 and 0.3 ns [8, 98–100].

<sup>2</sup> The FDV SR is optimized for the Bino-Wino coannihilation case, and differs in kinematics and range of parameters DFSZ axino Higgs channel in several ways. For all axino models studied, the Higgs boson is required to be produced on-shell, while for the Bino-Wino coannihilation models the Higgs boson is instead produced off-shell. This explains why this SR does not display an optimal sensitivity for the axino Higgs channel.

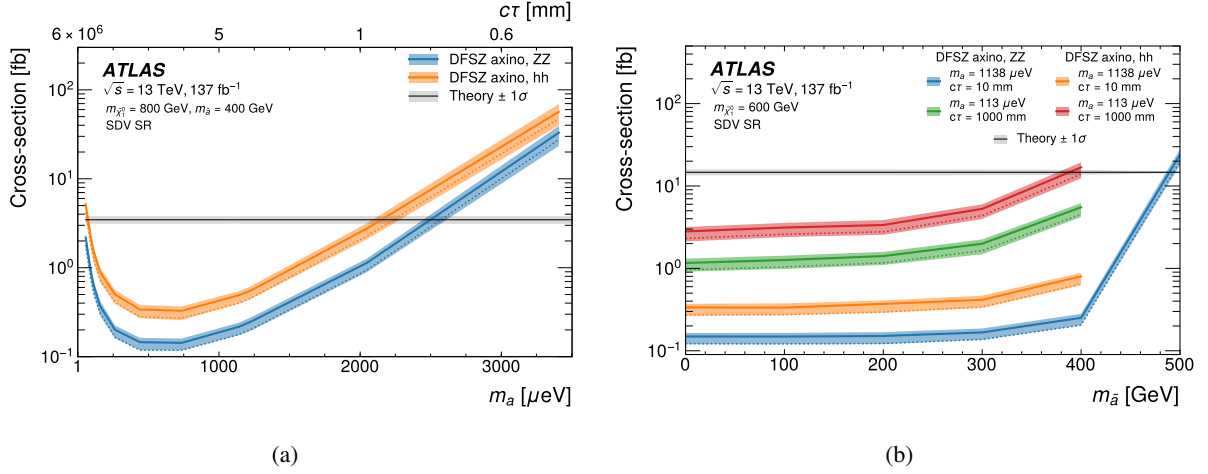


Figure 11: Expected and observed limits at 95% confidence level on the cross-section of the DFSZ axino model as a function of axino and axino mass, in which either (a) the axino mass  $m_{\tilde{a}}$  is held constant or (b) the neutralino mass  $m_{\tilde{\chi}_1^0}$  is held constant. Limits are drawn separately for two choices of the axion mass parameter  $m_a$ , which correspond to a range of  $\tilde{\chi}_1^0$  lifetimes as discussed in Section 2.3. The theoretical Higgsino pair production cross-section used is included for reference [56, 57]. Cross-sections above the contours are excluded.

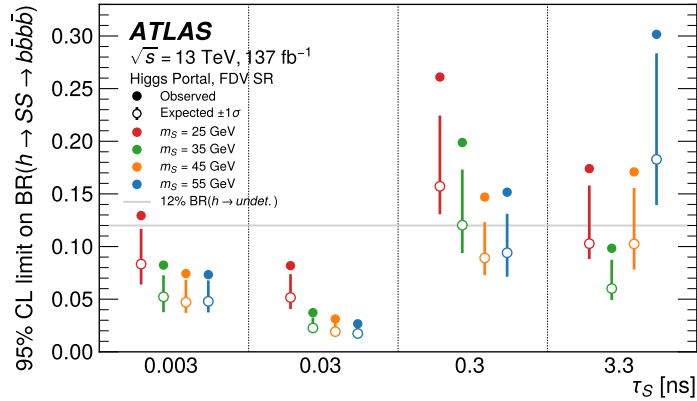


Figure 12: Expected and observed limits on the branching ratio of  $h \rightarrow SS \rightarrow 4b$  in the Higgs portal model at 95% confidence level, shown as a function of the lifetime  $\tau$  of the new heavy pseudoscalar  $S$ . Limits are evaluated for several values of the pseudoscalar mass  $m_S$ , and compared to a 12% branching ratio for the Higgs boson decaying into BSM final states [97]. Each color indicates a specific value of  $m_S$ . The weaker constraint on the observed limit compared to the expected limit is due to a small excess in FDV SR.

The shape of the exclusion contours in Figures 9–12 reflects the interplay between displaced vertex reconstruction efficiency and LLP decay kinematics. Sensitivity peaks at intermediate DV mass and lifetime, where decays are typically well-contained within the tracking volume and produce vertices that pass all selection and cleaning requirements. At low DV mass, signal vertices are more likely to mimic common background topologies and are frequently removed by the cleaning cuts. At large lifetimes, LLPs increasingly decay outside the detector volume, reducing the probability of reconstructing a displaced vertex. In models predicting two displaced decays per event, some sensitivity is retained even at long lifetimes when one LLP decays within the tracker and the other escapes, contributing to the event's  $E_T^{\text{miss}}$ .

However, such events still require at least one well-reconstructed displaced vertex to satisfy the analysis selection, and the overall efficiency drops sharply in this regime.

## 8 Conclusion

The results of a multi-faceted search for BSM physics processes characterized by displaced vertices and missing transverse momentum using  $137 \text{ fb}^{-1}$  of proton–proton collision data delivered by the LHC and collected by the ATLAS detector at  $\sqrt{s} = 13 \text{ TeV}$  are presented. This analysis employed both inclusive event selection criteria and dedicated displaced vertex reconstruction algorithms to maximize sensitivity across a broad range of theoretical models predicting long-lived particle signatures.

No statistically significant excess above the SM background expectation was observed, thus allowing constraints to be placed on the four primary BSM signal models considered: long-lived gluinos which hadronize into  $R$ -hadrons before decaying, neutralinos decaying via Higgs-mediated channels, long-lived Higgsinos decaying to axinos, and an exotic Higgs portal model predicting displaced decays of light pseudoscalars.

In the Gluino  $R$ -hadron model, constraints reached gluino masses of 1.8–2.5 TeV for a range of neutralino masses and gluino lifetimes, improving previous gluino mass results by more than 200 GeV. In the Bino-Wino coannihilation model, the lightest neutralino masses are constrained to be greater than approximately 350–650 GeV for a range of lifetimes and mass splittings. In the DFSZ axino model the analysis constrains axion masses between 100 and 2500  $\mu\text{eV}$  when the neutralino mass is fixed at 800 GeV, and for neutralino masses below 400 GeV for fixed axion mass parameters. Finally, the excluded Higgs branching ratio in the Higgs portal model reaches 2.6% for a pseudoscalar with a mass of 55 GeV and lifetime of 0.03 ns.

## Acknowledgements

We thank CERN for the very successful operation of the LHC and its injectors, as well as the support staff at CERN and at our institutions worldwide without whom ATLAS could not be operated efficiently.

The crucial computing support from all WLCG partners is acknowledged gratefully, in particular from CERN, the ATLAS Tier-1 facilities at TRIUMF/SFU (Canada), NDGF (Denmark, Norway, Sweden), CC-IN2P3 (France), KIT/GridKA (Germany), INFN-CNAF (Italy), NL-T1 (Netherlands), PIC (Spain), RAL (UK) and BNL (USA), the Tier-2 facilities worldwide and large non-WLCG resource providers. Major contributors of computing resources are listed in Ref. [101].

We gratefully acknowledge the support of ANPCyT, Argentina; YerPhI, Armenia; ARC, Australia; BMWFW and FWF, Austria; ANAS, Azerbaijan; CNPq and FAPESP, Brazil; NSERC, NRC and CFI, Canada; CERN; ANID, Chile; CAS, MOST and NSFC, China; Minciencias, Colombia; MEYS CR, Czech Republic; DNRF and DNSRC, Denmark; IN2P3-CNRS and CEA-DRF/IRFU, France; SRNSFG, Georgia; BMFTR, HGF and MPG, Germany; GSRI, Greece; RGC and Hong Kong SAR, China; ICHEP and Academy of Sciences and Humanities, Israel; INFN, Italy; MEXT and JSPS, Japan; CNRST, Morocco; NWO, Netherlands; RCN, Norway; MNiSW, Poland; FCT, Portugal; MNE/IFA, Romania; MSTDI, Serbia; MSSR, Slovakia; ARIS and MVZI, Slovenia; DSI/NRF, South Africa; MICIU/AEI, Spain; SRC and Wallenberg Foundation, Sweden; SERI, SNSF and Cantons of Bern and Geneva, Switzerland; NSTC, Taipei; TENMAK, Türkiye; STFC/UKRI, United Kingdom; DOE and NSF, United States of America.

Individual groups and members have received support from BCKDF, CANARIE, CRC and DRAC, Canada; CERN-CZ, FORTE and PRIMUS, Czech Republic; COST, ERC, ERDF, Horizon 2020 and Marie Skłodowska-Curie Actions, European Union; Investissements d’Avenir Labex, Investissements d’Avenir IDEX and ANR, France; DFG and AvH Foundation, Germany; Herakleitos, Thales and Aristeia programmes co-financed by EU-ESF and the Greek NSRF, Greece; BSF-NSF and MINERVA, Israel; NCN and NAWA, Poland; La Caixa Banking Foundation, CERCA and AGAUR programs from Generalitat de Catalunya and PROMETEO and GenT Programmes Generalitat Valenciana, Spain; Göran Gustafssons Stiftelse, Sweden; The Royal Society and Leverhulme Trust, United Kingdom; Eric and Wendy Schmidt Fund for Strategic Innovation, United States of America.

In addition, individual members wish to acknowledge support from Chile: Agencia Nacional de Investigación y Desarrollo (ANID FONDECYT reg. 1230987, FONDECYT 1230812, FONDECYT 1240864, Fondecyt 3240661, Fondecyt Regular 1240721); China: Chinese Ministry of Science and Technology (MOST-2023YFA1605700, MOST-2023YFA1609300), National Natural Science Foundation of China (NSFC 12275265, NSFC-W2543005); Czech Republic: Czech Science Foundation (GACR - 24-11373S), Ministry of Education Youth and Sports (ERC-CZ-LL2327, FORTE CZ.02.01.01/00/22\_008/0004632), PRIMUS Research Programme (PRIMUS/21/SCI/017); EU: H2020 European Research Council (ERC - 101002463); European Union: European Research Council (BARD No. 101116429, ERC - 948254, ERC 101089007), European Regional Development Fund (HE COFUND GA No.101081355, ERDF), Marie Skłodowska-Curie Actions (GAP-101168829); France: Agence Nationale de la Recherche (ANR-21-CE31-0013, ANR-22-EDIR-0002, ANR-24-CE31-0504-01); Germany: Deutsche Forschungsgemeinschaft (DFG - 469666862); China: Research Grants Council (GRF); Italy: Ministero dell’Università e della Ricerca (NextGenEU 153D23001490006 M4C2.1.1, NextGenEU I53D23000820006 M4C2.1.1, NextGenEU I53D23001490006 M4C2.1.1, SOE2024\_0000023); Japan: Japan Society for the Promotion of Science (JSPS KAKENHI JP25H0063, JSPS KAKENHI JP22H01227, JSPS KAKENHI JP22H04944, JSPS KAKENHI JP22KK0227, JSPS KAKENHI JP24K23939, JSPS KAKENHI JP24KK0251, JSPS KAKENHI JP25H00650, JSPS KAKENHI JP25H01291, JSPS KAKENHI JP25K01023); Norway: Research Council of Norway (RCN-314472); Poland: Polish National Science Centre (NCN 2021/42/E/ST2/00350, NCN OPUS 2023/51/B/ST2/02507, NCN OPUS nr 2022/47/B/ST2/03059, NCN UMO-2019/34/E/ST2/00393, UMO-2022/47/O/ST2/00148, UMO-2023/49/B/ST2/04085, UMO-2023/51/B/ST2/00920, UMO-2024/53/N/ST2/00869); Spain: Agència de Gestió d’Ajuts Universitaris i de Recerca. (AGAUR - 2023 BP 00141), Ministry of Science and Innovation (RYC2019-028510-I, RYC2020-030254-I, RYC2021-031273-I, RYC2022-038164-I), Ministerio de Ciencia, Innovación y Universidades/Agencia Estatal de Investigación (PID2022-142604OB-C22); Sweden: Carl Trygger Foundation (Carl Trygger Foundation CTS 22:2312), Swedish Research Council (Swedish Research Council 2023-04654, VR 2021-03651, VR 2022-03845, VR 2022-04683, VR 2023-03403, VR 2024-05451, VR 2025-05940), Knut and Alice Wallenberg Foundation (KAW 2023.0366); Switzerland: Swiss National Science Foundation (SNSF - PCEFP2\_194658); United Kingdom: The Binks Trust, Royal Society (NIF-R1-231091); United States of America: U.S. Department of Energy (ECA DE-AC02-76SF00515), John Templeton Foundation (John Templeton Foundation 63206), Neubauer Family Foundation.

## References

- [1] S. Knapen and S. Lowette, *A Guide to Hunting Long-Lived Particles at the LHC*, *Ann. Rev. Nucl. Part. Sci.* **73** (2023) 421, arXiv: [2212.03883](https://arxiv.org/abs/2212.03883) [hep-ph].
- [2] L. Evans and P. Bryant, *LHC Machine*, *JINST* **3** (2008) S08001.

- [3] ATLAS Collaboration, *The ATLAS Experiment at the CERN Large Hadron Collider*, [JINST \*\*3\*\* \(2008\) S08003](#).
- [4] ATLAS Collaboration, *Luminosity determination in  $pp$  collisions at  $\sqrt{s} = 13$  TeV using the ATLAS detector at the LHC*, [Eur. Phys. J. C \*\*83\*\* \(2023\) 982](#), arXiv: [2212.09379 \[hep-ex\]](#).
- [5] ATLAS Collaboration, *Search for long-lived, massive particles in events with displaced vertices and missing transverse momentum in  $\sqrt{s} = 13$  TeV  $pp$  collisions with the ATLAS detector*, [Phys. Rev. D \*\*97\*\* \(2018\) 052012](#), arXiv: [1710.04901 \[hep-ex\]](#).
- [6] ATLAS Collaboration, *Search for long-lived, massive particles in events with displaced vertices and multiple jets in  $pp$  collisions at  $\sqrt{s} = 13$  TeV with the ATLAS detector*, [JHEP \*\*06\*\* \(2023\) 200](#), arXiv: [2301.13866 \[hep-ex\]](#).
- [7] ATLAS Collaboration, *Search for long-lived, massive particles in events with a displaced vertex and a muon with large impact parameter in  $pp$  collisions at  $\sqrt{s} = 13$  TeV with the ATLAS detector*, [Phys. Rev. D \*\*102\*\* \(2020\) 032006](#), arXiv: [2003.11956 \[hep-ex\]](#).
- [8] ATLAS Collaboration, *Search for events with one displaced vertex from long-lived neutral particles decaying into hadronic jets in the ATLAS muon spectrometer in  $pp$  collisions at  $\sqrt{s} = 13$  TeV*, [Phys. Rev. D \*\*112\*\* \(2025\) 092001](#), arXiv: [2503.20445 \[hep-ex\]](#).
- [9] CMS Collaboration, *Search for  $R$ -parity violating supersymmetry with displaced vertices in proton–proton collisions at  $\sqrt{s} = 8$  TeV*, [Phys. Rev. D \*\*95\*\* \(2017\) 012009](#), arXiv: [1610.05133 \[hep-ex\]](#).
- [10] CMS Collaboration, *Search for new long-lived particles at  $\sqrt{s} = 13$  TeV*, [Phys. Lett. B \*\*780\*\* \(2018\) 432](#), arXiv: [1711.09120 \[hep-ex\]](#).
- [11] CMS Collaboration, *Search for long-lived particles with displaced vertices in multijet events in proton–proton collisions at  $\sqrt{s} = 13$  TeV*, [Phys. Rev. D \*\*98\*\* \(2018\) 092011](#), arXiv: [1808.03078 \[hep-ex\]](#).
- [12] CMS Collaboration, *Search for long-lived particles decaying into displaced jets in proton–proton collisions at  $\sqrt{s} = 13$  TeV*, [Phys. Rev. D \*\*99\*\* \(2019\) 032011](#), arXiv: [1811.07991 \[hep-ex\]](#).
- [13] CMS Collaboration, *Search for long-lived particles decaying to jets with displaced vertices in proton–proton collisions at  $\sqrt{s} = 13$  TeV*, [Phys. Rev. D \*\*104\*\* \(2021\) 052011](#), arXiv: [2104.13474 \[hep-ex\]](#).
- [14] CMS Collaboration, *Search for long-lived particles using displaced jets in proton–proton collisions at  $\sqrt{s} = 13$  TeV*, [Phys. Rev. D \*\*104\*\* \(2021\) 012015](#), arXiv: [2012.01581 \[hep-ex\]](#).
- [15] CMS Collaboration, *Search for long-lived heavy neutral leptons with displaced vertices in proton–proton collisions at  $\sqrt{s} = 13$  TeV*, [JHEP \*\*07\*\* \(2022\) 081](#), arXiv: [2201.05578 \[hep-ex\]](#).
- [16] CMS Collaboration, *Search for long-lived particles using displaced vertices and missing transverse momentum in proton–proton collisions at  $\sqrt{s} = 13$  TeV*, [Phys. Rev. D \*\*109\*\* \(2024\) 112005](#), arXiv: [2402.15804 \[hep-ex\]](#).
- [17] R. Aaij et al., *Updated search for long-lived particles decaying to jet pairs*, [Eur. Phys. J. C \*\*77\*\* \(2017\) 812](#), arXiv: [1705.07332 \[hep-ex\]](#).

- [18] R. Aaij et al., *Search for long-lived particles decaying to  $e^\pm \mu^\mp \nu$* , *Eur. Phys. J. C* **81** (2021) 261, arXiv: [2012.02696 \[hep-ex\]](#).
- [19] R. Aaij et al., *Search for massive long-lived particles decaying semileptonically at  $\sqrt{s} = 13$  TeV*, *Eur. Phys. J. C* **82** (2022) 373, arXiv: [2110.07293 \[hep-ex\]](#).
- [20] N. Sakai, *Naturalness in supersymmetric GUTS*, *Z. Phys. C* **11** (1981) 153.
- [21] S. Dimopoulos, S. Raby and F. Wilczek, *Supersymmetry and the scale of unification*, *Phys. Rev. D* **24** (1981) 1681.
- [22] Yu. A. Gol'fand and E. P. Likhtman, *Extension of the Algebra of Poincare Group Generators and Violation of P Invariance*, *JETP Lett.* **13** (1971) 20, [*Pisma Zh. Eksp. Teor. Fiz.* **13** (1971) 452].
- [23] D. V. Volkov and V. P. Akulov, *Is the neutrino a goldstone particle?*, *Phys. Lett. B* **46** (1973) 109.
- [24] J. Wess and B. Zumino, *Supergauge transformations in four dimensions*, *Nucl. Phys. B* **70** (1974) 39.
- [25] J. Wess and B. Zumino, *Supergauge invariant extension of quantum electrodynamics*, *Nucl. Phys. B* **78** (1974) 1.
- [26] S. Ferrara and B. Zumino, *Supergauge invariant Yang-Mills theories*, *Nucl. Phys. B* **79** (1974) 413.
- [27] A. Salam and J. Strathdee, *Super-symmetry and non-Abelian gauges*, *Phys. Lett. B* **51** (1974) 353.
- [28] G. R. Farrar and P. Fayet, *Phenomenology of the production, decay, and detection of new hadronic states associated with supersymmetry*, *Phys. Lett. B* **76** (1978) 575.
- [29] H. Goldberg, *Constraint on the Photino Mass from Cosmology*, *Phys. Rev. Lett.* **50** (1983) 1419, Erratum: *Phys. Rev. Lett.* **103** (2009) 099905.
- [30] J. Ellis, J. Hagelin, D. V. Nanopoulos, K. A. Olive and M. Srednicki, *Supersymmetric relics from the big bang*, *Nucl. Phys. B* **238** (1984) 453.
- [31] G. Hoshino et al., *Bridging the divide: axion searches and axino phenomenology at colliders*, (2025), arXiv: [2511.07224 \[hep-ph\]](#).
- [32] G. Giudice and A. Romanino, *Split supersymmetry*, *Nucl. Phys. B* **699** (2004) 65, arXiv: [hep-ph/0406088](#), Erratum: *Nucl. Phys. B* **706** (2005) 487.
- [33] N. Nagata, H. Otono and S. Shirai, *Probing Bino-Wino Coannihilation at the LHC*, *JHEP* **10** (2015) 086, arXiv: [1506.08206 \[hep-ph\]](#).
- [34] K. Rolbiecki and K. Sakurai, *Long-lived bino and wino in supersymmetry with heavy scalars and higgsinos*, *JHEP* **11** (2015) 091, arXiv: [1506.08799 \[hep-ph\]](#).
- [35] G. Arcadi, A. Djouadi and M. Raidal, *Dark Matter through the Higgs portal*, *Phys. Rept.* **842** (2020) 1, arXiv: [1903.03616 \[hep-ph\]](#).
- [36] N. Arkani-Hamed and S. Dimopoulos, *Supersymmetric unification without low energy supersymmetry and signatures for fine-tuning at the LHC*, *JHEP* **06** (2005) 073, arXiv: [hep-th/0405159](#).
- [37] A. Djouadi et al., *The Minimal Supersymmetric Standard Model: Group Summary Report*, 1998, arXiv: [hep-ph/9901246](#).
- [38] A. R. Zhitnitsky, *On Possible Suppression of the Axion Hadron Interactions*, *Sov. J. Nucl. Phys.* **31** (1980) 260.

- [39] M. Dine, W. Fischler and M. Srednicki, *A Simple Solution to the Strong CP Problem with a Harmless Axion*, *Phys. Lett. B* **104** (1981) 199.
- [40] J. Alwall et al., *The automated computation of tree-level and next-to-leading order differential cross sections, and their matching to parton shower simulations*, *JHEP* **07** (2014) 079, arXiv: [1405.0301 \[hep-ph\]](#).
- [41] P. Nason, *A new method for combining NLO QCD with shower Monte Carlo algorithms*, *JHEP* **11** (2004) 040, arXiv: [hep-ph/0409146](#).
- [42] S. Frixione, P. Nason and C. Oleari, *Matching NLO QCD computations with parton shower simulations: the POWHEG method*, *JHEP* **11** (2007) 070, arXiv: [0709.2092 \[hep-ph\]](#).
- [43] P. Artoisenet, R. Frederix, O. Mattelaer and R. Rietkerk, *Automatic spin-entangled decays of heavy resonances in Monte Carlo simulations*, *JHEP* **03** (2013) 015, arXiv: [1212.3460 \[hep-ph\]](#).
- [44] S. Frixione, E. Laenen, P. Motylinski and B. R. Webber, *Angular correlations of lepton pairs from vector boson and top quark decays in Monte Carlo simulations*, *JHEP* **04** (2007) 081, arXiv: [hep-ph/0702198](#).
- [45] T. Sjöstrand et al., *An introduction to PYTHIA 8.2*, *Comput. Phys. Commun.* **191** (2015) 159, arXiv: [1410.3012 \[hep-ph\]](#).
- [46] D. J. Lange, *The EvtGen particle decay simulation package*, *Nucl. Instrum. Meth. A* **462** (2001) 152.
- [47] T. Gleisberg et al., *Event generation with SHERPA 1.1*, *JHEP* **02** (2009) 007, arXiv: [0811.4622 \[hep-ph\]](#).
- [48] E. Bothmann et al., *Event generation with Sherpa 2.2*, *SciPost Phys.* **7** (2019) 034, arXiv: [1905.09127 \[hep-ph\]](#).
- [49] S. Agostinelli et al., *GEANT4 – a simulation toolkit*, *Nucl. Instrum. Meth. A* **506** (2003) 250.
- [50] ATLAS Collaboration, *Generation and Simulation of R-Hadrons in the ATLAS Experiment*, ATL-PHYS-PUB-2019-019, 2019, URL: <https://cds.cern.ch/record/2676309>.
- [51] ATLAS Collaboration, *Emulating the impact of additional proton–proton interactions in the ATLAS simulation by presampling sets of inelastic Monte Carlo events*, *Comput. Softw. Big Sci.* **6** (2022) 3, arXiv: [2102.09495 \[hep-ex\]](#).
- [52] ATLAS Collaboration, *ATLAS Pythia 8 tunes to 7 TeV data*, ATL-PHYS-PUB-2014-021, 2014, URL: <https://cds.cern.ch/record/1966419>.
- [53] NNPDF Collaboration, R. D. Ball et al., *Parton distributions with LHC data*, *Nucl. Phys. B* **867** (2013) 244, arXiv: [1207.1303 \[hep-ph\]](#).
- [54] W. Beenakker et al., *NNLL resummation for squark and gluino production at the LHC*, *JHEP* **12** (2014) 023, arXiv: [1404.3134 \[hep-ph\]](#).
- [55] J. Butterworth et al., *PDF4LHC recommendations for LHC Run II*, *J. Phys. G* **43** (2016) 023001, arXiv: [1510.03865 \[hep-ph\]](#).
- [56] B. Fuks, M. Klasen, D. R. Lamprea and M. Rothering, *Gaugino production in proton-proton collisions at a center-of-mass energy of 8 TeV*, *JHEP* **10** (2012) 081, arXiv: [1207.2159 \[hep-ph\]](#).

- [57] B. Fuks, M. Klasen, D. R. Lamprea and M. Rothering, *Precision predictions for electroweak superpartner production at hadron colliders with RESUMMINO*, *Eur. Phys. J. C* **73** (2013) 2480, arXiv: [1304.0790 \[hep-ph\]](#).
- [58] D. de Florian et al., *Handbook of LHC Higgs Cross Sections: 4. Deciphering the Nature of the Higgs Sector*, (2017), arXiv: [1610.07922 \[hep-ph\]](#).
- [59] C. Bierlich et al., *A comprehensive guide to the physics and usage of PYTHIA 8.3*, *SciPost Phys. Codebases* (2022) 8, arXiv: [2203.11601 \[hep-ph\]](#).
- [60] G. Avoni et al., *The new LUCID-2 detector for luminosity measurement and monitoring in ATLAS*, *JINST* **13** (2018) P07017.
- [61] ATLAS Collaboration, *Performance of the ATLAS trigger system in 2015*, *Eur. Phys. J. C* **77** (2017) 317, arXiv: [1611.09661 \[hep-ex\]](#).
- [62] ATLAS Collaboration, *Software and computing for Run 3 of the ATLAS experiment at the LHC*, *Eur. Phys. J. C* **85** (2025) 234, arXiv: [2404.06335 \[hep-ex\]](#),  
Erratum: *Eur. Phys. J. C* **85** (2025) 907.
- [63] ATLAS Collaboration, *ATLAS data quality operations and performance for 2015–2018 data-taking*, *JINST* **15** (2020) P04003, arXiv: [1911.04632 \[physics.ins-det\]](#).
- [64] ATLAS Collaboration, *Operation of the ATLAS trigger system in Run 2*, *JINST* **15** (2020) P10004, arXiv: [2007.12539 \[physics.ins-det\]](#).
- [65] ATLAS Collaboration, *Performance of electron and photon triggers in ATLAS during LHC Run 2*, *Eur. Phys. J. C* **80** (2020) 47, arXiv: [1909.00761 \[hep-ex\]](#).
- [66] ATLAS Collaboration, *Configuration and performance of the ATLAS b-jet triggers in Run 2*, *Eur. Phys. J. C* **81** (2021) 1087, arXiv: [2106.03584 \[hep-ex\]](#).
- [67] ATLAS Collaboration, *Performance of the ATLAS track reconstruction algorithms in dense environments in LHC Run 2*, *Eur. Phys. J. C* **77** (2017) 673, arXiv: [1704.07983 \[hep-ex\]](#).
- [68] ATLAS Collaboration, *Performance of the reconstruction of large impact parameter tracks in the inner detector of ATLAS*, ATL-PHYS-PUB-2017-014, 2017, URL: <https://cds.cern.ch/record/2275635>.
- [69] ATLAS Collaboration, *Vertex Reconstruction Performance of the ATLAS Detector at  $\sqrt{s} = 13$  TeV*, ATL-PHYS-PUB-2015-026, 2015, URL: <https://cds.cern.ch/record/2037717>.
- [70] ATLAS Collaboration, *Performance of vertex reconstruction algorithms for detection of new long-lived particle decays within the ATLAS inner detector*, ATL-PHYS-PUB-2019-013, 2019, URL: <https://cds.cern.ch/record/2669425>.
- [71] V. Kostyukhin, *VKalVrt - package for vertex reconstruction in ATLAS.*, tech. rep., revised version number 1 submitted on 2003-09-24 11:10:53: CERN, 2003, URL: <https://cds.cern.ch/record/685551>.
- [72] A. Hoecker et al., *TMVA - Toolkit for Multivariate Data Analysis*, 2009, arXiv: [physics/0703039 \[physics.data-an\]](#).

- [73] ATLAS Collaboration, *Muon reconstruction and identification efficiency in ATLAS using the full Run 2  $pp$  collision data set at  $\sqrt{s} = 13$  TeV*, *Eur. Phys. J. C* **81** (2021) 578, arXiv: [2012.00578](https://arxiv.org/abs/2012.00578) [hep-ex].
- [74] ATLAS Collaboration, *Electron and photon performance measurements with the ATLAS detector using the 2015–2017 LHC proton–proton collision data*, *JINST* **14** (2019) P12006, arXiv: [1908.00005](https://arxiv.org/abs/1908.00005) [hep-ex].
- [75] ATLAS Collaboration, *Electron and photon efficiencies in LHC Run 2 with the ATLAS experiment*, *JHEP* **05** (2024) 162, arXiv: [2308.13362](https://arxiv.org/abs/2308.13362) [hep-ex].
- [76] ATLAS Collaboration, *Electron reconstruction and identification in the ATLAS experiment using the 2015 and 2016 LHC proton–proton collision data at  $\sqrt{s} = 13$  TeV*, *Eur. Phys. J. C* **79** (2019) 639, arXiv: [1902.04655](https://arxiv.org/abs/1902.04655) [physics.ins-det].
- [77] ATLAS Collaboration, *Topological cell clustering in the ATLAS calorimeters and its performance in LHC Run 1*, *Eur. Phys. J. C* **77** (2017) 490, arXiv: [1603.02934](https://arxiv.org/abs/1603.02934) [hep-ex].
- [78] M. Cacciari, G. P. Salam and G. Soyez, *The anti- $k_t$  jet clustering algorithm*, *JHEP* **04** (2008) 063, arXiv: [0802.1189](https://arxiv.org/abs/0802.1189) [hep-ph].
- [79] M. Cacciari, G. P. Salam and G. Soyez, *FastJet user manual*, *Eur. Phys. J. C* **72** (2012) 1896, arXiv: [1111.6097](https://arxiv.org/abs/1111.6097) [hep-ph].
- [80] ATLAS Collaboration, *Selection of jets produced in 13 TeV proton–proton collisions with the ATLAS detector*, ATLAS-CONF-2015-029, 2015, URL: <https://cds.cern.ch/record/2037702>.
- [81] ATLAS Collaboration, *ATLAS  $b$ -jet identification performance and efficiency measurement with  $t\bar{t}$  events in  $pp$  collisions at  $\sqrt{s} = 13$  TeV*, *Eur. Phys. J. C* **79** (2019) 970, arXiv: [1907.05120](https://arxiv.org/abs/1907.05120) [hep-ex].
- [82] ATLAS Collaboration, *The performance of missing transverse momentum reconstruction and its significance with the ATLAS detector using  $140\text{fb}^{-1}$  of  $\sqrt{s} = 13$  TeV  $pp$  collisions*, *Eur. Phys. J. C* **85** (2025) 606, arXiv: [2402.05858](https://arxiv.org/abs/2402.05858) [hep-ex].
- [83] ATLAS Collaboration, *Tagging and suppression of pileup jets with the ATLAS detector*, ATLAS-CONF-2014-018, 2014, URL: <https://cds.cern.ch/record/1700870>.
- [84] ATLAS Collaboration, *Forward Jet Vertex Tagging: A new technique for the identification and rejection of forward pileup jets*, ATL-PHYS-PUB-2015-034, 2015, URL: <https://cds.cern.ch/record/2042098>.
- [85] A. I. Drozhdin, N. V. Mokhov and S. I. Striganov, *Beam Losses and Background Loads on Collider Detectors Due to Beam-Gas Interactions in the LHC*, (2010), URL: <https://cds.cern.ch/record/1370157>.
- [86] A. I. Drozhdin, M. Huhtinen and N. V. Mokhov, *Accelerator related background in the CMS detector at LHC*, *Nucl. Instrum. Methods Phys. Res., A* **381** (1996) 531.
- [87] R. Bruce et al., *Sources of machine-induced background in the ATLAS and CMS detectors at the CERN Large Hadron Collider*, *Nucl. Instrum. Methods Phys. Res., A* **729** (2013) 825.
- [88] ATLAS Collaboration, *Jet energy scale and resolution measured in proton–proton collisions at  $\sqrt{s} = 13$  TeV with the ATLAS detector*, *Eur. Phys. J. C* **81** (2021) 689, arXiv: [2007.02645](https://arxiv.org/abs/2007.02645) [hep-ex].

- [89] W. A. Rolke, A. M. López and J. Conrad, *Limits and confidence intervals in the presence of nuisance parameters*, *Nucl. Instrum. Meth. A* **551** (2005) 493, ed. by L. Lyons and M. Karagoz, arXiv: [physics/0403059](https://arxiv.org/abs/physics/0403059).
- [90] G. Cowan, K. Cranmer, E. Gross and O. Vitells, *Asymptotic formulae for likelihood-based tests of new physics*, *Eur. Phys. J. C* **71** (2011) 1554, arXiv: [1007.1727](https://arxiv.org/abs/1007.1727) [[physics.data-an](https://arxiv.org/archive/physics)], Erratum: *Eur. Phys. J. C* **73** (2013) 2501.
- [91] A. L. Read, *Presentation of search results: the  $CL_s$  technique*, *J. Phys. G* **28** (2002) 2693.
- [92] L. Heinrich, M. Feickert and G. Stark, *scikit-hep/pyhf: v0.7.6*, 2024, URL: <https://doi.org/10.5281/zenodo.10470033>.
- [93] L. Heinrich, M. Feickert, G. Stark and K. Cranmer, *pyhf: pure-Python implementation of HistFactory statistical models*, *J. Open Source Softw.* **6** (2021) 2823.
- [94] A. Held et al., *scikit-hep/cabinetry: v0.6.0*, 2023, URL: <https://doi.org/10.5281/zenodo.8360833>.
- [95] K. Cranmer and A. Held, *Building and steering binned template fits with cabinetry*, *EPJ Web Conf.* **251** (2021) 03067.
- [96] ATLAS Collaboration, *Search for charginos and neutralinos in final states with two boosted hadronically decaying bosons and missing transverse momentum in  $pp$  collisions at  $\sqrt{s} = 13$  TeV with the ATLAS detector*, *Phys. Rev. D* **104** (2021) 112010, arXiv: [2108.07586](https://arxiv.org/abs/2108.07586) [[hep-ex](https://arxiv.org/archive/hep)].
- [97] ATLAS Collaboration, *A detailed map of Higgs boson interactions by the ATLAS experiment ten years after the discovery*, *Nature* **607** (2022) 52, arXiv: [2207.00092](https://arxiv.org/abs/2207.00092) [[hep-ex](https://arxiv.org/archive/hep)], Erratum: *Nature* **612** (2022) E24.
- [98] ATLAS Collaboration, *Search for Light Long-Lived Particles in  $pp$  Collisions at  $\sqrt{s} = 13$  TeV Using Displaced Vertices in the ATLAS Inner Detector*, *Phys. Rev. Lett.* **133** (2024) 161803, arXiv: [2403.15332](https://arxiv.org/abs/2403.15332) [[hep-ex](https://arxiv.org/archive/hep)].
- [99] ATLAS Collaboration, *Search for neutral long-lived particles that decay into displaced jets in the ATLAS calorimeter in association with leptons or jets using  $pp$  collisions at  $\sqrt{s} = 13$  TeV*, *JHEP* **11** (2024) 036, arXiv: [2407.09183](https://arxiv.org/abs/2407.09183) [[hep-ex](https://arxiv.org/archive/hep)], Erratum: *JHEP* **11** (2025) 061.
- [100] ATLAS Collaboration, *Summary plots for Higgs boson mediated hidden sector involving long-lived particles*, ATL-PHYS-PUB-2025-039, 2025, URL: <https://cds.cern.ch/record/2946396>.
- [101] ATLAS Collaboration, *ATLAS Computing Acknowledgements*, ATL-SOFT-PUB-2026-001, 2026, URL: <https://cds.cern.ch/record/2952666>.

## The ATLAS Collaboration

G. Aad <sup>102</sup>, E. Aakvaag <sup>17</sup>, B. Abbott <sup>122</sup>, S. Abdelhameed <sup>118a</sup>, K. Abeling <sup>54</sup>, N.J. Abicht <sup>48</sup>, S.H. Abidi <sup>30</sup>, M. Aboeela <sup>44</sup>, A. Aboulhorma <sup>36e</sup>, H. Abramowicz <sup>155</sup>, B.S. Acharya <sup>68a,68b,m</sup>, A. Ackermann <sup>62a</sup>, C. Adam Bourdarios <sup>4</sup>, L. Adamczyk <sup>85a</sup>, S.V. Addepalli <sup>147</sup>, M.J. Addison <sup>101</sup>, J. Adelman <sup>117</sup>, A. Adiguzel <sup>22c</sup>, T. Adye <sup>136</sup>, A.A. Affolder <sup>138</sup>, Y. Afik <sup>39</sup>, M.N. Agaras <sup>13</sup>, A. Aggarwal <sup>100</sup>, C. Agheorghiesei <sup>28c</sup>, A. Ahmad <sup>83a</sup>, F. Ahmadov <sup>38,ad</sup>, S. Ahuja <sup>95</sup>, S. Ahuja <sup>166</sup>, X. Ai <sup>113c</sup>, G. Aielli <sup>75a,75b</sup>, A. Aikot <sup>166</sup>, M. Ait Tamlihat <sup>36e</sup>, T.P.A. Åkesson <sup>98</sup>, D. Akiyama <sup>171</sup>, N.N. Akolkar <sup>25</sup>, S. Aktas <sup>169</sup>, G.L. Alberghi <sup>24b</sup>, J. Albert <sup>168</sup>, U. Alberti <sup>20</sup>, P. Albicocco <sup>52</sup>, S. Alderweireldt <sup>51</sup>, Z.L. Alegria <sup>123</sup>, M. Aleksa <sup>37</sup>, I.N. Aleksandrov <sup>38</sup>, C. Alexa <sup>28b</sup>, T. Alexopoulos <sup>10</sup>, F. Alfonsi <sup>24b</sup>, M. Algren <sup>55</sup>, M. Alhroob <sup>170</sup>, B. Ali <sup>134</sup>, H.M.J. Ali <sup>91,v</sup>, S. Ali <sup>32</sup>, S.W. Alibocus <sup>92</sup>, M. Aliev <sup>34c</sup>, G. Alimonti <sup>70a</sup>, C. Allaire <sup>65</sup>, B.M.M. Allbrooke <sup>150</sup>, D.R. Allen <sup>123</sup>, J.S. Allen <sup>101</sup>, J.F. Allen <sup>51</sup>, C.S. Alley <sup>1</sup>, E.R. Almazan <sup>138</sup>, A. Aloisio <sup>71a,71b</sup>, F. Alonso <sup>90</sup>, C. Alpigiani <sup>141</sup>, A. Alvarez Fernandez <sup>100</sup>, M. Alves Cardoso <sup>55</sup>, M.G. Alviggi <sup>71a,71b</sup>, M. Aly <sup>101</sup>, Y. Amaral Coutinho <sup>81b</sup>, A. Ambler <sup>104</sup>, C. Amelung <sup>37</sup>, M. Amerl <sup>101</sup>, T. Amezza <sup>129</sup>, B. Amini <sup>53</sup>, K. Amirie <sup>159</sup>, A. Amirkhanov <sup>38</sup>, D. Amperidou <sup>156</sup>, S. An <sup>82</sup>, C. Anastopoulos <sup>143</sup>, T. Andeen <sup>11</sup>, J.K. Anders <sup>92</sup>, A.C. Anderson <sup>58</sup>, A. Andreazza <sup>70a,70b</sup>, S. Angelidakis <sup>9</sup>, A. Angerami <sup>41</sup>, A.V. Anisenkov <sup>38</sup>, A. Annovi <sup>73a</sup>, C. Antel <sup>37</sup>, E. Antipov <sup>149</sup>, M. Antonelli <sup>52</sup>, F. Anulli <sup>74a</sup>, M. Aoki <sup>82</sup>, T. Aoki <sup>157</sup>, M.A. Aparo <sup>13</sup>, L. Aperio Bella <sup>47</sup>, M. Apicella <sup>31</sup>, C. Appelt <sup>155</sup>, A. Apyan <sup>27</sup>, M. Arampatzi <sup>10</sup>, S.J. Arbiol Val <sup>86</sup>, C. Arcangeletti <sup>52</sup>, A.T.H. Arce <sup>50</sup>, J-F. Arguin <sup>108</sup>, S. Argyropoulos <sup>156</sup>, J.-H. Arling <sup>47</sup>, O. Arnaez <sup>4</sup>, H. Arnold <sup>149</sup>, G. Artoni <sup>74a,74b</sup>, H. Asada <sup>111</sup>, S. Asatryan <sup>176</sup>, N.A. Asbah <sup>37</sup>, R.A. Ashby Pickering <sup>170</sup>, A.M. Aslam <sup>95</sup>, J. Assahsah <sup>36d</sup>, K. Assamagan <sup>30</sup>, R. Astalos <sup>29a</sup>, K.S.V. Astrand <sup>98</sup>, S. Atashi <sup>163</sup>, R.J. Atkin <sup>34a</sup>, H. Atmani <sup>36f</sup>, P.A. Atmasiddha <sup>130</sup>, K. Augsten <sup>134</sup>, A.D. Auriol <sup>40</sup>, V.A. Austrup <sup>101</sup>, A.S. Avad <sup>94</sup>, G. Avolio <sup>37</sup>, K. Axiotis <sup>55</sup>, A. Azzam <sup>13</sup>, D. Babal <sup>29b</sup>, H. Bachacou <sup>137</sup>, K. Bachas <sup>156,p</sup>, A. Bachiou <sup>35</sup>, E. Bachmann <sup>49</sup>, M.J. Backes <sup>62a</sup>, A. Badea <sup>39</sup>, T.M. Baer <sup>106</sup>, M. Bahmani <sup>19</sup>, D. Bahner <sup>53</sup>, K. Bai <sup>125</sup>, L. Baines <sup>94</sup>, O.K. Baker <sup>175</sup>, D. Bakshi Gupta <sup>8</sup>, L.E. Balabram Filho <sup>81b</sup>, V. Balakrishnan <sup>122</sup>, R. Balasubramanian <sup>4</sup>, P. Balek <sup>85a</sup>, E. Ballabene <sup>24b,24a</sup>, F. Balli <sup>137</sup>, L.M. Baltes <sup>62a</sup>, W.K. Balunas <sup>128</sup>, I. Bamwidhi <sup>118b</sup>, E. Banas <sup>86</sup>, M. Bandieramonte <sup>131</sup>, A. Bandyopadhyay <sup>25</sup>, S. Bansal <sup>25</sup>, L. Barak <sup>155</sup>, M. Barakat <sup>47</sup>, E.L. Barberio <sup>105</sup>, D. Barberis <sup>18b</sup>, M. Barbero <sup>102</sup>, M.Z. Barel <sup>116</sup>, T. Barillari <sup>110</sup>, M-S. Barisits <sup>37</sup>, T. Barklow <sup>147</sup>, P. Baron <sup>135</sup>, D.A. Baron Moreno <sup>101</sup>, A. Baroncelli <sup>61</sup>, A.J. Barr <sup>128</sup>, J.D. Barr <sup>96</sup>, F. Barreiro <sup>99</sup>, J. Barreiro Guimarães da Costa <sup>14</sup>, M.G. Barros Teixeira <sup>132a</sup>, F. Bartels <sup>62a</sup>, R. Bartoldus <sup>147</sup>, A.E. Barton <sup>91</sup>, P. Bartos <sup>29a</sup>, M. Baselga <sup>48</sup>, S. Bashiri <sup>86</sup>, A. Bassalat <sup>65,b</sup>, M.J. Basso <sup>160a</sup>, S. Bataju <sup>44</sup>, R. Bate <sup>167</sup>, R.L. Bates <sup>58</sup>, S. Batlamous <sup>99</sup>, M. Battaglia <sup>138</sup>, D. Battulga <sup>19</sup>, M. Baucé <sup>74a,74b</sup>, L. Bauckhage <sup>47</sup>, P. Bauer <sup>25</sup>, L.T. Bayer <sup>47</sup>, L.T. Bazzano Hurrell <sup>31</sup>, T. Beau <sup>129</sup>, J.Y. Beaucamp <sup>90</sup>, S. Beauceron <sup>129</sup>, P.H. Beauchemin <sup>162</sup>, P. Bechtel <sup>25</sup>, H.P. Beck <sup>20,o</sup>, K. Becker <sup>170</sup>, A.J. Beddall <sup>80</sup>, V.A. Bednyakov <sup>38</sup>, C.P. Bee <sup>149</sup>, L.J. Beemster <sup>16</sup>, M. Begalli <sup>81d</sup>, M. Begel <sup>30</sup>, J.K. Behr <sup>47</sup>, J.F. Beirer <sup>37</sup>, F. Beisiegel <sup>25</sup>, M. Belfkir <sup>118b</sup>, G. Bella <sup>155</sup>, L. Bellagamba <sup>24b</sup>, A. Bellerive <sup>35</sup>, C.D. Bellgraph <sup>67</sup>, P. Bellos <sup>21</sup>, I. Benaoumeur <sup>21</sup>, D. Benckekroun <sup>36a</sup>, F. Bendebba <sup>36a</sup>, Y. Benhammou <sup>155</sup>, K.C. Benkendorfer <sup>168</sup>, L. Beresford <sup>47</sup>, M. Beretta <sup>52</sup>, E. Bergeas Kuutmann <sup>164</sup>, N. Berger <sup>4</sup>, B. Bergmann <sup>134</sup>, J. Beringer <sup>18a</sup>, M. Berkat <sup>137</sup>, G. Bernardi <sup>5</sup>, C. Bernius <sup>147</sup>, F.U. Bernlochner <sup>25</sup>, A. Berrocal Guardia <sup>13</sup>, T. Berry <sup>95</sup>, P. Berta <sup>135</sup>, A. Berti <sup>132a</sup>,

R. Bertrand [ID](#)<sup>102</sup>, S. Bethke [ID](#)<sup>110</sup>, A. Betti [ID](#)<sup>74a,74b</sup>, T.F. Beumker [ID](#)<sup>174</sup>, A.J. Bevan [ID](#)<sup>94</sup>, L. Bezio [ID](#)<sup>55</sup>,  
 N.K. Bhalla [ID](#)<sup>53</sup>, S. Bharthuar [ID](#)<sup>110</sup>, S. Bhatta [ID](#)<sup>149</sup>, P. Bhattacharai [ID](#)<sup>147</sup>, Z.M. Bhatti [ID](#)<sup>119</sup>, K.D. Bhide [ID](#)<sup>53</sup>,  
 V.S. Bhopatkar [ID](#)<sup>123</sup>, R.M. Bianchi [ID](#)<sup>131</sup>, G. Bianco [ID](#)<sup>24b,24a</sup>, O. Biebel [ID](#)<sup>109</sup>, M. Biglietti [ID](#)<sup>76a</sup>, P. Bijl [ID](#)<sup>53</sup>,  
 C.S. Billingsley [ID](#)<sup>44</sup>, Y. Bimgdi [ID](#)<sup>36f</sup>, M. Bindi [ID](#)<sup>54</sup>, A. Bingham [ID](#)<sup>174</sup>, A. Bingul [ID](#)<sup>22b</sup>, C. Bini [ID](#)<sup>74a,74b</sup>,  
 G.A. Bird [ID](#)<sup>33</sup>, M. Biroš [ID](#)<sup>135</sup>, S. Biryukov [ID](#)<sup>150</sup>, T. Bisanz [ID](#)<sup>48</sup>, E. Bisceglie [ID](#)<sup>24b,24a</sup>, J.P. Biswal [ID](#)<sup>136</sup>,  
 D. Biswas [ID](#)<sup>145</sup>, M. Biyabi [ID](#)<sup>14</sup>, I. Bloch [ID](#)<sup>47</sup>, A. Blue [ID](#)<sup>58</sup>, U. Blumenschein [ID](#)<sup>94</sup>, V.S. Bobrovnikov [ID](#)<sup>38</sup>,  
 L. Boccardo [ID](#)<sup>56b,56a</sup>, M. Boehler [ID](#)<sup>53</sup>, B. Boehm [ID](#)<sup>169</sup>, D. Bogavac [ID](#)<sup>13</sup>, L.S. Boggia [ID](#)<sup>129</sup>,  
 V. Boisvert [ID](#)<sup>95</sup>, P. Bokan [ID](#)<sup>164</sup>, T. Bold [ID](#)<sup>85a</sup>, M. Bomben [ID](#)<sup>5</sup>, M. Bona [ID](#)<sup>94</sup>, M. Boonekamp [ID](#)<sup>137</sup>,  
 A.G. Borbély [ID](#)<sup>58</sup>, G. Borissov [ID](#)<sup>91</sup>, A. Borkar [ID](#)<sup>169</sup>, D. Bortoletto [ID](#)<sup>128</sup>, D. Boscherini [ID](#)<sup>24b</sup>,  
 M. Bosman [ID](#)<sup>13</sup>, K. Bouaouda [ID](#)<sup>36a</sup>, L. Boudet [ID](#)<sup>4</sup>, J. Boudreau [ID](#)<sup>131</sup>, E.V. Bouhova-Thacker [ID](#)<sup>91</sup>,  
 D. Boumediene [ID](#)<sup>40</sup>, R. Bouquet [ID](#)<sup>56b,56a</sup>, A. Boveia [ID](#)<sup>121</sup>, J. Boyd [ID](#)<sup>37</sup>, D. Boye [ID](#)<sup>30</sup>, I.R. Boyko [ID](#)<sup>38</sup>,  
 L. Bozianu [ID](#)<sup>55</sup>, J. Bracinić [ID](#)<sup>21</sup>, N. Brahimi [ID](#)<sup>4</sup>, G. Brandt [ID](#)<sup>174</sup>, O. Brandt [ID](#)<sup>33</sup>, B. Brau [ID](#)<sup>103</sup>,  
 R. Brenner [ID](#)<sup>172</sup>, L. Brenner [ID](#)<sup>116</sup>, R. Brenner [ID](#)<sup>164</sup>, S. Bressler [ID](#)<sup>172</sup>, M. Brettell [ID](#)<sup>96</sup>, G. Brianti [ID](#)<sup>116</sup>,  
 D. Britton [ID](#)<sup>58</sup>, D. Britzger [ID](#)<sup>110</sup>, I. Brock [ID](#)<sup>25</sup>, R. Brock [ID](#)<sup>107</sup>, H. Bronson [ID](#)<sup>130</sup>, G. Brooijmans [ID](#)<sup>41</sup>,  
 A.J. Brooks [ID](#)<sup>67</sup>, E.M. Brooks [ID](#)<sup>160b</sup>, E. Brost [ID](#)<sup>30</sup>, L.M. Brown [ID](#)<sup>168,160a</sup>, L.E. Bruce [ID](#)<sup>60</sup>,  
 T.L. Bruckler [ID](#)<sup>128</sup>, P.A. Bruckman de Renstrom [ID](#)<sup>86</sup>, B. Brüers [ID](#)<sup>47</sup>, A. Bruni [ID](#)<sup>24b</sup>, G. Bruni [ID](#)<sup>24b</sup>,  
 D. Brunner [ID](#)<sup>46a,46b</sup>, M. Bruschi [ID](#)<sup>24b</sup>, N. Bruscinò [ID](#)<sup>74a,74b</sup>, T. Buanes [ID](#)<sup>17</sup>, Q. Buat [ID](#)<sup>141</sup>,  
 D. Buchin [ID](#)<sup>110</sup>, A.G. Buckley [ID](#)<sup>58</sup>, J. Bucko [ID](#)<sup>135</sup>, M. Bühring [ID](#)<sup>49</sup>, O. Bulekov [ID](#)<sup>80</sup>, B.A. Bullard [ID](#)<sup>147</sup>,  
 T.O. Buratovich [ID](#)<sup>90</sup>, S. Burdin [ID](#)<sup>92</sup>, C.D. Burgard [ID](#)<sup>48</sup>, A.M. Burger [ID](#)<sup>89</sup>, B. Burghgrave [ID](#)<sup>8</sup>,  
 O. Burlayenko [ID](#)<sup>53</sup>, J. Burleson [ID](#)<sup>165</sup>, J.C. Burzynski [ID](#)<sup>122</sup>, V. Büscher [ID](#)<sup>100</sup>, P.J. Bussey [ID](#)<sup>58</sup>, O. But [ID](#)<sup>25</sup>,  
 J.M. Butler [ID](#)<sup>26</sup>, C.M. Buttar [ID](#)<sup>58</sup>, J.M. Butterworth [ID](#)<sup>96</sup>, P. Butti [ID](#)<sup>37</sup>, W. Buttinger [ID](#)<sup>136</sup>,  
 C.J. Buxo Vazquez [ID](#)<sup>107</sup>, A.R. Buzykaev [ID](#)<sup>38</sup>, S. Cabrera Urbán [ID](#)<sup>166</sup>, L. Cadamuro [ID](#)<sup>65</sup>, H. Cai [ID](#)<sup>37</sup>,  
 Y. Cai [ID](#)<sup>24b,112c,24a</sup>, Y. Cai [ID](#)<sup>112a</sup>, M.A. Cairo [ID](#)<sup>130</sup>, V.M.M. Cairo [ID](#)<sup>37</sup>, O. Cakir [ID](#)<sup>3a</sup>, N. Calace [ID](#)<sup>37</sup>,  
 P. Calafiura [ID](#)<sup>18a</sup>, G. Calderini [ID](#)<sup>129</sup>, P. Calfayan [ID](#)<sup>35</sup>, L. Calic [ID](#)<sup>98</sup>, G. Callea [ID](#)<sup>58</sup>, L.P. Caloba [ID](#)<sup>81b</sup>,  
 D. Calvet [ID](#)<sup>40</sup>, S. Calvet [ID](#)<sup>40</sup>, R. Camacho Toro [ID](#)<sup>129</sup>, S. Camarda [ID](#)<sup>37</sup>, D. Camarero Munoz [ID](#)<sup>27</sup>,  
 P. Camarri [ID](#)<sup>75a,75b</sup>, C. Camincher [ID](#)<sup>37</sup>, M. Campanelli [ID](#)<sup>96</sup>, A. Camplani [ID](#)<sup>42</sup>, V. Canale [ID](#)<sup>71a,71b</sup>,  
 A.C. Canbay [ID](#)<sup>3a</sup>, E. Canonero [ID](#)<sup>95</sup>, J. Cantero [ID](#)<sup>166</sup>, F. Capocasa [ID](#)<sup>27</sup>, P. Cappelli [ID](#)<sup>27</sup>, M. Capua [ID](#)<sup>43b,43a</sup>,  
 A. Carbone [ID](#)<sup>70a,70b</sup>, R. Cardarelli [ID](#)<sup>75a</sup>, J.C.J. Cardenas [ID](#)<sup>8</sup>, M.P. Cardiff [ID](#)<sup>27</sup>, G. Carducci [ID](#)<sup>43b,43a</sup>,  
 T. Carli [ID](#)<sup>37</sup>, G. Carlino [ID](#)<sup>71a</sup>, J.I. Carlotto [ID](#)<sup>13</sup>, B.T. Carlson [ID](#)<sup>131,q</sup>, E.M. Carlson [ID](#)<sup>168</sup>,  
 L. Carminati [ID](#)<sup>70a,70b</sup>, A. Carnelli [ID](#)<sup>4</sup>, M. Carnesale [ID](#)<sup>37</sup>, S. Caron [ID](#)<sup>115</sup>, E. Carquin [ID](#)<sup>139g</sup>, I.B. Carr [ID](#)<sup>105</sup>,  
 S. Carrá [ID](#)<sup>72a,72b</sup>, G. Carratta [ID](#)<sup>24b,24a</sup>, C. Carrion Martinez [ID](#)<sup>166</sup>, A.M. Carroll [ID](#)<sup>125</sup>, N. Cartalade [ID](#)<sup>40</sup>,  
 M.P. Casado [ID](#)<sup>13,h</sup>, P. Casolaro [ID](#)<sup>71a,71b</sup>, M. Caspar [ID](#)<sup>47</sup>, F. Cassinese [ID](#)<sup>90</sup>, W.R. Castiglioni [ID](#)<sup>39</sup>,  
 F.L. Castillo [ID](#)<sup>4</sup>, L. Castillo Garcia [ID](#)<sup>13</sup>, V. Castillo Gimenez [ID](#)<sup>166</sup>, N.F. Castro [ID](#)<sup>132a,132e</sup>,  
 A. Catinaccio [ID](#)<sup>37</sup>, J.R. Catmore [ID](#)<sup>127</sup>, T. Cavaliere [ID](#)<sup>4</sup>, V. Cavaliere [ID](#)<sup>30</sup>, E. Celebi [ID](#)<sup>80</sup>, S. Cella [ID](#)<sup>30</sup>,  
 V. Cepaitis [ID](#)<sup>55</sup>, K. Cerny [ID](#)<sup>124</sup>, A.S. Cerqueira [ID](#)<sup>81a</sup>, A. Cerri [ID](#)<sup>73a,ap</sup>, L. Cerrito [ID](#)<sup>75a,75b</sup>, F. Cerutti [ID](#)<sup>18a</sup>,  
 B. Cervato [ID](#)<sup>70a,70b</sup>, A. Cervelli [ID](#)<sup>24b</sup>, G. Cesarini [ID](#)<sup>52</sup>, S.A. Cetin [ID](#)<sup>80</sup>, P.M. Chabrilat [ID](#)<sup>129</sup>,  
 R. Chakkappai [ID](#)<sup>65</sup>, S. Chakraborty [ID](#)<sup>170</sup>, A. Chambers [ID](#)<sup>60</sup>, J. Chan [ID](#)<sup>18a</sup>, J.D. Chapman [ID](#)<sup>33</sup>,  
 E. Chapon [ID](#)<sup>137</sup>, B. Chargeishvili [ID](#)<sup>153b</sup>, D.G. Charlton [ID](#)<sup>21</sup>, C. Chauhan [ID](#)<sup>133</sup>, Y. Che [ID](#)<sup>112a</sup>,  
 S. Chekanov [ID](#)<sup>6</sup>, G.A. Chelkov [ID](#)<sup>38,a</sup>, H. Chen [ID](#)<sup>30</sup>, J. Chen [ID](#)<sup>142a</sup>, J. Chen [ID](#)<sup>146</sup>, M. Chen [ID](#)<sup>59</sup>,  
 S. Chen [ID](#)<sup>87</sup>, S.J. Chen [ID](#)<sup>112a</sup>, X. Chen [ID](#)<sup>142a</sup>, X. Chen [ID](#)<sup>15,ai</sup>, Z. Chen [ID](#)<sup>61</sup>, C.L. Cheng [ID](#)<sup>173</sup>,  
 H.C. Cheng [ID](#)<sup>63a</sup>, S. Cheong [ID](#)<sup>147</sup>, A. Cheplakov [ID](#)<sup>38</sup>, E. Cherepanova [ID](#)<sup>116</sup>, E. Cheu [ID](#)<sup>7</sup>, K. Cheung [ID](#)<sup>64</sup>,  
 L. Chevalier [ID](#)<sup>137</sup>, G. Chiarelli [ID](#)<sup>73a</sup>, G. Chiodini [ID](#)<sup>69a</sup>, A.S. Chisholm [ID](#)<sup>21</sup>, A. Chitan [ID](#)<sup>28b</sup>,  
 M. Chitishvili [ID](#)<sup>166</sup>, M.V. Chizhov [ID](#)<sup>38,r</sup>, K. Choi [ID](#)<sup>11</sup>, Y. Chou [ID](#)<sup>141</sup>, E.Y.S. Chow [ID](#)<sup>115</sup>, K.L. Chu [ID](#)<sup>172</sup>,  
 M.C. Chu [ID](#)<sup>63a</sup>, Z. Chubinidze [ID](#)<sup>52</sup>, J. Chudoba [ID](#)<sup>133</sup>, J.J. Chwastowski [ID](#)<sup>86</sup>, D. Cieri [ID](#)<sup>110</sup>,  
 K.M. Ciesla [ID](#)<sup>85a</sup>, V. Cindro [ID](#)<sup>93</sup>, A. Ciocio [ID](#)<sup>18a</sup>, F. Ciotto [ID](#)<sup>71a,71b</sup>, Z.H. Citron [ID](#)<sup>172</sup>, M. Citterio [ID](#)<sup>70a</sup>,  
 D.A. Ciubotaru [ID](#)<sup>28b</sup>, A. Clark [ID](#)<sup>55</sup>, P.J. Clark [ID](#)<sup>51</sup>, N. Clarke Hall [ID](#)<sup>96</sup>, C. Clarry [ID](#)<sup>159</sup>, S.E. Clawson [ID](#)<sup>47</sup>,  
 C. Clement [ID](#)<sup>46a,46b</sup>, L. Clissa [ID](#)<sup>24b,24a</sup>, Y. Coadou [ID](#)<sup>102</sup>, M. Cobal [ID](#)<sup>68a,68c</sup>, A. Coccaro [ID](#)<sup>56b</sup>,

M.G. Cochran Branson [ID](#)<sup>141</sup>, R.F. Coelho Barrue [ID](#)<sup>132a</sup>, R. Coelho Lopes De Sa [ID](#)<sup>103</sup>, S. Coelli [ID](#)<sup>70a</sup>,  
M.M. Cohen [ID](#)<sup>130</sup>, L.S. Colangeli [ID](#)<sup>159</sup>, B. Cole [ID](#)<sup>41</sup>, P. Collado Soto [ID](#)<sup>99</sup>, J. Collot [ID](#)<sup>59</sup>,  
M.R. Coluccia [ID](#)<sup>69a</sup>, I. Combes<sup>65</sup>, P. Conde Muiño [ID](#)<sup>132a,132g</sup>, M.P. Connell [ID](#)<sup>34c</sup>, S.H. Connell [ID](#)<sup>34c</sup>,  
E.I. Conroy [ID](#)<sup>128</sup>, M. Contreras Cossio [ID](#)<sup>11</sup>, F. Conventi [ID](#)<sup>71a,ak</sup>, A.M. Cooper-Sarkar [ID](#)<sup>128</sup>,  
L. Corazzina [ID](#)<sup>74a,74b</sup>, F.A. Corchia [ID](#)<sup>24b,24a</sup>, A. Cordeiro Oudot Choi [ID](#)<sup>141</sup>, L.D. Corpe [ID](#)<sup>40</sup>,  
M. Corradi [ID](#)<sup>74a,74b</sup>, F. Corriveau [ID](#)<sup>104,ab</sup>, A. Cortes-Gonzalez [ID](#)<sup>157</sup>, M.J. Costa [ID](#)<sup>166</sup>, F. Costanza [ID](#)<sup>4</sup>,  
D. Costanzo [ID](#)<sup>143</sup>, J. Couthures [ID](#)<sup>4</sup>, G. Cowan [ID](#)<sup>95</sup>, K. Cranmer [ID](#)<sup>173</sup>, L. Cremer [ID](#)<sup>48</sup>,  
D. Cremonini [ID](#)<sup>24b,24a</sup>, S. Crépé-Renaudin [ID](#)<sup>59</sup>, F. Crescioli [ID](#)<sup>129</sup>, T. Cresta [ID](#)<sup>72a,72b</sup>, M. Cristinziani [ID](#)<sup>145</sup>,  
M. Cristoforetti [ID](#)<sup>77a,77b</sup>, E. Critelli [ID](#)<sup>96</sup>, A. Cueto [ID](#)<sup>99</sup>, H. Cui [ID](#)<sup>96</sup>, Z. Cui [ID](#)<sup>7</sup>, B.M. Cunnett [ID](#)<sup>150</sup>,  
W.R. Cunningham [ID](#)<sup>58</sup>, E. Cuppini<sup>110</sup>, F. Curcio [ID](#)<sup>166</sup>, J.R. Curran [ID](#)<sup>51</sup>,  
M.J. Da Cunha Sargedas De Sousa [ID](#)<sup>56b,56a</sup>, J.V. Da Fonseca Pinto [ID](#)<sup>81b</sup>, C. Da Via [ID](#)<sup>101</sup>,  
W. Dabrowski [ID](#)<sup>85a</sup>, T. Dado [ID](#)<sup>37</sup>, S. Dahbi [ID](#)<sup>152</sup>, T. Dai [ID](#)<sup>106</sup>, D. Dal Santo [ID](#)<sup>20</sup>, C. Dallapiccola [ID](#)<sup>103</sup>,  
M. Dam [ID](#)<sup>42</sup>, G. D'amen [ID](#)<sup>30</sup>, V. D'Amico [ID](#)<sup>109</sup>, J.R. Dandoy [ID](#)<sup>35</sup>, M. D'Andrea [ID](#)<sup>56b,56a</sup>,  
D. Dannheim [ID](#)<sup>37</sup>, G. D'anniballe [ID](#)<sup>73a,73b</sup>, M. Danninger [ID](#)<sup>146</sup>, V. Dao [ID](#)<sup>149</sup>, G. Darbo [ID](#)<sup>56b</sup>,  
F. Dattola [ID](#)<sup>47</sup>, S. D'Auria [ID](#)<sup>70a,70b</sup>, A. D'Avanzo [ID](#)<sup>71a,71b</sup>, T. Davidek [ID](#)<sup>135</sup>, J. Davidson [ID](#)<sup>170</sup>,  
I. Dawson [ID](#)<sup>94</sup>, K. De [ID](#)<sup>8</sup>, C. De Almeida Rossi [ID](#)<sup>159</sup>, N. De Biase [ID](#)<sup>47</sup>, S. De Castro [ID](#)<sup>24b,24a</sup>,  
N. De Groot [ID](#)<sup>115</sup>, P. de Jong [ID](#)<sup>116</sup>, H. De la Torre [ID](#)<sup>117</sup>, A. De Maria [ID](#)<sup>112a</sup>, S. De Miranda Rimes [ID](#)<sup>81d</sup>,  
A. De Salvo [ID](#)<sup>74a</sup>, U. De Sanctis [ID](#)<sup>75a,75b</sup>, F. De Santis [ID](#)<sup>69a,69b</sup>, A. De Santo [ID](#)<sup>150</sup>,  
J.B. De Vivie De Regie [ID](#)<sup>59</sup>, K.G. De Vries [ID](#)<sup>116</sup>, J. Debevc [ID](#)<sup>93</sup>, D.V. Dedovich<sup>38</sup>, J. Degens [ID](#)<sup>92</sup>,  
A.M. Deiana [ID](#)<sup>44</sup>, J. Del Peso [ID](#)<sup>99</sup>, L. Delagrangé [ID](#)<sup>27</sup>, F. Deliot [ID](#)<sup>137</sup>, C.M. Delitzsch [ID](#)<sup>48</sup>,  
M. Della Pietra [ID](#)<sup>71a,71b</sup>, D. Della Volpe [ID](#)<sup>55</sup>, A. Dell'Acqua [ID](#)<sup>37</sup>, L. Dell'Asta [ID](#)<sup>70a,70b</sup>, M. Delmastro [ID](#)<sup>4</sup>,  
C.C. Delogu [ID](#)<sup>56b,56a</sup>, P.A. Delsart [ID](#)<sup>59</sup>, S. Demers [ID](#)<sup>175</sup>, M. Demichev [ID](#)<sup>38</sup>, H. Denizli [ID](#)<sup>22a,1</sup>,  
M.G. Depala [ID](#)<sup>92</sup>, L. D'Eramo [ID](#)<sup>40</sup>, D. Derendarz [ID](#)<sup>86</sup>, L. Derin [ID](#)<sup>56b,56a</sup>, F. Derue [ID](#)<sup>129</sup>, P. Dervan [ID](#)<sup>92,\*</sup>,  
A.M. Desai [ID](#)<sup>1</sup>, K. Desch [ID](#)<sup>25</sup>, F.A. Di Bello [ID](#)<sup>73a,73b</sup>, A. Di Ciaccio [ID](#)<sup>75a,75b</sup>, L. Di Ciaccio [ID](#)<sup>4</sup>,  
D. Di Croce [ID](#)<sup>37</sup>, C. Di Donato [ID](#)<sup>71a,71b</sup>, A. Di Girolamo [ID](#)<sup>37</sup>, G. Di Gregorio [ID](#)<sup>65</sup>, A. Di Luca [ID](#)<sup>77a,77b</sup>,  
B. Di Micco [ID](#)<sup>76a,76b</sup>, R. Di Nardo [ID](#)<sup>76a,76b</sup>, K.F. Di Petrillo [ID](#)<sup>39</sup>, M. Diamantopoulou [ID](#)<sup>35</sup>, F.A. Dias [ID](#)<sup>116</sup>,  
M.A. Diaz [ID](#)<sup>139a,139b</sup>, A.R. Didenko [ID](#)<sup>38</sup>, M. Didenko [ID](#)<sup>166</sup>, S.D. Diefenbacher [ID](#)<sup>18a</sup>, E.B. Diehl [ID](#)<sup>106</sup>,  
S. Díez Cornell [ID](#)<sup>47</sup>, C. Díez Pardos [ID](#)<sup>145</sup>, C. Dimitriadi [ID](#)<sup>148</sup>, A. Dimitrievska [ID](#)<sup>21</sup>, A. Dimri [ID](#)<sup>149</sup>,  
Y. Ding<sup>61</sup>, J. Dingfelder [ID](#)<sup>25</sup>, T. Dingley [ID](#)<sup>128</sup>, I-M. Dinu [ID](#)<sup>28b</sup>, S.J. Dittmeier [ID](#)<sup>62b</sup>, F. Dittus [ID](#)<sup>37</sup>,  
M. Divisek [ID](#)<sup>135</sup>, B. Dixit [ID](#)<sup>92</sup>, F. Djama [ID](#)<sup>102</sup>, T. Djobava [ID](#)<sup>153b</sup>, C. Doglioni [ID](#)<sup>101,98</sup>, A. Dohnalova [ID](#)<sup>29a</sup>,  
Z. Dolezal [ID](#)<sup>135</sup>, K. Domijan [ID](#)<sup>85a</sup>, K.M. Dona [ID](#)<sup>39</sup>, M. Donadelli [ID](#)<sup>81d</sup>, B. Dong [ID](#)<sup>107</sup>, J. Donini [ID](#)<sup>40</sup>,  
A. D'Onofrio [ID](#)<sup>71a,71b</sup>, M. D'Onofrio [ID](#)<sup>92</sup>, J. Dopke [ID](#)<sup>136</sup>, A. Doria [ID](#)<sup>71a</sup>, N. Dos Santos Fernandes [ID](#)<sup>132a</sup>,  
I.A. Dos Santos Luz [ID](#)<sup>81e</sup>, P. Dougan [ID](#)<sup>44</sup>, M.T. Dova [ID](#)<sup>90</sup>, A.T. Doyle [ID](#)<sup>58</sup>, M.P. Drescher [ID](#)<sup>54</sup>,  
E. Dreyer [ID](#)<sup>172</sup>, I. Drivas-koulouris [ID](#)<sup>10</sup>, M. Drnevich [ID](#)<sup>119</sup>, D. Du [ID](#)<sup>61</sup>, T. Du [ID](#)<sup>39</sup>, T.A. du Pree [ID](#)<sup>116</sup>,  
Z. Duan<sup>112a</sup>, M. Dubau [ID](#)<sup>4</sup>, F. Dubinin [ID](#)<sup>38</sup>, M. Dubovsky [ID](#)<sup>29a</sup>, E. Duchovni [ID](#)<sup>172</sup>, G. Duckeck [ID](#)<sup>109</sup>,  
P.K. Duckett<sup>96</sup>, O.A. Ducu [ID](#)<sup>28b</sup>, D. Duda [ID](#)<sup>51</sup>, A. Dudarev [ID](#)<sup>37</sup>, M.M. Dudek [ID](#)<sup>86</sup>, E.R. Duden [ID](#)<sup>27</sup>,  
M. D'uffizi [ID](#)<sup>101</sup>, L. Dufлот [ID](#)<sup>65</sup>, M. Dührssen [ID](#)<sup>37</sup>, I. Duminica [ID](#)<sup>28g</sup>, A.E. Dumitriu [ID](#)<sup>28b</sup>,  
M. Dunford [ID](#)<sup>62a</sup>, T. Duong<sup>4</sup>, A. Duperrin [ID](#)<sup>102</sup>, A.F. Duque Bran [ID](#)<sup>40</sup>, H. Duran Yildiz [ID](#)<sup>3a</sup>,  
A. Durglishvili [ID](#)<sup>153b</sup>, G.I. Dyckes [ID](#)<sup>18a</sup>, M. Dyndal [ID](#)<sup>85a</sup>, B.S. Dziedzic [ID](#)<sup>37</sup>, G.H. Eberwein [ID](#)<sup>128</sup>,  
B. Eckerova [ID](#)<sup>29a</sup>, J.C. Egan [ID](#)<sup>96</sup>, S. Eggebrecht [ID](#)<sup>54</sup>, E. Egidio Purcino De Souza [ID](#)<sup>81e</sup>, G. Eigen [ID](#)<sup>17</sup>,  
K. Einsweiler [ID](#)<sup>18a</sup>, T. Ekelof [ID](#)<sup>164</sup>, P.A. Ekman [ID](#)<sup>98</sup>, S. El Farkh [ID](#)<sup>36b</sup>, Y. El Ghazali [ID](#)<sup>61</sup>,  
H. El Jarrari [ID](#)<sup>104</sup>, A. El Moussaouy [ID](#)<sup>36a</sup>, I. Elbaz [ID](#)<sup>155</sup>, D. Elitez [ID](#)<sup>37</sup>, M. Ellert [ID](#)<sup>164</sup>, F. Ellinghaus [ID](#)<sup>174</sup>,  
T.A. Elliot [ID](#)<sup>95</sup>, J. Elmsheuser [ID](#)<sup>30</sup>, M. Elsayy [ID](#)<sup>118a</sup>, M. Elsing [ID](#)<sup>37</sup>, D. Emeliyanov [ID](#)<sup>136</sup>, Y. Enari [ID](#)<sup>82</sup>,  
S. Epari [ID](#)<sup>108</sup>, D. Ernani Martins Neto [ID](#)<sup>86</sup>, F. Ernst<sup>37</sup>, M. Escalier [ID](#)<sup>65</sup>, C. Escobar [ID](#)<sup>166</sup>,  
R. Estevam De Paula [ID](#)<sup>81c</sup>, E. Etzion [ID](#)<sup>155</sup>, G. Evans [ID](#)<sup>132a,132b</sup>, H. Evans [ID](#)<sup>67</sup>, L.S. Evans [ID](#)<sup>47</sup>,  
S. Ezzarqtouni [ID](#)<sup>36a</sup>, F. Fabbri [ID](#)<sup>24b,24a</sup>, L. Fabbri [ID](#)<sup>24b,24a</sup>, G. Facini [ID](#)<sup>96</sup>, V. Fadeyev [ID](#)<sup>138</sup>,  
D. Fakoudis [ID](#)<sup>100</sup>, S. Falciano [ID](#)<sup>74a</sup>, L.F. Falda Ulhoa Coelho [ID](#)<sup>27</sup>, F. Fallavollita [ID](#)<sup>110</sup>, G. Falsetti [ID](#)<sup>43b,43a</sup>,

J. Faltova [ID](#)<sup>135</sup>, C. Fan [ID](#)<sup>165</sup>, K.Y. Fan [ID](#)<sup>63b</sup>, Y. Fan [ID](#)<sup>14</sup>, Y. Fang [ID](#)<sup>14,112c</sup>, M. Fanti [ID](#)<sup>70a,70b</sup>,  
 M. Faraj [ID](#)<sup>68a,68c</sup>, Z. Farazpay [ID](#)<sup>97</sup>, A. Farbin [ID](#)<sup>8</sup>, A. Farilla [ID](#)<sup>76a</sup>, K. Farman [ID](#)<sup>152</sup>, J.N. Farr [ID](#)<sup>175</sup>,  
 M.S. Farrington [ID](#)<sup>60</sup>, S.M. Farrington [ID](#)<sup>136,51</sup>, F. Fassi [ID](#)<sup>36e</sup>, D. Fassouliotis [ID](#)<sup>9</sup>, L. Fayard [ID](#)<sup>65</sup>,  
 P. Federic [ID](#)<sup>135</sup>, P. Federicova [ID](#)<sup>133</sup>, M. Feickert [ID](#)<sup>173</sup>, L. Feligioni [ID](#)<sup>102</sup>, D.E. Fellers [ID](#)<sup>18a</sup>, C. Feng [ID](#)<sup>113b</sup>,  
 Y. Feng [ID](#)<sup>14</sup>, Z. Feng [ID](#)<sup>65</sup>, B. Fernandez Barbadillo [ID](#)<sup>91</sup>, P. Fernandez Martinez [ID](#)<sup>66</sup>, C. Fernandez Ruiz [ID](#)<sup>33</sup>,  
 J. Ferrando [ID](#)<sup>91</sup>, A. Ferrari [ID](#)<sup>164</sup>, P. Ferrari [ID](#)<sup>116,115</sup>, R. Ferrari [ID](#)<sup>72a</sup>, D. Ferrere [ID](#)<sup>55</sup>, C. Ferretti [ID](#)<sup>106</sup>,  
 M.P. Fewell [ID](#)<sup>1</sup>, D. Fiacco [ID](#)<sup>74a,74b</sup>, F. Fiedler [ID](#)<sup>100</sup>, P. Fiedler [ID](#)<sup>134</sup>, S. Filimonov [ID](#)<sup>38</sup>, M.S. Filip [ID](#)<sup>28b,s</sup>,  
 A. Filipčič [ID](#)<sup>93</sup>, E.K. Filmer [ID](#)<sup>160a</sup>, F. Filthaut [ID](#)<sup>115</sup>, M.C.N. Fiolhais [ID](#)<sup>132a,132c,c</sup>, L. Fiorini [ID](#)<sup>166</sup>,  
 W.C. Fisher [ID](#)<sup>107</sup>, T. Fitschen [ID](#)<sup>101</sup>, I. Fleck [ID](#)<sup>145</sup>, P. Fleischmann [ID](#)<sup>106</sup>, T. Flick [ID](#)<sup>174</sup>, M. Flores [ID](#)<sup>34d,ag</sup>,  
 L.R. Flores Castillo [ID](#)<sup>63a</sup>, M. Foll [ID](#)<sup>127</sup>, F.M. Follega [ID](#)<sup>77a,77b</sup>, N. Fomin [ID](#)<sup>33</sup>, J.H. Foo [ID](#)<sup>159</sup>,  
 A. Formica [ID](#)<sup>137</sup>, M. Fornasiero [ID](#)<sup>150</sup>, A.C. Forti [ID](#)<sup>101</sup>, E. Fortin [ID](#)<sup>102</sup>, A.W. Fortman [ID](#)<sup>18a</sup>, L. Foster [ID](#)<sup>18a</sup>,  
 L. Fountas [ID](#)<sup>9</sup>, H. Fox [ID](#)<sup>91</sup>, P. Francavilla [ID](#)<sup>73a,73b</sup>, S. Francescato [ID](#)<sup>60</sup>, S. Franchellucci [ID](#)<sup>20</sup>,  
 M. Franchini [ID](#)<sup>24b,24a</sup>, S. Franchino [ID](#)<sup>62a</sup>, D. Francis [ID](#)<sup>37</sup>, L. Franco [ID](#)<sup>47</sup>, L. Franconi [ID](#)<sup>47</sup>, M. Franklin [ID](#)<sup>60</sup>,  
 G. Frattari [ID](#)<sup>27</sup>, Y.Y. Frid [ID](#)<sup>155</sup>, N. Fritzsche [ID](#)<sup>37</sup>, A. Froch [ID](#)<sup>55</sup>, D. Froidevaux [ID](#)<sup>37</sup>, J.A. Frost [ID](#)<sup>136</sup>,  
 Y. Fu [ID](#)<sup>107</sup>, S. Fuenzalida Garrido [ID](#)<sup>139g</sup>, Y.C. Fujikake [ID](#)<sup>138</sup>, M. Fujimoto [ID](#)<sup>149</sup>, K.Y. Fung [ID](#)<sup>63a</sup>,  
 E. Furtado De Simas Filho [ID](#)<sup>81e</sup>, M. Furukawa [ID](#)<sup>157</sup>, M. Fuste Costa [ID](#)<sup>47</sup>, J. Fuster [ID](#)<sup>166</sup>, A. Gaa [ID](#)<sup>54</sup>,  
 A. Gabrielli [ID](#)<sup>24b,24a</sup>, A. Gabrielli [ID](#)<sup>159</sup>, G. Gagliardi [ID](#)<sup>56b,56a</sup>, L.G. Gagnon [ID](#)<sup>18a</sup>, S. Galantzan [ID](#)<sup>155</sup>,  
 J. Gallagher [ID](#)<sup>1</sup>, E.J. Gallas [ID](#)<sup>128</sup>, A.L. Gallen [ID](#)<sup>164</sup>, B.J. Gallop [ID](#)<sup>136</sup>, K.K. Gan [ID](#)<sup>121</sup>, Y. Gao [ID](#)<sup>51</sup>,  
 Z. Gao [ID](#)<sup>112a</sup>, A. Garabaglu [ID](#)<sup>141</sup>, F.M. Garay Walls [ID](#)<sup>139a,139b</sup>, C. García [ID](#)<sup>166</sup>, A. Garcia Alonso [ID](#)<sup>116</sup>,  
 A.G. Garcia Caffaro [ID](#)<sup>175</sup>, J.E. García Navarro [ID](#)<sup>166</sup>, M.A. Garcia Ruiz [ID](#)<sup>23b</sup>, M. Garcia-Sciveres [ID](#)<sup>18a</sup>,  
 G.L. Gardner [ID](#)<sup>130</sup>, R.W. Gardner [ID](#)<sup>39</sup>, N. Garelli [ID](#)<sup>162</sup>, R.B. Garg [ID](#)<sup>147</sup>, J.M. Gargan [ID](#)<sup>33</sup>, C.A. Garner [ID](#)<sup>159</sup>,  
 C.M. Garvey [ID](#)<sup>34a</sup>, V.K. Gassmann [ID](#)<sup>162</sup>, G. Gaudio [ID](#)<sup>72a</sup>, A.J. Gavin [ID](#)<sup>94</sup>, J. Gavranovic [ID](#)<sup>93</sup>,  
 I.L. Gavrilenko [ID](#)<sup>132a</sup>, C. Gay [ID](#)<sup>167</sup>, G. Gaycken [ID](#)<sup>125</sup>, A. Gekow [ID](#)<sup>121</sup>, C. Gemme [ID](#)<sup>56b</sup>, M.H. Genest [ID](#)<sup>59</sup>,  
 A.D. Gentry [ID](#)<sup>114</sup>, S. George [ID](#)<sup>95</sup>, T. Geralis [ID](#)<sup>45</sup>, A.A. Gerwin [ID](#)<sup>122</sup>, P. Gessinger-Befurt [ID](#)<sup>37</sup>,  
 M. Ghani [ID](#)<sup>170</sup>, K. Ghorbanian [ID](#)<sup>94</sup>, A. Ghosal [ID](#)<sup>145</sup>, A. Ghosh [ID](#)<sup>163</sup>, A. Ghosh [ID](#)<sup>7</sup>, B. Giacobbe [ID](#)<sup>24b</sup>,  
 S. Giagu [ID](#)<sup>74a,74b</sup>, A. Giannini [ID](#)<sup>61</sup>, S.M. Gibson [ID](#)<sup>95</sup>, D.T. Gil [ID](#)<sup>85b</sup>, A.K. Gilbert [ID](#)<sup>85a</sup>, B.J. Gilbert [ID](#)<sup>41</sup>,  
 D. Gillberg [ID](#)<sup>35</sup>, G. Gilles [ID](#)<sup>116</sup>, D.M. Gingrich [ID](#)<sup>2,aj</sup>, M.P. Giordani [ID](#)<sup>68a,68c</sup>, P.F. Giraud [ID](#)<sup>137</sup>,  
 G. Giugliarelli [ID](#)<sup>68a,68c</sup>, D. Giugni [ID](#)<sup>70a</sup>, F. Giuli [ID](#)<sup>75a,75b,al</sup>, I. Gkialas [ID](#)<sup>9,i</sup>, C. Glasman [ID](#)<sup>99</sup>,  
 M. Glazewska [ID](#)<sup>20</sup>, R.M. Gleason [ID](#)<sup>163</sup>, G. Glemža [ID](#)<sup>47</sup>, I. Gnesi [ID](#)<sup>24b,24a,am</sup>, Y. Go [ID](#)<sup>30</sup>,  
 M. Goblirsch-Kolb [ID](#)<sup>37</sup>, B. Gocke [ID](#)<sup>48</sup>, D. Godin [ID](#)<sup>108</sup>, B. Gokturk [ID](#)<sup>22a</sup>, S. Goldfarb [ID](#)<sup>105</sup>, T. Golling [ID](#)<sup>55</sup>,  
 M.G.D. Gololo [ID](#)<sup>34c</sup>, A. Golub [ID](#)<sup>141</sup>, J.P. Gombas [ID](#)<sup>107</sup>, A. Gomes [ID](#)<sup>132a,132b</sup>, G. Gomes Da Silva [ID](#)<sup>145</sup>,  
 A.J. Gomez Delegido [ID](#)<sup>37</sup>, R. Gonçalves [ID](#)<sup>132a</sup>, A. Gongadze [ID](#)<sup>153c</sup>, F. Gonnella [ID](#)<sup>21</sup>, J.L. Gonski [ID](#)<sup>147</sup>,  
 R.Y. González Andana [ID](#)<sup>51</sup>, S. González de la Hoz [ID](#)<sup>166</sup>, M.V. Gonzalez Rodrigues [ID](#)<sup>47</sup>,  
 R. Gonzalez Suarez [ID](#)<sup>164</sup>, S. Gonzalez-Sevilla [ID](#)<sup>55</sup>, L. Goossens [ID](#)<sup>37</sup>, B. Gorini [ID](#)<sup>37</sup>, E. Gorini [ID](#)<sup>69a,69b</sup>,  
 A. Gorišek [ID](#)<sup>93</sup>, T.C. Gosart [ID](#)<sup>130</sup>, A.T. Goshaw [ID](#)<sup>50</sup>, M.I. Gostkin [ID](#)<sup>38</sup>, S. Goswami [ID](#)<sup>123</sup>,  
 C.A. Gottardo [ID](#)<sup>37</sup>, S.A. Gotz [ID](#)<sup>109</sup>, M. Goughri [ID](#)<sup>36b</sup>, A.G. Goussiou [ID](#)<sup>141</sup>, N. Govender [ID](#)<sup>34c</sup>,  
 R.P. Grabarczyk [ID](#)<sup>128</sup>, I. Grabowska-Bold [ID](#)<sup>85a</sup>, K. Graham [ID](#)<sup>35</sup>, E. Gramstad [ID](#)<sup>127</sup>,  
 S. Grancagnolo [ID](#)<sup>69a,69b</sup>, C.M. Grant [ID](#)<sup>1</sup>, P.M. Gravila [ID](#)<sup>28f</sup>, F.G. Gravili [ID](#)<sup>69a,69b</sup>, H.M. Gray [ID](#)<sup>18a</sup>,  
 M. Greco [ID](#)<sup>110</sup>, M.J. Green [ID](#)<sup>1</sup>, C. Grefe [ID](#)<sup>25</sup>, A.S. Grefsrud [ID](#)<sup>17</sup>, I.M. Gregor [ID](#)<sup>47</sup>, K.T. Greif [ID](#)<sup>163</sup>,  
 P. Grenier [ID](#)<sup>147</sup>, S.G. Grewe [ID](#)<sup>110</sup>, K. Grimm [ID](#)<sup>32</sup>, S. Grinstein [ID](#)<sup>13,x</sup>, E. Gross [ID](#)<sup>172</sup>, J. Grosse-Knetter [ID](#)<sup>54</sup>,  
 L.H. Grossman [ID](#)<sup>18b</sup>, L. Guan [ID](#)<sup>106</sup>, G. Guerrieri [ID](#)<sup>37</sup>, R. Guevara [ID](#)<sup>127</sup>, R. Gugel [ID](#)<sup>100</sup>,  
 J.A.M. Guhit [ID](#)<sup>106</sup>, A. Guida [ID](#)<sup>19</sup>, E. Guilloton [ID](#)<sup>170</sup>, S. Guindon [ID](#)<sup>37</sup>, F. Guo [ID](#)<sup>14,112c</sup>, J. Guo [ID](#)<sup>142a</sup>,  
 L. Guo [ID](#)<sup>47</sup>, L. Guo [ID](#)<sup>112b,u</sup>, Y. Guo [ID](#)<sup>106</sup>, Y. Guo [ID](#)<sup>41</sup>, A. Gupta [ID](#)<sup>48</sup>, R. Gupta [ID](#)<sup>131</sup>, S. Gupta [ID](#)<sup>27</sup>,  
 S. Gurbuz [ID](#)<sup>25</sup>, S.S. Gurdasani [ID](#)<sup>47</sup>, G. Gustavino [ID](#)<sup>74a,74b</sup>, P. Gutierrez [ID](#)<sup>122</sup>,  
 L.F. Gutierrez Zagazeta [ID](#)<sup>130</sup>, M. Gutsche [ID](#)<sup>49</sup>, C. Gutschow [ID](#)<sup>96</sup>, W. Guérin [ID](#)<sup>89</sup>, C. Gwenlan [ID](#)<sup>128</sup>,  
 C.B. Gwilliam [ID](#)<sup>92</sup>, E.S. Haaland [ID](#)<sup>127</sup>, A. Haas [ID](#)<sup>119</sup>, M. Habedank [ID](#)<sup>58</sup>, C. Haber [ID](#)<sup>18a</sup>,  
 R.J. Haberle [ID](#)<sup>172</sup>, H.K. Hadavand [ID](#)<sup>8</sup>, A. Haddad [ID](#)<sup>40</sup>, A. Hadeef [ID](#)<sup>49</sup>, A.I. Hagan [ID](#)<sup>91</sup>, J.J. Hahn [ID](#)<sup>145</sup>,

M. Haleem <sup>169</sup>, J. Haley <sup>123</sup>, G.D. Hallewell <sup>102</sup>, J.A. Hallford <sup>47</sup>, K. Hamano <sup>168</sup>,  
H. Hamdaoui <sup>164</sup>, M. Hamer <sup>25</sup>, S.E.D. Hammoud <sup>65</sup>, E.J. Hampshire <sup>95</sup>, L. Han <sup>112a</sup>,  
L. Han <sup>61</sup>, S. Han <sup>14</sup>, K. Hanagaki <sup>82</sup>, M. Hance <sup>138</sup>, D.A. Hangal <sup>41</sup>, H. Hanif <sup>146</sup>,  
M.D. Hank <sup>130</sup>, J.B. Hansen <sup>42</sup>, P.H. Hansen <sup>42</sup>, T. Harenberg <sup>174</sup>, S. Harkusha <sup>176</sup>,  
M.L. Harris <sup>103</sup>, Y.T. Harris <sup>25</sup>, J. Harrison <sup>13</sup>, P.F. Harrison <sup>170</sup>, M.L.E. Hart <sup>96</sup>,  
N.M. Hartman <sup>110</sup>, N.M. Hartmann <sup>109</sup>, R.Z. Hasan <sup>95,136</sup>, Y. Hasegawa <sup>144</sup>, D. Hashimoto <sup>111</sup>,  
F. Haslbeck <sup>37</sup>, S. Hassan <sup>127</sup>, R. Hauser <sup>107</sup>, M. Haviernik <sup>135</sup>, C.M. Hawkes <sup>21</sup>,  
R.J. Hawkings <sup>37</sup>, Y. Hayashi <sup>157</sup>, D. Hayden <sup>107</sup>, R.L. Hayes <sup>116</sup>, C.P. Hays <sup>128</sup>, J.M. Hays <sup>94</sup>,  
H.S. Hayward <sup>92</sup>, M. He <sup>14,112c</sup>, Y. He <sup>47</sup>, Y. He <sup>96</sup>, N.B. Heatley <sup>94</sup>, V. Hedberg <sup>98</sup>,  
J. Heilman <sup>35</sup>, S. Heim <sup>47</sup>, T. Heim <sup>18a</sup>, J.J. Heinrich <sup>125</sup>, L. Heinrich <sup>110</sup>, J. Hejbal <sup>133</sup>,  
M. Helbig <sup>49</sup>, A. Held <sup>173</sup>, S. Hellesund <sup>17</sup>, C.M. Helling <sup>167</sup>, F.N.E. Henry <sup>58</sup>, H. Herde <sup>98</sup>,  
Y. Hernández Jiménez <sup>149</sup>, G. Herten <sup>53</sup>, R. Hertenberger <sup>109</sup>, L. Hervas <sup>37</sup>, M.E. Hesping <sup>100</sup>,  
N.P. Hessey <sup>160a</sup>, J. Hessler <sup>110</sup>, R. Hicks <sup>130</sup>, M. Hidaoui <sup>36b</sup>, N. Hidic <sup>135</sup>, E. Hill <sup>159</sup>,  
T.S. Hillersoy <sup>17</sup>, S.J. Hillier <sup>21</sup>, J.R. Hinds <sup>107</sup>, F. Hinterkeuser <sup>25</sup>, M. Hirose <sup>126</sup>, S. Hirose <sup>161</sup>,  
D. Hirschbuehl <sup>174</sup>, B. Hiti <sup>93</sup>, J. Hobbs <sup>149</sup>, R. Hobincu <sup>28e</sup>, N. Hod <sup>172</sup>, A.M. Hodges <sup>165</sup>,  
M.C. Hodgkinson <sup>143</sup>, B.H. Hodgkinson <sup>128</sup>, A. Hoecker <sup>37</sup>, D.D. Hofer <sup>106</sup>, J. Hofer <sup>166</sup>,  
J. Hofner <sup>100</sup>, M. Holzbock <sup>37</sup>, L.B.A.H. Hommels <sup>33</sup>, V. Homsak <sup>128</sup>, J.J. Hong <sup>67</sup>,  
T.M. Hong <sup>131</sup>, B.H. Hooberman <sup>165</sup>, W.H. Hopkins <sup>6</sup>, M.C. Hoppesch <sup>165</sup>, Y. Horii <sup>111</sup>,  
M.E. Horstmann <sup>110</sup>, M.M. Horzela <sup>54</sup>, S. Hou <sup>152</sup>, M.R. Housenga <sup>165</sup>, J. Howarth <sup>58</sup>,  
J. Hoya <sup>6</sup>, M. Hrabovsky <sup>124</sup>, T. Hryn'ova <sup>4</sup>, P.J. Hsu <sup>64</sup>, S.-C. Hsu <sup>141</sup>, T. Hsu <sup>65</sup>, M. Hu <sup>18a</sup>,  
P. Hu <sup>63b</sup>, Q. Hu <sup>61</sup>, S. Huang <sup>33</sup>, X. Huang <sup>14,112c</sup>, Y. Huang <sup>135</sup>, Y. Huang <sup>112b</sup>, Y. Huang <sup>14</sup>,  
Z. Huang <sup>65</sup>, Z. Hubacek <sup>134</sup>, F. Huegging <sup>25</sup>, T.B. Huffman <sup>128</sup>,  
M. Hufnagel Maranha De Faria <sup>81a</sup>, C.A. Hugli <sup>47</sup>, M. Huhtinen <sup>37</sup>, S.K. Huiberts <sup>17</sup>,  
R. Hulsken <sup>104</sup>, C.E. Hultquist <sup>18a</sup>, D.L. Humphreys <sup>103</sup>, N. Huseynov <sup>12</sup>, J. Huston <sup>107</sup>,  
B. Huth <sup>37</sup>, J. Huth <sup>60</sup>, L. Huth <sup>47</sup>, R. Hyneman <sup>7</sup>, G. Iacobucci <sup>55</sup>, G. Iakovidis <sup>30</sup>,  
L. Iconomidou-Fayard <sup>65</sup>, J.P. Iddon <sup>37</sup>, P. Iengo <sup>71a,71b</sup>, Y. Iiyama <sup>157</sup>, T. Iizawa <sup>157</sup>,  
Y. Ikegami <sup>82</sup>, D. Iliadis <sup>156</sup>, N. Ilic <sup>159</sup>, H. Imam <sup>36a</sup>, G. Inacio Goncalves <sup>81d</sup>,  
S.A. Infante Cabanas <sup>139c</sup>, T. Ingebretsen Carlson <sup>46a,46b</sup>, J.M. Inglis <sup>94</sup>, G. Introzzi <sup>72a,72b</sup>,  
M. Iodice <sup>76a</sup>, V. Ippolito <sup>74a,74b</sup>, R.K. Irwin <sup>92</sup>, M. Ishino <sup>157</sup>, W. Islam <sup>173</sup>, C. Issever <sup>19</sup>,  
S. Istin <sup>22a,ar</sup>, K. Itabashi <sup>126</sup>, H. Ito <sup>171</sup>, R. Iuppa <sup>77a,77b</sup>, A. Ivina <sup>172</sup>, F. Ivone <sup>37</sup>,  
S. Izumiyama <sup>111</sup>, V. Izzo <sup>71a</sup>, P. Jacka <sup>134</sup>, P. Jackson <sup>1</sup>, P.R. Jacobson <sup>50</sup>, P. Jain <sup>47</sup>,  
K. Jakobs <sup>53</sup>, J. Jamieson <sup>58</sup>, W. Jang <sup>157</sup>, S. Jankovych <sup>116</sup>, B.K. Jashal <sup>136</sup>, M. Javurkova <sup>103</sup>,  
P. Jawahar <sup>101</sup>, L. Jeanty <sup>125</sup>, J. Jejelava <sup>153a,ae</sup>, P. Jenni <sup>53,f</sup>, L. Jerala <sup>93</sup>, C.E. Jessiman <sup>35</sup>,  
H. Jia <sup>167</sup>, J. Jia <sup>149</sup>, X. Jia <sup>110,112c</sup>, C. Jiang <sup>51</sup>, Q. Jiang <sup>63b</sup>, S. Jiggins <sup>47</sup>,  
M. Jimenez Ortega <sup>166</sup>, J. Jimenez Pena <sup>13</sup>, S. Jin <sup>112a</sup>, A. Jinaru <sup>28b</sup>, O. Jinnouchi <sup>140</sup>,  
P. Johansson <sup>143</sup>, K.A. Johns <sup>7</sup>, J.W. Johnson <sup>138</sup>, F.A. Jolly <sup>47</sup>, D.M. Jones <sup>150</sup>, E. Jones <sup>47</sup>,  
K.S. Jones <sup>8</sup>, P. Jones <sup>33</sup>, R.W.L. Jones <sup>91</sup>, T.J. Jones <sup>92</sup>, H.L. Joos <sup>37</sup>, R. Joshi <sup>121</sup>,  
J. Jovicevic <sup>16</sup>, X. Ju <sup>18a</sup>, J.J. Junggeburth <sup>37</sup>, T. Junkermann <sup>62a</sup>, A. Juste Rozas <sup>13,x</sup>,  
M.K. Juzek <sup>86</sup>, S. Kabana <sup>139f</sup>, A. Kaczmarska <sup>86</sup>, S.A. Kadir <sup>147</sup>, M. Kado <sup>110</sup>, H. Kagan <sup>121</sup>,  
M. Kagan <sup>147</sup>, A. Kahn <sup>130</sup>, C. Kahra <sup>100</sup>, T. Kaji <sup>157</sup>, E. Kajomovitz <sup>154</sup>, N. Kakati <sup>172</sup>,  
N. Kakoty <sup>13</sup>, S. Kandel <sup>8</sup>, N. Kanellos <sup>10</sup>, D. Kar <sup>34j,\*</sup>, E. Karentzos <sup>25</sup>, K. Karki <sup>8</sup>,  
O. Karkout <sup>116</sup>, S.N. Karpov <sup>38</sup>, Z.M. Karpova <sup>38</sup>, V. Kartvelishvili <sup>91,153b</sup>, E. Kasimi <sup>156</sup>,  
J. Katzy <sup>47</sup>, S. Kaur <sup>35</sup>, R. Kavak <sup>165</sup>, K. Kawade <sup>144</sup>, M.P. Kawale <sup>122</sup>, C. Kawamoto <sup>87</sup>,  
E.F. Kay <sup>37</sup>, S. Kazakos <sup>107</sup>, K. Kazakova <sup>102</sup>, J.M. Keaveney <sup>34a</sup>, R. Keeler <sup>168</sup>, G.V. Kehris <sup>60</sup>,  
J.S. Keller <sup>35</sup>, J.M. Kelly <sup>168</sup>, J.J. Kempster <sup>150</sup>, O. Kepka <sup>133</sup>, J. Kerr <sup>160b</sup>, B.P. Kerridge <sup>136</sup>,  
B.P. Kerševan <sup>93</sup>, L. Keszeghova <sup>29a</sup>, R.A. Khan <sup>131</sup>, A. Khanov <sup>123</sup>, M. Kholodenko <sup>132a</sup>,  
T.J. Khoo <sup>19</sup>, G. Khoraiuli <sup>169</sup>, Y. Khoulaki <sup>36a</sup>, Y.A.R. Khwaira <sup>129</sup>, D. Kim <sup>6</sup>, D.W. Kim <sup>18b</sup>,

Y.K. Kim <sup>39</sup>, N. Kimura <sup>96</sup>, M.K. Kingston <sup>54</sup>, F. Kirfel <sup>25</sup>, J. Kirk <sup>136</sup>, A.E. Kiryunin <sup>110</sup>,  
 S. Kita <sup>161</sup>, O. Kivernyk <sup>25</sup>, M. Klassen <sup>162</sup>, C. Klein <sup>35</sup>, L. Klein <sup>169</sup>, M.H. Klein <sup>44</sup>,  
 S.B. Klein <sup>55</sup>, U. Klein <sup>92</sup>, A. Klimentov <sup>30</sup>, P. Kluit <sup>116</sup>, S. Kluth <sup>110</sup>, E. Kneringer <sup>78</sup>,  
 T.M. Knight <sup>159</sup>, A. Knue <sup>48</sup>, M. Kobel <sup>49</sup>, D. Kobylanski <sup>172</sup>, S.F. Koch <sup>37</sup>, M. Kocian <sup>147</sup>,  
 P. Kodyš <sup>135</sup>, D.M. Koeck <sup>125</sup>, T. Koffas <sup>35</sup>, K. Kojima <sup>82</sup>, O. Kolay <sup>49</sup>, I. Koletsou <sup>4</sup>,  
 T. Komarek <sup>86</sup>, S. Kondo <sup>157</sup>, K. Köneke <sup>54</sup>, A.X.Y. Kong <sup>1</sup>, T. Kono <sup>120</sup>, N. Konstantinidis <sup>96</sup>,  
 P. Kontaxakis <sup>55</sup>, B. Konya <sup>98</sup>, R. Kopeliansky <sup>41</sup>, S. Koperny <sup>35a</sup>, R. Koppenhofer <sup>53</sup>,  
 K. Korcyl <sup>86</sup>, K. Kordas <sup>156,d</sup>, A. Korn <sup>96</sup>, S. Korn <sup>54</sup>, I. Korolkov <sup>13</sup>, B. Kortman <sup>116</sup>,  
 O. Kortner <sup>110</sup>, S. Kortner <sup>110</sup>, W.H. Kostecka <sup>117</sup>, M. Kostov <sup>29a</sup>, V.V. Kostyukhin <sup>145</sup>,  
 A. Kotskechagia <sup>37</sup>, A. Kotwal <sup>50</sup>, A. Koulouris <sup>37</sup>, A. Kourkoumeli-Charalampidi <sup>72a,72b</sup>,  
 O. Kovanda <sup>125</sup>, R. Kowalewski <sup>168</sup>, W. Kozanecki <sup>125</sup>, G. Kramberger <sup>93</sup>, P. Kramer <sup>25</sup>,  
 A. Krasznahorkay <sup>103</sup>, A.C. Kraus <sup>117</sup>, J.W. Kraus <sup>174</sup>, J.A. Kremer <sup>47</sup>, N.B. Krenzel <sup>145</sup>,  
 T. Kresse <sup>159</sup>, L. Kretschmann <sup>174</sup>, J. Kretschmar <sup>92</sup>, P. Krieger <sup>159</sup>, K. Krizka <sup>21</sup>,  
 K. Kroeninger <sup>48</sup>, H. Kroha <sup>110</sup>, J. Kroll <sup>133</sup>, J. Kroll <sup>130</sup>, K.S. Krowpman <sup>107</sup>, U. Kruchonak <sup>38</sup>,  
 H. Krüger <sup>25</sup>, N. Krumnack <sup>79</sup>, J. Krupa <sup>147</sup>, M.C. Kruse <sup>50</sup>, O. Kuchinskaia <sup>38</sup>, S. Kудay <sup>3a</sup>,  
 S. Kuehn <sup>37</sup>, R. Kuesters <sup>53</sup>, T. Kuhl <sup>47</sup>, V. Kukhtin <sup>38</sup>, Y. Kulchitsky <sup>38</sup>, S. Kuleshov <sup>139d,139b</sup>,  
 J. Kull <sup>1</sup>, E.V. Kumar <sup>109</sup>, M. Kumar <sup>34j</sup>, N. Kumari <sup>47</sup>, P. Kumari <sup>160b</sup>, A. Kupco <sup>133</sup>,  
 O. Kuprash <sup>53</sup>, H. Kurashige <sup>84</sup>, L.L. Kurchaninov <sup>160a</sup>, O. Kurdysh <sup>4</sup>, M. Kuze <sup>140</sup>,  
 A.K. Kvam <sup>103</sup>, J. Kvita <sup>124</sup>, N.G. Kyriacou <sup>141</sup>, M. Laassiri <sup>30</sup>, C. Lacasta <sup>166</sup>, H. Lacker <sup>19</sup>,  
 D. Lacour <sup>129</sup>, E. Ladygin <sup>38</sup>, A. Lafarge <sup>40</sup>, B. Laforge <sup>129</sup>, T. Lagouri <sup>175</sup>, F.Z. Lahbabi <sup>36a</sup>,  
 S. Lai <sup>54</sup>, W.S. Lai <sup>96</sup>, I.K. Lakomic <sup>54</sup>, J.E. Lambert <sup>168</sup>, S. Lammers <sup>67</sup>, W. Lampl <sup>7</sup>,  
 C. Lampoudis <sup>156</sup>, G. Lamprinoudis <sup>169</sup>, A.N. Lancaster <sup>117</sup>, U. Landgraf <sup>53</sup>, M.P.J. Landon <sup>94</sup>,  
 V.S. Lang <sup>53</sup>, A.J. Lankford <sup>163</sup>, F. Lanni <sup>37</sup>, C.S. Lantz <sup>165</sup>, K. Lantzsch <sup>25</sup>, A. Lanza <sup>72a</sup>,  
 M. Lanzac Berrocal <sup>166</sup>, T. Lari <sup>70a</sup>, D. Larsen <sup>17</sup>, L. Larson <sup>11</sup>, F. Lasagni Manghi <sup>24b</sup>,  
 M. Lassnig <sup>37</sup>, H.C. Lau <sup>168</sup>, S.D. Lawlor <sup>143</sup>, R. Lazaridou <sup>163</sup>, M. Lazzaroni <sup>70a,70b</sup>, E.T.T. Le <sup>163</sup>,  
 H.D.M. Le <sup>107</sup>, E.M. Le Boulicaut <sup>175</sup>, L.T. Le Pottier <sup>18a</sup>, B. Leban <sup>24b,24a</sup>, F. Ledroit-Guillon <sup>59</sup>,  
 T.F. Lee <sup>160b</sup>, L.L. Leeuw <sup>34h</sup>, M. Lefebvre <sup>168</sup>, C. Leggett <sup>18a</sup>, L.M. Lehmann <sup>116</sup>,  
 G. Lehmann Miotto <sup>37</sup>, M. Leigh <sup>55</sup>, W.A. Leight <sup>103</sup>, W. Leinonen <sup>115</sup>, A. Leisos <sup>156,t</sup>,  
 M.A.L. Leite <sup>81c</sup>, C.E. Leitgeb <sup>19</sup>, R. Leitner <sup>135</sup>, K.J.C. Leney <sup>44</sup>, T. Lenz <sup>25</sup>, S. Leone <sup>73a</sup>,  
 C. Leonidopoulos <sup>51</sup>, A. Leopold <sup>148</sup>, J. LePage-Bourbonnais <sup>35</sup>, R. Les <sup>107</sup>, C.G. Lester <sup>33</sup>,  
 J. Levêque <sup>4</sup>, L.J. Levinson <sup>172</sup>, G. Levrini <sup>24b,24a</sup>, M.P. Lewicki <sup>86</sup>, C. Lewis <sup>141</sup>, D.J. Lewis <sup>4</sup>,  
 L. Lewitt <sup>143</sup>, A. Li <sup>30</sup>, B. Li <sup>113b</sup>, C. Li <sup>106</sup>, C-Q. Li <sup>110</sup>, H. Li <sup>113b</sup>, H. Li <sup>101</sup>, H. Li <sup>15</sup>, H. Li <sup>61</sup>,  
 H. Li <sup>113b</sup>, J. Li <sup>142a</sup>, L. Li <sup>142a</sup>, R. Li <sup>175</sup>, S. Li <sup>142b,142a</sup>, T. Li <sup>5</sup>, Y. Li <sup>14</sup>, Z. Li <sup>14,112c</sup>,  
 Z. Li <sup>61</sup>, S. Liang <sup>14,112c</sup>, Z. Liang <sup>14</sup>, M. Liberatore <sup>137</sup>, B. Liberti <sup>75a</sup>, G.B. Libotte <sup>81d</sup>,  
 K. Lie <sup>63c</sup>, J. Lieber Marin <sup>81e</sup>, H. Lien <sup>67</sup>, H. Lin <sup>106</sup>, S.F. Lin <sup>149</sup>, L. Linden <sup>109</sup>,  
 R.E. Lindley <sup>7</sup>, J.H. Lindon <sup>37</sup>, J. Ling <sup>60</sup>, E. Lipeles <sup>130</sup>, A. Lipniacka <sup>17</sup>, A. Lister <sup>167</sup>,  
 J.D. Little <sup>67</sup>, B. Liu <sup>113a</sup>, B.X. Liu <sup>112b</sup>, D. Liu <sup>154</sup>, D. Liu <sup>138</sup>, E.H.L. Liu <sup>21</sup>, H. Liu <sup>112b</sup>,  
 J.K.K. Liu <sup>119</sup>, K. Liu <sup>142b</sup>, K. Liu <sup>142b</sup>, M. Liu <sup>61</sup>, M.Y. Liu <sup>61</sup>, P. Liu <sup>113b</sup>, Q. Liu <sup>147</sup>,  
 S. Liu <sup>149</sup>, X. Liu <sup>113b</sup>, Y. Liu <sup>112b,112c</sup>, Y. Liu <sup>165</sup>, Y.L. Liu <sup>113b</sup>, Y.W. Liu <sup>61</sup>, Z. Liu <sup>65j</sup>,  
 S.L. Lloyd <sup>94</sup>, E.M. Lobodzinska <sup>47</sup>, P. Loch <sup>7</sup>, E. Lodhi <sup>159</sup>, K. Lohwasser <sup>143</sup>, E. Loiacono <sup>123</sup>,  
 J.D. Lomas <sup>21</sup>, I. Longarini <sup>163</sup>, R. Longo <sup>24b,24a,am</sup>, A. Lopez Solis <sup>13</sup>, N.A. Lopez-canelas <sup>7</sup>,  
 N. Lorenzo Martinez <sup>4</sup>, A.M. Lory <sup>109</sup>, M. Losada <sup>118a</sup>, G. Lösckke Centeno <sup>4</sup>, X. Lou <sup>14,112c</sup>,  
 P.A. Love <sup>91</sup>, M. Lu <sup>65</sup>, S. Lu <sup>130</sup>, Y.J. Lu <sup>152</sup>, H.J. Lubatti <sup>141</sup>, C. Luci <sup>74a,74b</sup>,  
 F.L. Lucio Alves <sup>112a</sup>, F. Luehring <sup>67</sup>, B.S. Lunday <sup>130</sup>, O. Lundberg <sup>148</sup>, J. Lunde <sup>37</sup>,  
 N.A. Luongo <sup>6</sup>, M.S. Lutz <sup>159</sup>, A.B. Lux <sup>26</sup>, D. Lynn <sup>30</sup>, R. Lysak <sup>133</sup>, V. Lysenko <sup>134</sup>,  
 E. Lytken <sup>98</sup>, V. Lyubushkin <sup>38</sup>, T. Lyubushkina <sup>38</sup>, M.M. Lyukova <sup>149</sup>, H. Ma <sup>30</sup>, K. Ma <sup>61</sup>,  
 L.L. Ma <sup>113b</sup>, W. Ma <sup>61</sup>, Y. Ma <sup>113b</sup>, J.C. MacDonald <sup>100</sup>, P.C. Machado De Abreu Farias <sup>81e</sup>,

D. Macina <sup>37</sup>, R. Madar <sup>40</sup>, T. Madula <sup>96</sup>, J. Maeda <sup>84</sup>, T. Maeno <sup>30</sup>, P.T. Mafa <sup>34f</sup>,  
 H. Maguire <sup>143</sup>, M. Maheshwari <sup>33</sup>, V. Maiboroda <sup>65</sup>, A. Maio <sup>132a,132b,132d</sup>, K. Maj <sup>85a</sup>,  
 O. Majersky <sup>47</sup>, S. Majewski <sup>125</sup>, A. Makita <sup>157</sup>, N. Makovec <sup>65</sup>, V. Maksimovic <sup>16</sup>,  
 B. Malaescu <sup>129</sup>, J. Malamant <sup>127</sup>, Pa. Malecki <sup>86</sup>, F. Malek <sup>59,n</sup>, M. Mali <sup>93</sup>, D. Malito <sup>95</sup>,  
 A. Maloizel <sup>5</sup>, A. Malvezzi Lopes <sup>81d</sup>, S. Malyukov <sup>38</sup>, J. Mamuzic <sup>93</sup>, G. Mancini <sup>52</sup>,  
 M.N. Mancini <sup>27</sup>, G. Manco <sup>72a,72b</sup>, S.S. Mandarry <sup>150</sup>, I. Mandić <sup>93</sup>,  
 L. Manhaes de Andrade Filho <sup>81a</sup>, I.M. Maniatis <sup>172</sup>, J. Manjarres Ramos <sup>89</sup>, D.C. Mankad <sup>172</sup>,  
 A. Mann <sup>109</sup>, T. Manoussos <sup>37</sup>, M.N. Mantinan <sup>39</sup>, S. Manzoni <sup>37</sup>, L. Mao <sup>142a</sup>,  
 X. Mapekula <sup>34c</sup>, A. Marantis <sup>156</sup>, R.R. Marcelo Gregorio <sup>1</sup>, G. Marchiori <sup>5</sup>, C. Marcon <sup>70a</sup>,  
 E. Maricic <sup>16</sup>, M. Marinescu <sup>47</sup>, S. Marium <sup>47</sup>, M. Marjanovic <sup>122</sup>, A. Markhoos <sup>53</sup>,  
 M. Markovitch <sup>65</sup>, M.K. Maroun <sup>103</sup>, M.C. Marr <sup>146</sup>, G.T. Marsden <sup>101</sup>, Z. Marshall <sup>18a</sup>,  
 S. Marti-Garcia <sup>166</sup>, J. Martin <sup>96</sup>, T.A. Martin <sup>136</sup>, V.J. Martin <sup>51</sup>, B. Martin dit Latour <sup>17</sup>,  
 L. Martinelli <sup>74a,74b</sup>, V.I. Martinez Outschoorn <sup>103</sup>, P. Martinez Suarez <sup>37</sup>, S. Martin-Haugh <sup>136</sup>,  
 G. Martinovicova <sup>135</sup>, V.S. Martoiu <sup>28b</sup>, A. Martone <sup>89</sup>, A.C. Martyniuk <sup>96</sup>, A. Marzin <sup>37</sup>,  
 D. Mascione <sup>77a,77b</sup>, L. Masetti <sup>100</sup>, J. Masik <sup>101</sup>, A.L. Maslennikov <sup>38</sup>, S.L. Mason <sup>41</sup>,  
 P. Massarotti <sup>71a,71b</sup>, P. Mastrandrea <sup>73a,73b</sup>, A. Mastroberardino <sup>43b,43a</sup>, T. Masubuchi <sup>126</sup>,  
 T.T. Mathew <sup>125</sup>, J. Matousek <sup>135</sup>, D.M. Mattern <sup>48</sup>, K. Mauer <sup>47</sup>, J. Maurer <sup>28b</sup>, T. Maurin <sup>58</sup>,  
 A.J. Maury <sup>65</sup>, B. Maček <sup>93</sup>, C. Mavungu Tsava <sup>102</sup>, A.E. May <sup>101</sup>, E. Mayer <sup>40</sup>, R. Mazini <sup>34j</sup>,  
 S.M. Mazza <sup>138</sup>, E. Mazzeo <sup>37</sup>, J.P. Mc Gowan <sup>168</sup>, S.P. Mc Kee <sup>106</sup>, C.C. McCracken <sup>167</sup>,  
 E.F. McDonald <sup>105</sup>, L.F. Mcelhinney <sup>91</sup>, J.A. Mcfayden <sup>150</sup>, R.P. McGovern <sup>130</sup>,  
 R.P. Mckenzie <sup>34j</sup>, D.J. McLaughlin <sup>96</sup>, S.J. McMahan <sup>136</sup>, C.M. Mcpartland <sup>92</sup>,  
 R.A. McPherson <sup>168,ab</sup>, S. Mehlhase <sup>109</sup>, A. Mehta <sup>92</sup>, D. Melini <sup>166</sup>, B.R. Mellado Garcia <sup>14,ah</sup>,  
 A.H. Melo <sup>54</sup>, F. Meloni <sup>47</sup>, A.M. Mendes Jacques Da Costa <sup>101</sup>, L. Meng <sup>91</sup>, S. Menke <sup>110</sup>,  
 M. Mentink <sup>37</sup>, E. Meoni <sup>43b,43a</sup>, G. Mercado <sup>117</sup>, S. Merianos <sup>156</sup>, C. Merlassino <sup>68a,68c</sup>,  
 C. Meroni <sup>70a,70b</sup>, J. Metcalfe <sup>6</sup>, A.S. Mete <sup>6</sup>, E. Meuser <sup>100</sup>, C. Meyer <sup>67</sup>, J-P. Meyer <sup>137</sup>,  
 Y. Miao <sup>112a</sup>, R.P. Middleton <sup>136</sup>, M. Mihovilovic <sup>65</sup>, L. Mijović <sup>51</sup>, G. Mikenberg <sup>172</sup>,  
 M. Mikestikova <sup>133</sup>, M. Mikuž <sup>93</sup>, H. Mildner <sup>100</sup>, A. Milic <sup>37</sup>, D.W. Miller <sup>39</sup>, E.H. Miller <sup>147</sup>,  
 A. Milov <sup>172</sup>, D.A. Milstead <sup>46a,46b</sup>, T. Min <sup>112a</sup>, I.A. Minashvili <sup>153b</sup>, A.I. Mincer <sup>119</sup>, B. Mindur <sup>85a</sup>,  
 M. Mineev <sup>38</sup>, Y. Mino <sup>87</sup>, L.M. Mir <sup>13</sup>, M. Miralles Lopez <sup>58</sup>, M. Mironova <sup>18a</sup>, M. Missio <sup>40</sup>,  
 A. Mitra <sup>170</sup>, V.A. Mitsou <sup>166</sup>, Y. Mitsumori <sup>111</sup>, P.S. Miyagawa <sup>94</sup>, R. Mizuhiki <sup>84</sup>,  
 T. Mkrtchyan <sup>37</sup>, M. Mlinarevic <sup>96</sup>, T. Mlinarevic <sup>96</sup>, M. Mlynarikova <sup>135</sup>, L. Mlynarska <sup>85a</sup>,  
 C. Mo <sup>142a</sup>, S. Mobius <sup>20</sup>, M.H. Mohamed Farook <sup>114</sup>, S. Mohapatra <sup>41</sup>, M.F. Mohd Soberi <sup>51</sup>,  
 S. Mohiuddin <sup>123</sup>, G. Mokgatitswane <sup>34j</sup>, R. Mole <sup>21</sup>, L. Moleri <sup>172</sup>, U. Molinatti <sup>128</sup>,  
 L.G. Mollier <sup>20</sup>, B. Mondal <sup>133</sup>, S. Mondal <sup>135</sup>, K. Mönig <sup>47</sup>, E. Monnier <sup>102</sup>,  
 L. Monsonis Romero <sup>166</sup>, A. Montella <sup>46a,46b</sup>, M. Montella <sup>121</sup>, F. Montekali <sup>76a,76b</sup>,  
 F. Monticelli <sup>90</sup>, S. Monzani <sup>68a,68c</sup>, M.E.E. Moors <sup>25</sup>, A. Morancho Tarda <sup>42</sup>, N. Morange <sup>65</sup>,  
 M. Moreno Llácer <sup>166</sup>, C. Moreno Martinez <sup>55</sup>, J.M. Moreno Perez <sup>23b</sup>, P. Morettini <sup>56b</sup>,  
 S. Morgenstern <sup>62a</sup>, M. Morii <sup>60</sup>, M. Morinaga <sup>157</sup>, F. Morodei <sup>74a,74b</sup>, P. Moschovakos <sup>37</sup>,  
 B. Moser <sup>53</sup>, M. Mosidze <sup>153b</sup>, T. Moskalets <sup>44</sup>, P. Moskvitina <sup>115</sup>, C.J. Mosomane <sup>34b</sup>, J. Moss <sup>32</sup>,  
 T. Motta Quirino <sup>81d</sup>, A. Moussa <sup>36d</sup>, Y. Moyal <sup>172,k</sup>, H. Moyano Gomez <sup>13</sup>, E.J.W. Moyse <sup>103</sup>,  
 T.G. Mroz <sup>86</sup>, S. Muanza <sup>102</sup>, M. Mucha <sup>25</sup>, J. Mueller <sup>131</sup>, D. Muller <sup>145</sup>, G.A. Mullier <sup>164</sup>,  
 A.J. Mullin <sup>33</sup>, J.J. Mullin <sup>50</sup>, A.C. Mullins <sup>44</sup>, A.E. Mulski <sup>60</sup>, D.P. Mungo <sup>159</sup>, D. Munoz Perez <sup>123</sup>,  
 F.J. Munoz Sanchez <sup>101</sup>, W.J. Murray <sup>170,136</sup>, E. Musajan <sup>61</sup>, M. Muškinja <sup>93</sup>, C. Mwewa <sup>47</sup>,  
 A.J. Myers <sup>8</sup>, G. Myers <sup>106</sup>, M. Myska <sup>134</sup>, B.P. Nachman <sup>147</sup>, K. Nagai <sup>128</sup>, K. Nagano <sup>82</sup>,  
 R. Nagasaka <sup>157</sup>, J.L. Nagle <sup>30,ao</sup>, E. Nagy <sup>102</sup>, A.M. Nairz <sup>37</sup>, T. Nakagawa <sup>87</sup>, Y. Nakahama <sup>82</sup>,  
 K. Nakamura <sup>82</sup>, K. Nakkalil <sup>5</sup>, A. Nandi <sup>62b</sup>, H. Nanjo <sup>126</sup>, E.A. Narayanan <sup>44</sup>,  
 Y. Narukawa <sup>157</sup>, L. Nasella <sup>70a,70b</sup>, S. Nasri <sup>118b</sup>, C. Nass <sup>25</sup>, G. Navarro <sup>23a</sup>, A. Nayaz <sup>19</sup>,

S. Nechaeva <sup>24b,24a</sup>, F. Nechansky <sup>133</sup>, L. Nedic <sup>128</sup>, A. Negri <sup>72a,72b</sup>, M. Negrini <sup>24b</sup>,  
 C. Nellist <sup>116</sup>, C. Nelson <sup>104</sup>, K. Nelson <sup>106</sup>, S. Nemecek <sup>133</sup>, M. Nessi <sup>37.g</sup>, M.S. Neubauer <sup>165</sup>,  
 J. Newell <sup>92</sup>, P.R. Newman <sup>21</sup>, Y.W.Y. Ng <sup>165</sup>, B. Ngair <sup>118a</sup>, H.D.N. Nguyen <sup>108</sup>,  
 J.D. Nichols <sup>122</sup>, R. Nicolaidou <sup>137</sup>, J. Nielsen <sup>138</sup>, M. Niemeyer <sup>54</sup>, J. Niermann <sup>37</sup>,  
 N. Nikiforou <sup>37</sup>, I. Nikolic-Audit <sup>129</sup>, P. Nilsson <sup>30</sup>, G. Ninio <sup>155</sup>, A. Nisati <sup>74a</sup>, R. Nisius <sup>110</sup>,  
 N. Nitika <sup>172</sup>, E.K. Nkadimeng <sup>34b</sup>, T. Nobe <sup>157</sup>, D. Noll <sup>147</sup>, T. Nommensen <sup>151</sup>,  
 M.B. Norfolk <sup>143</sup>, B.J. Norman <sup>35</sup>, L.C. Nosler <sup>18a</sup>, M. Noury <sup>36a</sup>, J. Novak <sup>93</sup>, T. Novak <sup>93</sup>,  
 P. Novotny <sup>172</sup>, R. Novotny <sup>134</sup>, L. Nozka <sup>124</sup>, K. Ntekas <sup>37</sup>, D. Ntounis <sup>147</sup>,  
 N.M.J. Nunes De Moura Junior <sup>81b</sup>, J. Ocariz <sup>129</sup>, I. Ochoa <sup>132a</sup>, A. Odella Rodriguez <sup>13</sup>,  
 S. Oerdek <sup>47</sup>, J.T. Offermann <sup>39</sup>, A. Ogrodnik <sup>86</sup>, A. Oh <sup>101</sup>, C.C. Ohm <sup>148</sup>, H. Oide <sup>82</sup>,  
 M.L. Ojeda <sup>37</sup>, Y. Okumura <sup>157</sup>, L.F. Oleiro Seabra <sup>132a</sup>, I. Oleksiyuk <sup>55</sup>, G. Oliveira Correa <sup>13</sup>,  
 D. Oliveira Damazio <sup>30</sup>, J.L. Oliver <sup>1</sup>, R. Omar <sup>67</sup>, A.P. O'Neill <sup>20</sup>, Y. Onoda <sup>140</sup>,  
 A. Onofre <sup>132a,132e,e</sup>, P.U.E. Onyisi <sup>11</sup>, M.J. Oreglia <sup>39</sup>, D. Orestano <sup>76a,76b</sup>, R. Orlandini <sup>76a,76b</sup>,  
 R.S. Orr <sup>159</sup>, L.M. Osojnak <sup>41</sup>, Y. Osumi <sup>111</sup>, G. Otero y Garzón <sup>31</sup>, H. Otono <sup>88</sup>,  
 M. Ouchrif <sup>36d</sup>, F. Ould-Saada <sup>127</sup>, T. Ovsiannikova <sup>141</sup>, M. Owen <sup>58</sup>, R.E. Owen <sup>136</sup>,  
 S.A. Oyeniran <sup>114</sup>, V.E. Ozcan <sup>22a</sup>, F. Ozturk <sup>86</sup>, N. Ozturk <sup>8</sup>, S. Ozturk <sup>80</sup>, H.A. Pacey <sup>128</sup>,  
 K. Pachal <sup>160a</sup>, A. Pacheco Pages <sup>13</sup>, C. Padilla Aranda <sup>13</sup>, G. Padovano <sup>74a,74b</sup>,  
 S. Pagan Griso <sup>18a</sup>, L. Pagani <sup>75a,75b</sup>, J. Pampel <sup>25</sup>, D.K. Panchal <sup>11</sup>, C.E. Pandini <sup>59</sup>,  
 J.G. Panduro Vazquez <sup>136</sup>, H.D. Pandya <sup>1</sup>, H. Pang <sup>137</sup>, P. Pani <sup>47</sup>, G. Panizzo <sup>68a,68c</sup>,  
 L. Panwar <sup>129,w</sup>, L. Paolozzi <sup>55</sup>, S. Parajuli <sup>165</sup>, A. Paramonov <sup>6</sup>, C. Paraskevopoulos <sup>52</sup>,  
 D. Paredes Hernandez <sup>63b</sup>, S.R. Paredes Saenz <sup>51</sup>, A. Pareti <sup>72a,72b</sup>, K.R. Park <sup>41</sup>, T.H. Park <sup>110</sup>,  
 F. Parodi <sup>56b,56a</sup>, J.A. Parsons <sup>41</sup>, U. Parzefall <sup>53</sup>, B.A. Paschen <sup>18a</sup>, B. Pascual Dias <sup>40</sup>,  
 L. Pascual Dominguez <sup>99</sup>, E. Pasqualucci <sup>74a</sup>, S. Passaggio <sup>56b</sup>, F. Pastore <sup>95</sup>, P. Patel <sup>86</sup>,  
 U.M. Patel <sup>50</sup>, J.R. Pater <sup>101</sup>, T. Pauly <sup>37</sup>, A. Paunovic <sup>16</sup>, F. Pauwels <sup>135</sup>, C.I. Pazos <sup>162</sup>,  
 M. Pedersen <sup>127</sup>, R. Pedro <sup>132a</sup>, O. Penc <sup>133</sup>, C.C. Penelaud <sup>129</sup>, S. Peng <sup>15</sup>, G.D. Penn <sup>175</sup>,  
 B.S. Peralva <sup>81d</sup>, A.P. Pereira Peixoto <sup>141</sup>, L. Pereira Sanchez <sup>147</sup>, D.V. Perepelitsa <sup>30,ao</sup>,  
 G. Perera <sup>103</sup>, E. Perez Codina <sup>37</sup>, M. Perganti <sup>10</sup>, H. Pernegger <sup>37</sup>, S. Perrella <sup>74a,74b</sup>,  
 K. Peters <sup>47</sup>, R.F.Y. Peters <sup>101</sup>, B.A. Petersen <sup>37</sup>, T.C. Petersen <sup>42</sup>, E. Petit <sup>102</sup>, V. Petousis <sup>134</sup>,  
 A.R. Petri <sup>70a,70b</sup>, T. Petru <sup>135</sup>, M. Pettee <sup>18a</sup>, A. Petukhov <sup>80</sup>, K. Petukhova <sup>37</sup>, R. Pezoa <sup>139g</sup>,  
 L. Pezzotti <sup>24b,24a</sup>, G. Pezzullo <sup>175</sup>, L. Pfaffenbichler <sup>37</sup>, A.J. Pflieger <sup>78</sup>, T.M. Pham <sup>173</sup>,  
 T. Pham <sup>105</sup>, P.W. Phillips <sup>136</sup>, G. Piacquadio <sup>149</sup>, E. Pianori <sup>18a</sup>, F. Piazza <sup>125</sup>, R. Piegai <sup>31</sup>,  
 D. Pietreanu <sup>28b</sup>, A.D. Pilkington <sup>101</sup>, M. Pinamonti <sup>68a,68c</sup>, J.L. Pinfeld <sup>2</sup>, G. Pinheiro Matos <sup>41</sup>,  
 B.C. Pinheiro Pereira <sup>132a</sup>, J. Pinol Bel <sup>13</sup>, A.E. Pinto Pinoargote <sup>129</sup>, L. Pintucci <sup>68a,68c</sup>,  
 K.M. Piper <sup>150</sup>, A. Pirttikoski <sup>55</sup>, D.A. Pizzi <sup>35</sup>, L. Pizzimento <sup>63b</sup>, A. Plebani <sup>33</sup>,  
 M.-A. Pleier <sup>30</sup>, V. Pleskot <sup>135</sup>, E. Plotnikova <sup>38</sup>, G. Poddar <sup>94</sup>, R. Poettgen <sup>98</sup>, L. Poggioli <sup>129</sup>,  
 S. Polacek <sup>135</sup>, G. Polesello <sup>72a</sup>, A. Poley <sup>146</sup>, A. Polini <sup>24b</sup>, C.S. Pollard <sup>170</sup>, Z.B. Pollock <sup>121</sup>,  
 E. Pompa Pacchi <sup>122</sup>, N.I. Pond <sup>96</sup>, D. Ponomarenko <sup>67</sup>, L. Pontecorvo <sup>37</sup>, S. Popa <sup>28a</sup>,  
 G.A. Popeneciu <sup>28d</sup>, A. Poreba <sup>62a</sup>, D.M. Portillo Quintero <sup>160a</sup>, S. Pospisil <sup>134</sup>, M.A. Postill <sup>143</sup>,  
 P. Postolache <sup>28c</sup>, K. Potamianos <sup>170</sup>, P.A. Potepa <sup>85a</sup>, I.N. Potrap <sup>38</sup>, C.J. Potter <sup>33</sup>, H. Potti <sup>151</sup>,  
 J. Poveda <sup>166</sup>, M.E. Pozo Astigarraga <sup>37</sup>, R. Pozzi <sup>37</sup>, A. Prades Ibanez <sup>75a,75b</sup>, S.R. Pradhan <sup>143</sup>,  
 J. Pretel <sup>168</sup>, D. Price <sup>101</sup>, M. Primavera <sup>69a</sup>, L. Primomo <sup>68a,68c</sup>, M.A. Principe Martin <sup>99</sup>,  
 R. Privara <sup>124</sup>, T. Procter <sup>85b</sup>, M.L. Proffitt <sup>141</sup>, N. Proklova <sup>130</sup>, K. Prokofiev <sup>63c</sup>, G. Proto <sup>110</sup>,  
 J. Proudfoot <sup>6</sup>, M. Przybycien <sup>85a</sup>, W.W. Przygoda <sup>85b</sup>, A. Psallidas <sup>45</sup>, D. Pudzha <sup>52</sup>, P. Puhl <sup>57</sup>,  
 H.I. Purnell <sup>1</sup>, D. Pyatizbyantseva <sup>115</sup>, J. Qian <sup>106</sup>, R. Qian <sup>107</sup>, D. Qichen <sup>128</sup>, Y. Qin <sup>13</sup>,  
 T. Qiu <sup>51</sup>, A. Quadt <sup>54</sup>, M. Queitsch-Maitland <sup>101</sup>, G. Quetant <sup>55</sup>, R.P. Quinn <sup>167</sup>,  
 D. Rafanoharana <sup>110</sup>, J.L. Rainbolt <sup>39</sup>, S. Rajagopalan <sup>30</sup>, E. Ramakoti <sup>38</sup>, L. Rambelli <sup>56b,56a</sup>,  
 I.A. Ramirez-Berend <sup>35</sup>, K. Ran <sup>106,112c</sup>, S.D. Randles <sup>92</sup>, D.S. Rankin <sup>130</sup>, N.P. Rapheeha <sup>34j</sup>,

H. Rasheed <sup>28b</sup>, A. Rastogi <sup>18a</sup>, S. Rave <sup>100</sup>, S. Ravera <sup>56b,56a</sup>, B. Ravina <sup>37</sup>, I. Ravinovich <sup>172</sup>,  
 M. Raymond <sup>37</sup>, A.L. Read <sup>127</sup>, N.P. Readioff <sup>143</sup>, D.M. Rebuzzi <sup>72a,72b</sup>, A.S. Reed <sup>58</sup>,  
 K. Reeves <sup>27</sup>, D. Reikher <sup>37</sup>, A. Rej <sup>48</sup>, C. Rembser <sup>37</sup>, H. Ren <sup>61</sup>, M. Renda <sup>28b</sup>, F. Renner <sup>47</sup>,  
 A.G. Rennie <sup>58</sup>, M. Repik <sup>55</sup>, A.L. Rescia <sup>56b,56a</sup>, S. Resconi <sup>70a</sup>, M. Ressegotti <sup>56b</sup>,  
 S. Rettie <sup>116</sup>, W.F. Rettie <sup>35</sup>, M.M. Revering <sup>33</sup>, O.L. Rezanova <sup>38</sup>, P. Reznicek <sup>135</sup>, H. Riani <sup>36d</sup>,  
 N. Ribaric <sup>50</sup>, B. Ricci <sup>68a,68c</sup>, E. Ricci <sup>77a,77b</sup>, R. Richter <sup>110</sup>, E. Richter-Was <sup>85b</sup>, M. Ridel <sup>129</sup>,  
 S. Ridouani <sup>36d</sup>, P. Riedler <sup>37</sup>, E.M. Riefel <sup>46a,46b</sup>, J.O. Rieger <sup>116</sup>, M. Rimoldi <sup>34c</sup>,  
 L. Rinaldi <sup>24b,24a</sup>, P. Rincke <sup>164,54</sup>, G. Ripellino <sup>164</sup>, I. Riu <sup>13</sup>, J.C. Rivera Vergara <sup>168</sup>,  
 F. Rizatdinova <sup>123</sup>, E. Rizvi <sup>94</sup>, B.R. Roberts <sup>39</sup>, S.S. Roberts <sup>138</sup>, D. Robinson <sup>33</sup>, A. Robson <sup>58</sup>,  
 A. Rocchi <sup>75a,75b</sup>, C. Roda <sup>73a,73b</sup>, F.A. Rodriguez <sup>117</sup>, S. Rodriguez Bosca <sup>37</sup>,  
 Y. Rodriguez Garcia <sup>23a</sup>, A.M. Rodríguez Vera <sup>117</sup>, S. Roe <sup>37</sup>, J.T. Roemer <sup>37</sup>, O. Røhne <sup>127</sup>,  
 R.A. Rojas <sup>37</sup>, Z. Rokavec <sup>93</sup>, C.P.A. Roland <sup>129</sup>, A. Romaniouk <sup>78</sup>, E. Romano <sup>72a,72b</sup>,  
 M. Romano <sup>24b</sup>, N. Rompotis <sup>92</sup>, L. Roos <sup>129</sup>, S. Rosati <sup>74a</sup>, L. Roscher <sup>47</sup>, B.J. Rosser <sup>39</sup>,  
 E. Rossi <sup>128</sup>, E. Rossi <sup>71a,71b</sup>, L.P. Rossi <sup>60</sup>, L. Rossini <sup>53</sup>, R. Rosten <sup>121</sup>, M. Rotaru <sup>28b</sup>,  
 R. Roth <sup>37</sup>, D. Rousseau <sup>65</sup>, D. Rousso <sup>47</sup>, S. Roy-Garand <sup>159</sup>, A. Rozanov <sup>102</sup>,  
 Z.M.A. Rozario <sup>58</sup>, Y. Rozen <sup>154</sup>, A. Rubio Jimenez <sup>166</sup>, V.H. Ruelas Rivera <sup>19</sup>, T.A. Ruggeri <sup>1</sup>,  
 A. Ruggiero <sup>128</sup>, A. Ruiz-Martinez <sup>166</sup>, A. Rummler <sup>37</sup>, G.B. Rupnik Boero <sup>37</sup>,  
 N.A. Rusakovich <sup>38</sup>, S. Ruscelli <sup>48</sup>, H.L. Russell <sup>168</sup>, G. Russo <sup>138</sup>, J.P. Rutherford <sup>7</sup>,  
 S. Rutherford Colmenares <sup>119</sup>, M. Rybar <sup>135</sup>, P. Rybczynski <sup>85a</sup>, A. Ryzhov <sup>44</sup>,  
 F. Safai Tehrani <sup>74a</sup>, S. Saha <sup>1</sup>, B. Sahoo <sup>172</sup>, A. Saibel <sup>166</sup>, B.T. Saifuddin <sup>122</sup>, M. Saimpert <sup>137</sup>,  
 I. Sainz Saenz Diez <sup>62a</sup>, G.T. Saito <sup>81c</sup>, M. Saito <sup>157</sup>, T. Saito <sup>157</sup>, A. Sala <sup>70a,70b</sup>, O.T. Salin <sup>65</sup>,  
 A. Salnikov <sup>147</sup>, J. Salt <sup>166</sup>, A. Salvador Salas <sup>155</sup>, F. Salvatore <sup>150</sup>, A. Salzburger <sup>37</sup>,  
 D. Sammel <sup>53</sup>, E. Sampson <sup>91</sup>, D. Sampsonidis <sup>156,d</sup>, D. Sampsonidou <sup>125</sup>, M.A.A. Samy <sup>58</sup>,  
 J. Sánchez <sup>166</sup>, V. Sanchez Sebastian <sup>166</sup>, H. Sandaker <sup>127</sup>, C.O. Sander <sup>47</sup>, J.A. Sandesara <sup>173</sup>,  
 M. Sandhoff <sup>174</sup>, C. Sandoval <sup>23b</sup>, L. Sanfilippo <sup>62a</sup>, D.P.C. Sankey <sup>136</sup>, T. Sano <sup>87</sup>, A. Sansar <sup>22c</sup>,  
 A. Sansoni <sup>52</sup>, M. Santana Queiroz <sup>18b</sup>, L. Santi <sup>37</sup>, C. Santoni <sup>40</sup>, H. Santos <sup>132a,132b</sup>,  
 L. Santos Pereira Trigo <sup>47</sup>, E. Sanzani <sup>24b,24a</sup>, K.A. Saoucha <sup>83b</sup>, J.G. Saraiva <sup>132a,132d</sup>,  
 J. Sardain <sup>7</sup>, S. Sarkar <sup>50</sup>, O. Sasaki <sup>82</sup>, K. Sato <sup>161</sup>, C. Sauer <sup>37</sup>, E. Sauvan <sup>4</sup>, P. Savard <sup>159,aj</sup>,  
 R. Sawada <sup>157</sup>, C. Sawyer <sup>136</sup>, L. Sawyer <sup>97</sup>, A.M. Sayed <sup>27</sup>, C. Sbarra <sup>24b</sup>, A. Sbrizzi <sup>24b,24a</sup>,  
 R. Scaglioni <sup>72a,72b</sup>, T. Scanlon <sup>96</sup>, J. Schaarschmidt <sup>141</sup>, U. Schäfer <sup>100</sup>, A.C. Schaffer <sup>65,44</sup>,  
 D. Schaile <sup>109</sup>, R.D. Schamberger <sup>149</sup>, C. Scharf <sup>19</sup>, M.M. Schefer <sup>20</sup>, D. Scheirich <sup>135</sup>,  
 M. Schernau <sup>139f</sup>, C. Scheulen <sup>55</sup>, C. Schiavi <sup>56b,56a</sup>, M. Schioppa <sup>43b,43a</sup>, S. Schlenker <sup>37</sup>,  
 T. Schlomer <sup>54</sup>, J. Schmeing <sup>174</sup>, E. Schmidt <sup>110</sup>, M.A. Schmidt <sup>174</sup>, K. Schmieden <sup>25</sup>,  
 C. Schmitt <sup>100</sup>, N. Schmitt <sup>100</sup>, S. Schmitt <sup>47</sup>, N.A. Schneider <sup>109</sup>, L. Schoeffel <sup>137</sup>,  
 A. Schoening <sup>62b</sup>, P.G. Scholer <sup>35</sup>, E. Schopf <sup>145</sup>, M. Schott <sup>25</sup>, S. Schramm <sup>55</sup>, T. Schroer <sup>55</sup>,  
 H-C. Schultz-Coulon <sup>62a</sup>, M. Schumacher <sup>53</sup>, B.A. Schumm <sup>138</sup>, Ph. Schune <sup>137</sup>, H.R. Schwartz <sup>7</sup>,  
 A. Schwartzman <sup>147</sup>, T.A. Schwarz <sup>106</sup>, Ph. Schwemling <sup>137</sup>, R. Schwienhorst <sup>107</sup>,  
 F.G. Sciacca <sup>20</sup>, A. Sciandra <sup>30</sup>, G. Sciolla <sup>27</sup>, S.A. Scoville <sup>131</sup>, F. Scuri <sup>73a</sup>, C.D. Sebastiani <sup>37</sup>,  
 K. Sedlaczek <sup>117</sup>, A. Sehwat <sup>139b</sup>, S.C. Seidel <sup>114</sup>, B.D. Seidlitz <sup>41</sup>, C. Seitz <sup>47</sup>,  
 J.M. Seixas <sup>81b</sup>, G. Sekhniaidze <sup>71a</sup>, L. Selem <sup>129</sup>, N. Semprini-Cesari <sup>24b,24a</sup>, A. Semushin <sup>176</sup>,  
 V. Senthilkumar <sup>116</sup>, L. Serin <sup>65</sup>, M. Sessa <sup>71a,71b</sup>, H. Severini <sup>122</sup>, F. Sforza <sup>56b,56a</sup>, A. Sfyrla <sup>55</sup>,  
 Q. Sha <sup>14</sup>, H. Shaddix <sup>117</sup>, A.H. Shah <sup>33</sup>, R. Shaheen <sup>148</sup>, J.D. Shahinian <sup>130</sup>, M. Shamim <sup>37</sup>,  
 L.Y. Shan <sup>14</sup>, M. Shapiro <sup>18a</sup>, A. Sharma <sup>37</sup>, A.S. Sharma <sup>167</sup>, P. Sharma <sup>30</sup>, K. Shaw <sup>150</sup>,  
 S.M. Shaw <sup>101</sup>, D. Shemyakin <sup>172</sup>, Q. Shen <sup>14</sup>, D.J. Sheppard <sup>146</sup>, P. Sherwood <sup>96</sup>, L. Shi <sup>112b</sup>,  
 X. Shi <sup>14</sup>, S. Shimizu <sup>82</sup>, S. Shirabe <sup>88</sup>, M. Shiyakova <sup>38,z</sup>, M.J. Shochet <sup>39</sup>, D.R. Shope <sup>127</sup>,  
 B. Shrestha <sup>122</sup>, S. Shrestha <sup>121,aq</sup>, I. Shreyber <sup>38</sup>, M.J. Shroff <sup>104</sup>, P. Sicho <sup>133</sup>, A.M. Sickles <sup>165</sup>,  
 E. Sideras Haddad <sup>34j</sup>, A.C. Sidley <sup>116</sup>, A. Sidoti <sup>24b</sup>, F. Siegert <sup>49</sup>, Dj. Sijacki <sup>16</sup>, F. Sili <sup>61</sup>,

J.M. Silva <sup>51</sup>, I. Silva Ferreira <sup>81b</sup>, M.V. Silva Oliveira <sup>30</sup>, S.B. Silverstein <sup>46a</sup>, S. Simion <sup>65</sup>, R. Simoniello <sup>37</sup>, E.L. Simpson <sup>101</sup>, H. Simpson <sup>150</sup>, L.R. Simpson <sup>6</sup>, S. Simsek <sup>80</sup>, S. Sindhu <sup>54</sup>, S.N. Singh <sup>27</sup>, S. Singh <sup>30</sup>, S. Sinha <sup>47</sup>, S. Sinha <sup>101</sup>, M. Sioli <sup>24b,24a</sup>, K. Sioulas <sup>9</sup>, I. Siral <sup>37</sup>, E. Sitnikova <sup>47</sup>, J. Sjölin <sup>46a,46b</sup>, A. Skaf <sup>54</sup>, E. Skorda <sup>21</sup>, P. Skubic <sup>122</sup>, M. Slawinska <sup>86</sup>, I. Slazyk <sup>17</sup>, I. Sliusar <sup>127</sup>, V. Smakhtin <sup>172</sup>, B.H. Smart <sup>136</sup>, S.Yu. Smirnov <sup>139b</sup>, Y. Smirnov <sup>34c</sup>, O. Smirnova <sup>98</sup>, A.C. Smith <sup>41</sup>, J.L. Smith <sup>101</sup>, M.B. Smith <sup>35</sup>, R. Smith <sup>147</sup>, H. Smitmanns <sup>100</sup>, M. Smizanska <sup>91</sup>, K. Smolek <sup>134</sup>, P. Smolyanskiy <sup>134</sup>, A.A. Snesarev <sup>38</sup>, H.L. Snoek <sup>116</sup>, R.M. Snyder <sup>50</sup>, S. Snyder <sup>30</sup>, R. Sobie <sup>168,ab</sup>, A. Soffer <sup>155</sup>, C.A. Solans Sanchez <sup>37</sup>, E.Yu. Soldatov <sup>38</sup>, U. Soldevila <sup>166</sup>, A.A. Solodkov <sup>34j</sup>, S. Solomon <sup>27</sup>, A. Soloshenko <sup>38</sup>, O.V. Solovyanov <sup>40</sup>, P. Sommer <sup>49</sup>, A. Sopczak <sup>134</sup>, A.L. Sopio <sup>51</sup>, F. Sopkova <sup>29b</sup>, J.D. Sorenson <sup>114</sup>, I.R. Sotarriva Alvarez <sup>140</sup>, V. Sothilingam <sup>62a</sup>, O.J. Soto Sandoval <sup>139c,139b</sup>, S. Sottocornola <sup>67</sup>, R. Soualah <sup>83a</sup>, D. South <sup>47</sup>, N. Soybelman <sup>172</sup>, S. Spagnolo <sup>69a,69b</sup>, A.S. Spellman <sup>125</sup>, D. Sperlich <sup>53</sup>, B. Spisso <sup>71a,71b</sup>, L. Splendori <sup>102</sup>, M. Spousta <sup>135</sup>, E.J. Staats <sup>35</sup>, R. Stamen <sup>62a</sup>, E. Stanecka <sup>86</sup>, W. Stanek-Maslouska <sup>47</sup>, M.V. Stange <sup>49</sup>, B. Stanislaus <sup>18a</sup>, M.M. Stanitzki <sup>47</sup>, G.H. Stark <sup>138</sup>, J. Stark <sup>89</sup>, P. Staroba <sup>133</sup>, P. Starovoitov <sup>83b</sup>, R. Staszewski <sup>86</sup>, C. Stauch <sup>109</sup>, G. Stavropoulos <sup>45</sup>, A. Steff <sup>37</sup>, A. Stein <sup>100</sup>, P. Steinberg <sup>30</sup>, B. Stelzer <sup>146,160a</sup>, H.J. Stelzer <sup>131</sup>, O. Stelzer <sup>160a</sup>, H. Stenzel <sup>57</sup>, T.J. Stevenson <sup>150</sup>, G.A. Stewart <sup>47</sup>, G. Stoicea <sup>28b</sup>, M. Stolarski <sup>132a</sup>, S. Stonjek <sup>110</sup>, A. Straessner <sup>49</sup>, J. Strandberg <sup>148</sup>, S. Strandberg <sup>46a,46b</sup>, M. Stratmann <sup>174</sup>, M. Strauss <sup>122</sup>, T. Strebler <sup>102</sup>, P. Strizenec <sup>29b</sup>, R. Ströhmer <sup>169</sup>, D.M. Strom <sup>125</sup>, R. Stroynowski <sup>44</sup>, A. Strubig <sup>46a,46b</sup>, S.A. Stucci <sup>30</sup>, B. Stugu <sup>17</sup>, J. Stupak <sup>122</sup>, N.A. Styles <sup>47</sup>, D. Su <sup>147</sup>, S. Su <sup>61</sup>, X. Su <sup>61</sup>, D. Suchy <sup>29a</sup>, A.D. Sudhakar Ponnu <sup>54</sup>, L. Sudit <sup>172</sup>, Y. Sue <sup>82</sup>, K. Sugizaki <sup>130</sup>, D.M.S. Sultan <sup>128</sup>, L. Sultanliyeva <sup>25</sup>, S. Sultansoy <sup>3b</sup>, S. Sun <sup>173</sup>, W. Sun <sup>14</sup>, S. Sundar Raman <sup>167</sup>, N. Sur <sup>98</sup>, J.P. Surdutovich <sup>121</sup>, N. Suri Jr <sup>175</sup>, M.R. Sutton <sup>150</sup>, M. Svatos <sup>133</sup>, P.N. Swallow <sup>33</sup>, S.N. Swatman <sup>37</sup>, M. Swiatlowski <sup>160a</sup>, A. Swoboda <sup>37</sup>, I. Sykora <sup>29a</sup>, M. Sykora <sup>135</sup>, T. Sykora <sup>135</sup>, D. Ta <sup>100</sup>, K. Tackmann <sup>47,y</sup>, A. Taffard <sup>163</sup>, R. Tafirout <sup>160a</sup>, Y. Takubo <sup>82</sup>, M. Talby <sup>102</sup>, N.M. Tamir <sup>155</sup>, A. Tanaka <sup>157</sup>, J. Tanaka <sup>157</sup>, R. Tanaka <sup>65</sup>, M. Tanasini <sup>149</sup>, Z. Tao <sup>167</sup>, S. Tapia Araya <sup>139g</sup>, S. Tapprogge <sup>100</sup>, A. Tarek Abouelfadl Mohamed <sup>37</sup>, S. Tarem <sup>154</sup>, K. Tariq <sup>14</sup>, G. Tarna <sup>37</sup>, G.F. Tartarelli <sup>70a</sup>, M.J. Tartarin <sup>142b</sup>, P. Tas <sup>135</sup>, M. Tasevsky <sup>133</sup>, E. Tassi <sup>43b,43a</sup>, A.C. Tate <sup>165</sup>, Y. Tayalati <sup>36e,aa</sup>, G.N. Taylor <sup>105</sup>, W. Taylor <sup>160b</sup>, R.J. Taylor Vara <sup>166</sup>, A.S. Tegetmeier <sup>89</sup>, P. Teixeira-Dias <sup>95</sup>, J.J. Teoh <sup>159</sup>, K. Terashi <sup>157</sup>, J. Terron <sup>99</sup>, S. Terzo <sup>13</sup>, M. Testa <sup>52</sup>, R.J. Teuscher <sup>159,ab</sup>, A. Thaler <sup>78</sup>, T. Thevenaux-Pelzer <sup>102</sup>, J.P. Thomas <sup>21</sup>, E.A. Thompson <sup>18a</sup>, P.D. Thompson <sup>21</sup>, E. Thomson <sup>130</sup>, R.E. Thornberry <sup>30</sup>, T.M. Thory-Rao <sup>21</sup>, C. Tian <sup>61</sup>, Y. Tian <sup>55</sup>, V. Tikhomirov <sup>80</sup>, Yu.A. Tikhonov <sup>38</sup>, D. Timoshyn <sup>135</sup>, E.X.L. Ting <sup>1</sup>, P. Tipton <sup>175</sup>, A. Tishelman-Charny <sup>30</sup>, K. Todome <sup>140</sup>, S. Todorova-Nova <sup>135</sup>, L. Toffolin <sup>68a,68c</sup>, M. Togawa <sup>82</sup>, J. Tojo <sup>88</sup>, S. Tokár <sup>29a</sup>, O. Toldaiev <sup>67</sup>, G. Tolkachev <sup>102</sup>, M. Tomoto <sup>82</sup>, L. Tompkins <sup>147</sup>, E. Torrence <sup>125</sup>, H. Torres <sup>89</sup>, D.I. Torres Arza <sup>139g</sup>, E. Torres Reoyo <sup>166</sup>, E. Torró Pastor <sup>166</sup>, M. Toscani <sup>31</sup>, C. Tosciri <sup>39</sup>, M. Tost <sup>11</sup>, D.R. Tovey <sup>143</sup>, T. Trefzger <sup>169</sup>, P.M. Tricarico <sup>13</sup>, A. Tricoli <sup>30</sup>, I.M. Trigger <sup>160a</sup>, S. Trincaz-Duvoid <sup>129</sup>, D.A. Trischuk <sup>168</sup>, A. Tropina <sup>38</sup>, D. Truncali <sup>75a,75b</sup>, L. Truong <sup>34c</sup>, M. Trzebinski <sup>86</sup>, A. Trzupek <sup>86</sup>, F. Tsai <sup>149</sup>, A. Tsiamis <sup>156</sup>, P.V. Tsiarehka <sup>38</sup>, S. Tsigaridas <sup>160a</sup>, A. Tsirigotis <sup>156,t</sup>, V. Tsiskaridze <sup>153a</sup>, E.G. Tskhadadze <sup>153a</sup>, H.F. Tsoi <sup>130</sup>, Y. Tsujikawa <sup>87</sup>, V. Tsulaia <sup>18a</sup>, K. Tsurii <sup>120</sup>, D. Tsybychev <sup>149</sup>, Y. Tu <sup>63b</sup>, A. Tudorache <sup>28b</sup>, V. Tudorache <sup>28b</sup>, S.B. Tuncay <sup>128</sup>, S. Turchikhin <sup>56b,56a</sup>, I. Turk Cakir <sup>3a</sup>, R. Turra <sup>70a</sup>, T. Turtuvshin <sup>38,ac</sup>, P.M. Tuts <sup>41</sup>, Y. Uematsu <sup>82</sup>, F. Ukegawa <sup>161</sup>, P.A. Ulloa Poblete <sup>139c,139b</sup>, G. Unal <sup>37</sup>, A. Undrus <sup>30</sup>, J. Urban <sup>29b</sup>, P. Urrejola <sup>139e</sup>, G. Usai <sup>8</sup>, R. Ushioda <sup>158</sup>, M. Usman <sup>108</sup>, F. Ustuner <sup>51</sup>, Z. Uysal <sup>80</sup>, V. Vacek <sup>134</sup>, B. Vachon <sup>104</sup>,

T. Vafeiadis <sup>37</sup>, A. Vaitkus <sup>96</sup>, C. Valderanis <sup>109</sup>, E. Valdes Santurio <sup>46a,46b</sup>, M. Valente <sup>37</sup>,  
 S. Valentinetti <sup>24b,24a</sup>, A. Valero <sup>166</sup>, E. Valiente Moreno <sup>166</sup>, A. Vallier <sup>89</sup>, J.A. Valls Ferrer <sup>166</sup>,  
 D.R. Van Arneman <sup>116</sup>, R. Van Den Broucke <sup>129</sup>, A. Van Der Graaf <sup>48</sup>, H.Z. Van Der Schyf <sup>34j</sup>,  
 P. Van Gemmeren <sup>6</sup>, M. Van Rijnbach <sup>37</sup>, S. Van Stroud <sup>96</sup>, I. Van Vulpen <sup>116</sup>, P. Vana <sup>135</sup>,  
 M. Vanadia <sup>75a,75b</sup>, U.M. Vande Voorde <sup>148</sup>, W. Vandelli <sup>37</sup>, E.R. Vandewall <sup>147</sup>, D. Vannicola <sup>155</sup>,  
 R. Vari <sup>74a</sup>, M. Varma <sup>175</sup>, E.W. Varnes <sup>7</sup>, C. Varni <sup>85a</sup>, D. Varouchas <sup>65</sup>, L. Varriale <sup>166</sup>,  
 K.E. Varvell <sup>151</sup>, M.E. Vasile <sup>28b</sup>, A. Vasileiadou <sup>9</sup>, L. Vaslin <sup>82</sup>, M.D. Vassilev <sup>147</sup>, A. Vasyukov <sup>38</sup>,  
 L.M. Vaughan <sup>123</sup>, R. Vavricka <sup>135</sup>, T. Vazquez Schroeder <sup>13</sup>, J. Veatch <sup>32</sup>, V. Vecchio <sup>101</sup>,  
 M.J. Veen <sup>103</sup>, I. Veliscek <sup>30</sup>, I. Velkovska <sup>93</sup>, L.M. Veloce <sup>159</sup>, F. Veloso <sup>132a,132c</sup>,  
 A.G. Veltman <sup>51</sup>, S.H. Venetianer <sup>162</sup>, S. Veneziano <sup>74a</sup>, A. Ventura <sup>69a,69b</sup>, A. Verbytskyi <sup>110</sup>,  
 M. Verducci <sup>73a,73b</sup>, C. Vergis <sup>94</sup>, M. Verissimo De Araujo <sup>81b</sup>, W. Verkerke <sup>116</sup>,  
 J.C. Vermeulen <sup>116</sup>, C. Vernieri <sup>147</sup>, M. Vessella <sup>163</sup>, M.C. Vetterli <sup>146,aj</sup>, A. Vgenopoulos <sup>100</sup>,  
 N. Viaux Maira <sup>139g,af</sup>, L. Vicens <sup>134</sup>, T. Vickey <sup>143</sup>, O.E. Vickey Boeriu <sup>143</sup>,  
 G.H.A. Viehhauser <sup>128</sup>, L. Vigani <sup>62b</sup>, M. Vigi <sup>110</sup>, M. Villa <sup>24b,24a</sup>, M. Villaplana Perez <sup>166</sup>,  
 E.M. Villhauer <sup>39</sup>, E. Vilucchi <sup>52</sup>, M. Vincent <sup>166</sup>, M.G. Vincter <sup>35</sup>, A. Visibile <sup>116</sup>, A. Visive <sup>116</sup>,  
 C. Vittori <sup>162</sup>, I. Vivarelli <sup>24b,24a</sup>, M.I. Vivas Albornoz <sup>47</sup>, E. Voevodina <sup>110</sup>, F. Vogel <sup>109</sup>,  
 J.C. Voigt <sup>49</sup>, P. Vokac <sup>134</sup>, Yu. Volkotrub <sup>85b</sup>, L. Vomberg <sup>25</sup>, E. Von Toerne <sup>25</sup>,  
 B. Vormwald <sup>37</sup>, K. Vorobev <sup>50</sup>, M. Vos <sup>166</sup>, K. Voss <sup>145</sup>, M. Vozak <sup>37</sup>, L. Vozdecky <sup>122</sup>,  
 N. Vranjes <sup>16</sup>, M. Vranjes Milosavljevic <sup>16</sup>, M. Vreeswijk <sup>116</sup>, N.K. Vu <sup>112a</sup>, R. Vuillermet <sup>37</sup>,  
 O. Vujinovic <sup>100</sup>, I. Vukotic <sup>39</sup>, I.K. Vyas <sup>35</sup>, J.F. Wack <sup>33</sup>, A. Wada <sup>111</sup>, S. Wada <sup>161</sup>,  
 C. Wagner <sup>147</sup>, J.M. Wagner <sup>18a</sup>, W. Wagner <sup>174</sup>, S. Wahdan <sup>174</sup>, H. Wahlberg <sup>90</sup>, C.H. Waits <sup>122</sup>,  
 J. Walder <sup>136</sup>, R. Walker <sup>109</sup>, K. Walkingshaw Pass <sup>58</sup>, W. Walkowiak <sup>145</sup>, A. Wall <sup>130</sup>,  
 E.J. Wallin <sup>98</sup>, T. Wamorkar <sup>147</sup>, K. Wandall-Christensen <sup>166</sup>, A. Wang <sup>61</sup>, A.Z. Wang <sup>138</sup>,  
 C. Wang <sup>47</sup>, C. Wang <sup>11</sup>, H. Wang <sup>18a</sup>, J. Wang <sup>63c</sup>, P. Wang <sup>101</sup>, P. Wang <sup>96</sup>, R. Wang <sup>60</sup>,  
 R. Wang <sup>106</sup>, R. Wang <sup>6</sup>, S.M. Wang <sup>152</sup>, S. Wang <sup>14</sup>, T. Wang <sup>115</sup>, T. Wang <sup>61</sup>, W.T. Wang <sup>128</sup>,  
 X. Wang <sup>165</sup>, X. Wang <sup>142a</sup>, X. Wang <sup>47</sup>, Y. Wang <sup>149</sup>, Y. Wang <sup>114</sup>, Z. Wang <sup>106</sup>, Z. Wang <sup>14</sup>,  
 Z. Wang <sup>63b</sup>, C. Wanotayaroj <sup>82</sup>, A. Warburton <sup>104</sup>, A.L. Warnerbring <sup>145</sup>, S. Waterhouse <sup>96</sup>,  
 A.T. Watson <sup>21</sup>, H. Watson <sup>51</sup>, M.F. Watson <sup>21</sup>, E. Watton <sup>37</sup>, G. Watts <sup>141</sup>, B.M. Waugh <sup>96</sup>,  
 J.M. Webb <sup>53</sup>, C. Weber <sup>30</sup>, M.S. Weber <sup>20</sup>, C. Wei <sup>61</sup>, Y. Wei <sup>53</sup>, A.R. Weidberg <sup>128</sup>,  
 E.J. Weik <sup>119</sup>, J. Weingarten <sup>48</sup>, C. Weiser <sup>53</sup>, C.J. Wells <sup>47</sup>, T. Wenaus <sup>30</sup>, T. Wengler <sup>37</sup>,  
 N.S. Wenke <sup>110</sup>, N. Wermes <sup>25</sup>, M. Wessels <sup>62a</sup>, A.M. Wharton <sup>91</sup>, A.S. White <sup>37</sup>, A. White <sup>8</sup>,  
 M.J. White <sup>1</sup>, D. Whiteson <sup>163</sup>, L. Wickremasinghe <sup>126</sup>, W. Wiedenmann <sup>173</sup>, M. Wielers <sup>136</sup>,  
 R. Wierda <sup>148</sup>, C. Wiglesworth <sup>42</sup>, H.G. Wilkens <sup>37</sup>, J.J.H. Wilkinson <sup>33</sup>, S. Williams <sup>33</sup>,  
 S. Willocq <sup>103</sup>, D.J. Wilson <sup>101</sup>, P.J. Windischhofer <sup>39</sup>, F.I. Winkel <sup>31</sup>, F. Winklmeier <sup>125</sup>,  
 B.T. Winter <sup>53</sup>, M. Wittgen <sup>147</sup>, M. Wobisch <sup>97</sup>, T. Wojtkowski <sup>59</sup>, Z. Wolfs <sup>116</sup>, J. Wollrath <sup>37</sup>,  
 M.W. Wolter <sup>86</sup>, H. Wolters <sup>132a,132c</sup>, M.C. Wong <sup>138</sup>, E.L. Woodward <sup>41</sup>, S.D. Worm <sup>47</sup>,  
 B.K. Wosiek <sup>86</sup>, K.A. Wozniak <sup>55</sup>, K.W. Woźniak <sup>86</sup>, S. Wozniowski <sup>54</sup>, K. Wraight <sup>58</sup>,  
 C. Wu <sup>159</sup>, C. Wu <sup>21</sup>, J. Wu <sup>157</sup>, M. Wu <sup>112b</sup>, M. Wu <sup>115</sup>, S.L. Wu <sup>173</sup>, S. Wu <sup>14,an</sup>, X. Wu <sup>61</sup>,  
 Y.Q. Wu <sup>159</sup>, Y. Wu <sup>61</sup>, Z. Wu <sup>102</sup>, Z. Wu <sup>112a</sup>, J. Wuerzinger <sup>110</sup>, T.R. Wyatt <sup>101</sup>,  
 B.M. Wynne <sup>51</sup>, S. Xella <sup>42</sup>, L. Xia <sup>112a</sup>, M. Xie <sup>61</sup>, A. Xiong <sup>125</sup>, I. Xiotidis <sup>37</sup>, D. Xu <sup>14</sup>,  
 H. Xu <sup>61</sup>, L. Xu <sup>61</sup>, R. Xu <sup>130</sup>, T. Xu <sup>106</sup>, W. Xu <sup>112a</sup>, Y. Xu <sup>141</sup>, Z. Xu <sup>51</sup>, R. Xue <sup>131</sup>,  
 B. Yabsley <sup>151</sup>, S. Yacoob <sup>11</sup>, Y. Yamaguchi <sup>82</sup>, E. Yamashita <sup>157</sup>, H. Yamauchi <sup>161</sup>,  
 T. Yamazaki <sup>18a</sup>, Y. Yamazaki <sup>84</sup>, S. Yan <sup>58</sup>, Z. Yan <sup>103</sup>, C. Yang <sup>18a</sup>, H.J. Yang <sup>142a</sup>,  
 H.T. Yang <sup>61</sup>, S. Yang <sup>61</sup>, X. Yang <sup>37</sup>, X. Yang <sup>14</sup>, Y. Yang <sup>157</sup>, Y. Yang <sup>61</sup>, W-M. Yao <sup>18a</sup>,  
 C.L. Yardley <sup>150</sup>, J. Ye <sup>14</sup>, S. Ye <sup>30</sup>, X. Ye <sup>61</sup>, I. Yeletsikh <sup>38</sup>, B. Yeo <sup>18b</sup>, M.R. Yexley <sup>96</sup>,  
 T.P. Yildirim <sup>128</sup>, K. Yorita <sup>171</sup>, C.J.S. Young <sup>37</sup>, C. Young <sup>147</sup>, I.N.L. Young <sup>58</sup>, N.D. Young <sup>125</sup>,  
 Y. Yu <sup>61</sup>, J. Yuan <sup>14,112c,an</sup>, M. Yuan <sup>106</sup>, R. Yuan <sup>142b</sup>, L. Yue <sup>96</sup>, M. Zaazoua <sup>61</sup>,

B. Zabinski <sup>86</sup>, I. Zahir <sup>36a</sup>, Q.U.A. Zahoor <sup>51</sup>, A. Zaio<sup>56b,56a</sup>, Z.K. Zak <sup>86</sup>, T. Zakareishvili <sup>166</sup>, S. Zambito <sup>55</sup>, J. Zang <sup>157</sup>, R. Zanzottera <sup>70a,70b</sup>, O. Zaplatilek <sup>134</sup>, E. Zaya <sup>148</sup>, C. Zeitnitz <sup>174</sup>, H. Zeng <sup>14</sup>, D.T. Zenger Jr <sup>27</sup>, T. Ženiš <sup>29a</sup>, S. Zenz <sup>94</sup>, D. Zerwas <sup>65</sup>, B. Zhang <sup>170</sup>, D.F. Zhang <sup>143</sup>, G. Zhang <sup>14,an</sup>, J. Zhang <sup>113b</sup>, J. Zhang <sup>6</sup>, L. Zhang <sup>61</sup>, L. Zhang <sup>112a</sup>, P. Zhang <sup>14,112c</sup>, R. Zhang <sup>112a</sup>, S. Zhang <sup>89</sup>, Y. Zhang <sup>141</sup>, Y. Zhang <sup>96</sup>, Y. Zhang <sup>61</sup>, Y. Zhang <sup>112a</sup>, Z. Zhang <sup>18a</sup>, Z. Zhang <sup>113b</sup>, Z. Zhang <sup>65</sup>, H. Zhao <sup>141</sup>, T. Zhao <sup>113b</sup>, Y. Zhao <sup>35</sup>, Z. Zhao <sup>61</sup>, Z. Zhao <sup>61</sup>, A. Zhemchugov <sup>38</sup>, J. Zheng <sup>112a</sup>, K. Zheng <sup>165</sup>, L. Zheng <sup>113b</sup>, X. Zheng <sup>61</sup>, Z. Zheng <sup>147</sup>, D. Zhong <sup>165</sup>, B. Zhou <sup>106</sup>, B. Zhou <sup>142b,142a</sup>, N. Zhou <sup>142a</sup>, Y. Zhou <sup>15</sup>, Y. Zhou <sup>112a</sup>, Y. Zhou<sup>7</sup>, Z. Zhou <sup>61</sup>, J. Zhu <sup>106</sup>, X. Zhu <sup>142b</sup>, Y. Zhu <sup>142a</sup>, X. Zhuang <sup>14</sup>, K. Zhukov <sup>67</sup>, N.I. Zimine <sup>38</sup>, J. Zinsser <sup>62b</sup>, M. Ziolkowski <sup>145</sup>, L. Živković <sup>16</sup>, A. Zoccoli <sup>24b,24a</sup>, K. Zoch <sup>37</sup>, A. Zografos <sup>37</sup>, T.G. Zorbas <sup>143</sup>, L. Zwalinski <sup>37</sup>.

<sup>1</sup>Department of Physics, University of Adelaide, Adelaide; Australia.

<sup>2</sup>Department of Physics, University of Alberta, Edmonton AB; Canada.

<sup>3(a)</sup>Department of Physics, Ankara University, Ankara; <sup>(b)</sup>Division of Physics, TOBB University of Economics and Technology, Ankara; Türkiye.

<sup>4</sup>LAPP, Université Savoie Mont Blanc, CNRS/IN2P3, Annecy; France.

<sup>5</sup>APC, Université Paris Cité, CNRS/IN2P3, Paris; France.

<sup>6</sup>High Energy Physics Division, Argonne National Laboratory, Argonne IL; United States of America.

<sup>7</sup>Department of Physics, University of Arizona, Tucson AZ; United States of America.

<sup>8</sup>Department of Physics, University of Texas at Arlington, Arlington TX; United States of America.

<sup>9</sup>Physics Department, National and Kapodistrian University of Athens, Athens; Greece.

<sup>10</sup>Physics Department, National Technical University of Athens, Zografou; Greece.

<sup>11</sup>Department of Physics, University of Texas at Austin, Austin TX; United States of America.

<sup>12</sup>Institute of Physics, Azerbaijan Academy of Sciences, Baku; Azerbaijan.

<sup>13</sup>Institut de Física d'Altes Energies (IFAE), Barcelona Institute of Science and Technology, Barcelona; Spain.

<sup>14</sup>Institute of High Energy Physics, Chinese Academy of Sciences, Beijing; China.

<sup>15</sup>Physics Department, Tsinghua University, Beijing; China.

<sup>16</sup>Institute of Physics, University of Belgrade, Belgrade; Serbia.

<sup>17</sup>Department for Physics and Technology, University of Bergen, Bergen; Norway.

<sup>18(a)</sup>Physics Division, Lawrence Berkeley National Laboratory, Berkeley CA; <sup>(b)</sup>University of California, Berkeley CA; United States of America.

<sup>19</sup>Institut für Physik, Humboldt Universität zu Berlin, Berlin; Germany.

<sup>20</sup>Albert Einstein Center for Fundamental Physics and Laboratory for High Energy Physics, University of Bern, Bern; Switzerland.

<sup>21</sup>School of Physics and Astronomy, University of Birmingham, Birmingham; United Kingdom.

<sup>22(a)</sup>Department of Physics, Bogazici University, Istanbul; <sup>(b)</sup>Department of Physics Engineering, Gaziantep University, Gaziantep; <sup>(c)</sup>Department of Physics, Istanbul University, Istanbul; Türkiye.

<sup>23(a)</sup>Facultad de Ciencias y Centro de Investigaciones, Universidad Antonio Nariño, Bogotá; <sup>(b)</sup>Departamento de Física, Universidad Nacional de Colombia, Bogotá; Colombia.

<sup>24(a)</sup>Dipartimento di Fisica e Astronomia A. Righi, Università di Bologna, Bologna; <sup>(b)</sup>INFN Sezione di Bologna; Italy.

<sup>25</sup>Physikalisches Institut, Universität Bonn, Bonn; Germany.

<sup>26</sup>Department of Physics, Boston University, Boston MA; United States of America.

<sup>27</sup>Department of Physics, Brandeis University, Waltham MA; United States of America.

<sup>28(a)</sup>Transilvania University of Brasov, Brasov; <sup>(b)</sup>Horia Hulubei National Institute of Physics and Nuclear

- Engineering, Bucharest;<sup>(c)</sup> Department of Physics, Alexandru Ioan Cuza University of Iasi, Iasi;<sup>(d)</sup> National Institute for Research and Development of Isotopic and Molecular Technologies, Physics Department, Cluj-Napoca;<sup>(e)</sup> National University of Science and Technology Politehnica, Bucharest;<sup>(f)</sup> West University in Timisoara, Timisoara;<sup>(g)</sup> Faculty of Physics, University of Bucharest, Bucharest; Romania.
- <sup>29(a)</sup> Faculty of Mathematics, Physics and Informatics, Comenius University, Bratislava;<sup>(b)</sup> Department of Subnuclear Physics, Institute of Experimental Physics of the Slovak Academy of Sciences, Kosice; Slovak Republic.
- <sup>30</sup> Physics Department, Brookhaven National Laboratory, Upton NY; United States of America.
- <sup>31</sup> Universidad de Buenos Aires, Facultad de Ciencias Exactas y Naturales, Departamento de Física, y CONICET, Instituto de Física de Buenos Aires (IFIBA), Buenos Aires; Argentina.
- <sup>32</sup> California State University, CA; United States of America.
- <sup>33</sup> Cavendish Laboratory, University of Cambridge, Cambridge; United Kingdom.
- <sup>34(a)</sup> Department of Physics, University of Cape Town, Cape Town;<sup>(b)</sup> iThemba Labs, Western Cape;<sup>(c)</sup> Department of Mechanical Engineering Science, University of Johannesburg, Johannesburg;<sup>(d)</sup> National Institute of Physics, University of the Philippines Diliman (Philippines);<sup>(e)</sup> Department of Physics, Stellenbosch University, Matieland;<sup>(f)</sup> University of KwaZulu-Natal, School of Agriculture and Science, Mathematics, Westville;<sup>(g)</sup> University of South Africa, Department of Physics, Pretoria;<sup>(h)</sup> University of Pretoria, Department of Mechanical and Aeronautical Engineering, Pretoria;<sup>(i)</sup> University of Zululand, KwaDlangezwa;<sup>(j)</sup> School of Physics, University of the Witwatersrand, Johannesburg; South Africa.
- <sup>35</sup> Department of Physics, Carleton University, Ottawa ON; Canada.
- <sup>36(a)</sup> Faculté des Sciences Ain Chock, Université Hassan II de Casablanca;<sup>(b)</sup> Faculté des Sciences, Université Ibn-Tofail, Kénitra;<sup>(c)</sup> Faculté des Sciences Semlalia, Université Cadi Ayyad, LPHEA-Marrakech;<sup>(d)</sup> LPMR, Faculté des Sciences, Université Mohamed Premier, Oujda;<sup>(e)</sup> Faculté des sciences, Université Mohammed V, Rabat;<sup>(f)</sup> Institute of Applied Physics, Mohammed VI Polytechnic University, Ben Guerir; Morocco.
- <sup>37</sup> CERN, Geneva; Switzerland.
- <sup>38</sup> Affiliated with an international laboratory covered by a cooperation agreement with CERN.
- <sup>39</sup> Enrico Fermi Institute, University of Chicago, Chicago IL; United States of America.
- <sup>40</sup> LPC, Université Clermont Auvergne, CNRS/IN2P3, Clermont-Ferrand; France.
- <sup>41</sup> Nevis Laboratory, Columbia University, Irvington NY; United States of America.
- <sup>42</sup> Niels Bohr Institute, University of Copenhagen, Copenhagen; Denmark.
- <sup>43(a)</sup> Dipartimento di Fisica, Università della Calabria, Rende;<sup>(b)</sup> INFN Gruppo Collegato di Cosenza, Laboratori Nazionali di Frascati; Italy.
- <sup>44</sup> Physics Department, Southern Methodist University, Dallas TX; United States of America.
- <sup>45</sup> National Centre for Scientific Research "Demokritos", Agia Paraskevi; Greece.
- <sup>46(a)</sup> Department of Physics, Stockholm University;<sup>(b)</sup> Oskar Klein Centre, Stockholm; Sweden.
- <sup>47</sup> Deutsches Elektronen-Synchrotron DESY, Hamburg and Zeuthen; Germany.
- <sup>48</sup> Fakultät Physik, Technische Universität Dortmund, Dortmund; Germany.
- <sup>49</sup> Institut für Kern- und Teilchenphysik, Technische Universität Dresden, Dresden; Germany.
- <sup>50</sup> Department of Physics, Duke University, Durham NC; United States of America.
- <sup>51</sup> SUPA - School of Physics and Astronomy, University of Edinburgh, Edinburgh; United Kingdom.
- <sup>52</sup> INFN e Laboratori Nazionali di Frascati, Frascati; Italy.
- <sup>53</sup> Physikalisches Institut, Albert-Ludwigs-Universität Freiburg, Freiburg; Germany.
- <sup>54</sup> II. Physikalisches Institut, Georg-August-Universität Göttingen, Göttingen; Germany.
- <sup>55</sup> Département de Physique Nucléaire et Corpusculaire, Université de Genève, Genève; Switzerland.
- <sup>56(a)</sup> Dipartimento di Fisica, Università di Genova, Genova;<sup>(b)</sup> INFN Sezione di Genova; Italy.

- <sup>57</sup>II. Physikalisches Institut, Justus-Liebig-Universität Giessen, Giessen; Germany.
- <sup>58</sup>SUPA - School of Physics and Astronomy, University of Glasgow, Glasgow; United Kingdom.
- <sup>59</sup>LPSC, Université Grenoble Alpes, CNRS/IN2P3, Grenoble INP, Grenoble; France.
- <sup>60</sup>Laboratory for Particle Physics and Cosmology, Harvard University, Cambridge MA; United States of America.
- <sup>61</sup>Department of Modern Physics and State Key Laboratory of Particle Detection and Electronics, University of Science and Technology of China, Hefei; China.
- <sup>62</sup>(<sup>a</sup>) Kirchhoff-Institut für Physik, Ruprecht-Karls-Universität Heidelberg, Heidelberg; (<sup>b</sup>) Physikalisches Institut, Ruprecht-Karls-Universität Heidelberg, Heidelberg; Germany.
- <sup>63</sup>(<sup>a</sup>) Department of Physics, Chinese University of Hong Kong, Shatin, N.T., Hong Kong; (<sup>b</sup>) Department of Physics, University of Hong Kong, Hong Kong; (<sup>c</sup>) Department of Physics and Institute for Advanced Study, Hong Kong University of Science and Technology, Clear Water Bay, Kowloon, Hong Kong; China.
- <sup>64</sup>Department of Physics, National Tsing Hua University, Hsinchu; Taiwan.
- <sup>65</sup>IJCLab, Université Paris-Saclay, CNRS/IN2P3, 91405, Orsay; France.
- <sup>66</sup>Centro Nacional de Microelectrónica (IMB-CNM-CSIC), Barcelona; Spain.
- <sup>67</sup>Department of Physics, Indiana University, Bloomington IN; United States of America.
- <sup>68</sup>(<sup>a</sup>) INFN Gruppo Collegato di Udine, Sezione di Trieste, Udine; (<sup>b</sup>) ICTP, Trieste; (<sup>c</sup>) Dipartimento Politecnico di Ingegneria e Architettura, Università di Udine, Udine; Italy.
- <sup>69</sup>(<sup>a</sup>) INFN Sezione di Lecce; (<sup>b</sup>) Dipartimento di Matematica e Fisica, Università del Salento, Lecce; Italy.
- <sup>70</sup>(<sup>a</sup>) INFN Sezione di Milano; (<sup>b</sup>) Dipartimento di Fisica, Università di Milano, Milano; Italy.
- <sup>71</sup>(<sup>a</sup>) INFN Sezione di Napoli; (<sup>b</sup>) Dipartimento di Fisica, Università di Napoli, Napoli; Italy.
- <sup>72</sup>(<sup>a</sup>) INFN Sezione di Pavia; (<sup>b</sup>) Dipartimento di Fisica, Università di Pavia, Pavia; Italy.
- <sup>73</sup>(<sup>a</sup>) INFN Sezione di Pisa; (<sup>b</sup>) Dipartimento di Fisica E. Fermi, Università di Pisa, Pisa; Italy.
- <sup>74</sup>(<sup>a</sup>) INFN Sezione di Roma; (<sup>b</sup>) Dipartimento di Fisica, Sapienza Università di Roma, Roma; Italy.
- <sup>75</sup>(<sup>a</sup>) INFN Sezione di Roma Tor Vergata; (<sup>b</sup>) Dipartimento di Fisica, Università di Roma Tor Vergata, Roma; Italy.
- <sup>76</sup>(<sup>a</sup>) INFN Sezione di Roma Tre; (<sup>b</sup>) Dipartimento di Matematica e Fisica, Università Roma Tre, Roma; Italy.
- <sup>77</sup>(<sup>a</sup>) INFN-TIFPA; (<sup>b</sup>) Università degli Studi di Trento, Trento; Italy.
- <sup>78</sup>Universität Innsbruck, Department of Astro and Particle Physics, Innsbruck; Austria.
- <sup>79</sup>Department of Physics and Astronomy, Iowa State University, Ames IA; United States of America.
- <sup>80</sup>Istinye University, Sariyer, Istanbul; Türkiye.
- <sup>81</sup>(<sup>a</sup>) Departamento de Engenharia Elétrica, Universidade Federal de Juiz de Fora (UFJF), Juiz de Fora; (<sup>b</sup>) Universidade Federal do Rio De Janeiro COPPE/EE/IF, Rio de Janeiro; (<sup>c</sup>) Instituto de Física, Universidade de São Paulo, São Paulo; (<sup>d</sup>) Rio de Janeiro State University, Rio de Janeiro; (<sup>e</sup>) Federal University of Bahia, Bahia; Brazil.
- <sup>82</sup>KEK, High Energy Accelerator Research Organization, Tsukuba; Japan.
- <sup>83</sup>(<sup>a</sup>) Khalifa University of Science and Technology, Abu Dhabi; (<sup>b</sup>) University of Sharjah, Sharjah; United Arab Emirates.
- <sup>84</sup>Graduate School of Science, Kobe University, Kobe; Japan.
- <sup>85</sup>(<sup>a</sup>) AGH University of Krakow, Faculty of Physics and Applied Computer Science, Krakow; (<sup>b</sup>) Marian Smoluchowski Institute of Physics, Jagiellonian University, Krakow; Poland.
- <sup>86</sup>Institute of Nuclear Physics Polish Academy of Sciences, Krakow; Poland.
- <sup>87</sup>Faculty of Science, Kyoto University, Kyoto; Japan.
- <sup>88</sup>Research Center for Advanced Particle Physics and Department of Physics, Kyushu University, Fukuoka ; Japan.
- <sup>89</sup>L2IT, Université de Toulouse, CNRS/IN2P3, UPS, Toulouse; France.

- <sup>90</sup>Instituto de Física La Plata, Universidad Nacional de La Plata and CONICET, La Plata; Argentina.
- <sup>91</sup>Physics Department, Lancaster University, Lancaster; United Kingdom.
- <sup>92</sup>Oliver Lodge Laboratory, University of Liverpool, Liverpool; United Kingdom.
- <sup>93</sup>Department of Experimental Particle Physics, Jožef Stefan Institute and Department of Physics, University of Ljubljana, Ljubljana; Slovenia.
- <sup>94</sup>Department of Physics and Astronomy, Queen Mary University of London, London; United Kingdom.
- <sup>95</sup>Department of Physics, Royal Holloway University of London, Egham; United Kingdom.
- <sup>96</sup>Department of Physics and Astronomy, University College London, London; United Kingdom.
- <sup>97</sup>Louisiana Tech University, Ruston LA; United States of America.
- <sup>98</sup>Fysiska institutionen, Lunds universitet, Lund; Sweden.
- <sup>99</sup>Departamento de Física Teórica C-15 and CIAFF, Universidad Autónoma de Madrid, Madrid; Spain.
- <sup>100</sup>Institut für Physik, Universität Mainz, Mainz; Germany.
- <sup>101</sup>School of Physics and Astronomy, University of Manchester, Manchester; United Kingdom.
- <sup>102</sup>CPPM, Aix-Marseille Université, CNRS/IN2P3, Marseille; France.
- <sup>103</sup>Department of Physics, University of Massachusetts, Amherst MA; United States of America.
- <sup>104</sup>Department of Physics, McGill University, Montreal QC; Canada.
- <sup>105</sup>School of Physics, University of Melbourne, Victoria; Australia.
- <sup>106</sup>Department of Physics, University of Michigan, Ann Arbor MI; United States of America.
- <sup>107</sup>Department of Physics and Astronomy, Michigan State University, East Lansing MI; United States of America.
- <sup>108</sup>Group of Particle Physics, University of Montreal, Montreal QC; Canada.
- <sup>109</sup>Fakultät für Physik, Ludwig-Maximilians-Universität München, München; Germany.
- <sup>110</sup>Max-Planck-Institut für Physik (Werner-Heisenberg-Institut), München; Germany.
- <sup>111</sup>Graduate School of Science and Kobayashi-Maskawa Institute, Nagoya University, Nagoya; Japan.
- <sup>112</sup><sup>(a)</sup>Department of Physics, Nanjing University, Nanjing; <sup>(b)</sup>School of Science, Shenzhen Campus of Sun Yat-sen University; <sup>(c)</sup>University of Chinese Academy of Science (UCAS), Beijing; China.
- <sup>113</sup><sup>(a)</sup>School of Physics, Nankai University, Tianjin; <sup>(b)</sup>Institute of Frontier and Interdisciplinary Science and Key Laboratory of Particle Physics and Particle Irradiation (MOE), Shandong University, Qingdao; <sup>(c)</sup>School of Physics, Zhengzhou University; China.
- <sup>114</sup>Department of Physics and Astronomy, University of New Mexico, Albuquerque NM; United States of America.
- <sup>115</sup>Institute for Mathematics, Astrophysics and Particle Physics, Radboud University/Nikhef, Nijmegen; Netherlands.
- <sup>116</sup>Nikhef National Institute for Subatomic Physics and University of Amsterdam, Amsterdam; Netherlands.
- <sup>117</sup>Department of Physics, Northern Illinois University, DeKalb IL; United States of America.
- <sup>118</sup><sup>(a)</sup>New York University Abu Dhabi, Abu Dhabi; <sup>(b)</sup>United Arab Emirates University, Al Ain; United Arab Emirates.
- <sup>119</sup>Department of Physics, New York University, New York NY; United States of America.
- <sup>120</sup>Ochanomizu University, Otsuka, Bunkyo-ku, Tokyo; Japan.
- <sup>121</sup>Ohio State University, Columbus OH; United States of America.
- <sup>122</sup>Homer L. Dodge Department of Physics and Astronomy, University of Oklahoma, Norman OK; United States of America.
- <sup>123</sup>Department of Physics, Oklahoma State University, Stillwater OK; United States of America.
- <sup>124</sup>Palacký University, Joint Laboratory of Optics, Olomouc; Czech Republic.
- <sup>125</sup>Institute for Fundamental Science, University of Oregon, Eugene, OR; United States of America.
- <sup>126</sup>Graduate School of Science, University of Osaka, Osaka; Japan.

- <sup>127</sup>Department of Physics, University of Oslo, Oslo; Norway.
- <sup>128</sup>Department of Physics, Oxford University, Oxford; United Kingdom.
- <sup>129</sup>LPNHE, Sorbonne Université, Université Paris Cité, CNRS/IN2P3, Paris; France.
- <sup>130</sup>Department of Physics, University of Pennsylvania, Philadelphia PA; United States of America.
- <sup>131</sup>Department of Physics and Astronomy, University of Pittsburgh, Pittsburgh PA; United States of America.
- <sup>132</sup>(<sup>a</sup>) Laboratório de Instrumentação e Física Experimental de Partículas - LIP, Lisboa; (<sup>b</sup>) Departamento de Física, Faculdade de Ciências, Universidade de Lisboa, Lisboa; (<sup>c</sup>) Departamento de Física, Universidade de Coimbra, Coimbra; (<sup>d</sup>) Centro de Física Nuclear da Universidade de Lisboa, Lisboa; (<sup>e</sup>) Departamento de Física, Escola de Ciências, Universidade do Minho, Braga; (<sup>f</sup>) Departamento de Física Teórica y del Cosmos, Universidad de Granada, Granada (Spain); (<sup>g</sup>) Departamento de Física, Instituto Superior Técnico, Universidade de Lisboa, Lisboa; Portugal.
- <sup>133</sup>Institute of Physics of the Czech Academy of Sciences, Prague; Czech Republic.
- <sup>134</sup>Czech Technical University in Prague, Prague; Czech Republic.
- <sup>135</sup>Charles University, Faculty of Mathematics and Physics, Prague; Czech Republic.
- <sup>136</sup>Particle Physics Department, Rutherford Appleton Laboratory, Didcot; United Kingdom.
- <sup>137</sup>IRFU, CEA, Université Paris-Saclay, Gif-sur-Yvette; France.
- <sup>138</sup>Santa Cruz Institute for Particle Physics, University of California Santa Cruz, Santa Cruz CA; United States of America.
- <sup>139</sup>(<sup>a</sup>) Departamento de Física, Pontificia Universidad Católica de Chile, Santiago; (<sup>b</sup>) Millennium Institute for Subatomic physics at high energy frontier (SAPHIR), Santiago; (<sup>c</sup>) Instituto de Investigación Multidisciplinario en Ciencia y Tecnología, y Departamento de Física, Universidad de La Serena; (<sup>d</sup>) Universidad Andres Bello, Department of Physics, Santiago; (<sup>e</sup>) Universidad San Sebastian, Recoleta; (<sup>f</sup>) Instituto de Alta Investigación, Universidad de Tarapacá, Arica; (<sup>g</sup>) Departamento de Física, Universidad Técnica Federico Santa María, Valparaíso; Chile.
- <sup>140</sup>Department of Physics, Institute of Science, Tokyo; Japan.
- <sup>141</sup>Department of Physics, University of Washington, Seattle WA; United States of America.
- <sup>142</sup>(<sup>a</sup>) State Key Laboratory of Dark Matter Physics, School of Physics and Astronomy, Shanghai Jiao Tong University, Key Laboratory for Particle Astrophysics and Cosmology (MOE), SKLPPC, Shanghai; (<sup>b</sup>) State Key Laboratory of Dark Matter Physics, Tsung-Dao Lee Institute, Shanghai Jiao Tong University, Shanghai; China.
- <sup>143</sup>Department of Physics and Astronomy, University of Sheffield, Sheffield; United Kingdom.
- <sup>144</sup>Department of Physics, Shinshu University, Nagano; Japan.
- <sup>145</sup>Department Physik, Universität Siegen, Siegen; Germany.
- <sup>146</sup>Department of Physics, Simon Fraser University, Burnaby BC; Canada.
- <sup>147</sup>SLAC National Accelerator Laboratory, Stanford CA; United States of America.
- <sup>148</sup>Department of Physics, Royal Institute of Technology, Stockholm; Sweden.
- <sup>149</sup>Departments of Physics and Astronomy, Stony Brook University, Stony Brook NY; United States of America.
- <sup>150</sup>Department of Physics and Astronomy, University of Sussex, Brighton; United Kingdom.
- <sup>151</sup>School of Physics, University of Sydney, Sydney; Australia.
- <sup>152</sup>Institute of Physics, Academia Sinica, Taipei; Taiwan.
- <sup>153</sup>(<sup>a</sup>) E. Andronikashvili Institute of Physics, Iv. Javakhishvili Tbilisi State University, Tbilisi; (<sup>b</sup>) High Energy Physics Institute, Tbilisi State University, Tbilisi; (<sup>c</sup>) University of Georgia, Tbilisi; Georgia.
- <sup>154</sup>Department of Physics, Technion, Israel Institute of Technology, Haifa; Israel.
- <sup>155</sup>Raymond and Beverly Sackler School of Physics and Astronomy, Tel Aviv University, Tel Aviv; Israel.
- <sup>156</sup>Department of Physics, Aristotle University of Thessaloniki, Thessaloniki; Greece.

- <sup>157</sup>International Center for Elementary Particle Physics and Department of Physics, University of Tokyo, Tokyo; Japan.
- <sup>158</sup>Graduate School of Science and Technology, Tokyo Metropolitan University, Tokyo; Japan.
- <sup>159</sup>Department of Physics, University of Toronto, Toronto ON; Canada.
- <sup>160</sup>(<sup>a</sup>)TRIUMF, Vancouver BC; (<sup>b</sup>)Department of Physics and Astronomy, York University, Toronto ON; Canada.
- <sup>161</sup>Division of Physics and Tomonaga Center for the History of the Universe, Faculty of Pure and Applied Sciences, University of Tsukuba, Tsukuba; Japan.
- <sup>162</sup>Department of Physics and Astronomy, Tufts University, Medford MA; United States of America.
- <sup>163</sup>Department of Physics and Astronomy, University of California Irvine, Irvine CA; United States of America.
- <sup>164</sup>Department of Physics and Astronomy, University of Uppsala, Uppsala; Sweden.
- <sup>165</sup>Department of Physics, University of Illinois, Urbana IL; United States of America.
- <sup>166</sup>Instituto de Física Corpuscular (IFIC), Centro Mixto Universidad de Valencia - CSIC, Valencia; Spain.
- <sup>167</sup>Department of Physics, University of British Columbia, Vancouver BC; Canada.
- <sup>168</sup>Department of Physics and Astronomy, University of Victoria, Victoria BC; Canada.
- <sup>169</sup>Fakultät für Physik und Astronomie, Julius-Maximilians-Universität Würzburg, Würzburg; Germany.
- <sup>170</sup>Department of Physics, University of Warwick, Coventry; United Kingdom.
- <sup>171</sup>Waseda University, Tokyo; Japan.
- <sup>172</sup>Department of Particle Physics and Astrophysics, Weizmann Institute of Science, Rehovot; Israel.
- <sup>173</sup>Department of Physics, University of Wisconsin, Madison WI; United States of America.
- <sup>174</sup>Fakultät für Mathematik und Naturwissenschaften, Fachgruppe Physik, Bergische Universität Wuppertal, Wuppertal; Germany.
- <sup>175</sup>Department of Physics, Yale University, New Haven CT; United States of America.
- <sup>176</sup>Yerevan Physics Institute, Yerevan; Armenia.
- <sup>a</sup> Also at Affiliated with an institute formerly covered by a cooperation agreement with CERN.
- <sup>b</sup> Also at An-Najah National University, Nablus; Palestine.
- <sup>c</sup> Also at Borough of Manhattan Community College, City University of New York, New York NY; United States of America.
- <sup>d</sup> Also at Center for Interdisciplinary Research and Innovation (CIRI-AUTH), Thessaloniki; Greece.
- <sup>e</sup> Also at Centre of Physics of the Universities of Minho and Porto (CF-UM-UP); Portugal.
- <sup>f</sup> Also at CERN, Geneva; Switzerland.
- <sup>g</sup> Also at Département de Physique Nucléaire et Corpusculaire, Université de Genève, Genève; Switzerland.
- <sup>h</sup> Also at Departament de Física de la Universitat Autònoma de Barcelona, Barcelona; Spain.
- <sup>i</sup> Also at Department of Financial and Management Engineering, University of the Aegean, Chios; Greece.
- <sup>j</sup> Also at Department of Modern Physics and State Key Laboratory of Particle Detection and Electronics, University of Science and Technology of China, Hefei; China.
- <sup>k</sup> Also at Department of Physics, Ben Gurion University of the Negev, Beer Sheva; Israel.
- <sup>l</sup> Also at Department of Physics, Bolu Abant İzzet Baysal University, Bolu; Türkiye.
- <sup>m</sup> Also at Department of Physics, King's College London, London; United Kingdom.
- <sup>n</sup> Also at Department of Physics, Stellenbosch University; South Africa.
- <sup>o</sup> Also at Department of Physics, University of Fribourg, Fribourg; Switzerland.
- <sup>p</sup> Also at Department of Physics, University of Thessaly; Greece.
- <sup>q</sup> Also at Department of Physics, Westmont College, Santa Barbara; United States of America.
- <sup>r</sup> Also at Faculty of Physics, Sofia University, 'St. Kliment Ohridski', Sofia; Bulgaria.
- <sup>s</sup> Also at Faculty of Physics, University of Bucharest; Romania.

- <sup>t</sup> Also at Hellenic Open University, Patras; Greece.
- <sup>u</sup> Also at Henan University; China.
- <sup>v</sup> Also at Imam Mohammad Ibn Saud Islamic University; Saudi Arabia.
- <sup>w</sup> Also at Indian Institute of Technology (IIT), Jodhpur; India.
- <sup>x</sup> Also at Institutio Catalana de Recerca i Estudis Avancats, ICREA, Barcelona; Spain.
- <sup>y</sup> Also at Institut für Experimentalphysik, Universität Hamburg, Hamburg; Germany.
- <sup>z</sup> Also at Institute for Nuclear Research and Nuclear Energy (INRNE) of the Bulgarian Academy of Sciences, Sofia; Bulgaria.
- <sup>aa</sup> Also at Institute of Applied Physics, Mohammed VI Polytechnic University, Ben Guerir; Morocco.
- <sup>ab</sup> Also at Institute of Particle Physics (IPP); Canada.
- <sup>ac</sup> Also at Institute of Physics and Technology, Mongolian Academy of Sciences, Ulaanbaatar; Mongolia.
- <sup>ad</sup> Also at Institute of Physics, Azerbaijan Academy of Sciences, Baku; Azerbaijan.
- <sup>ae</sup> Also at Institute of Theoretical Physics, Ilia State University, Tbilisi; Georgia.
- <sup>af</sup> Also at Millennium Institute for Subatomic physics at high energy frontier (SAPHIR), Santiago; Chile.
- <sup>ag</sup> Also at National Institute of Physics, University of the Philippines Diliman (Philippines); Philippines.
- <sup>ah</sup> Also at School of Physics, University of the Witwatersrand, Johannesburg; South Africa.
- <sup>ai</sup> Also at The Collaborative Innovation Center of Quantum Matter (CICQM), Beijing; China.
- <sup>aj</sup> Also at TRIUMF, Vancouver BC; Canada.
- <sup>ak</sup> Also at Università di Napoli Parthenope, Napoli; Italy.
- <sup>al</sup> Also at Università degli Studi Link; Italy.
- <sup>am</sup> Also at University and INFN Torino, Torino; Italy.
- <sup>an</sup> Also at University of Chinese Academy of Sciences (UCAS), Beijing; China.
- <sup>ao</sup> Also at University of Colorado Boulder, Department of Physics, Colorado; United States of America.
- <sup>ap</sup> Also at University of Siena; Italy.
- <sup>aq</sup> Also at Washington College, Chestertown, MD; United States of America.
- <sup>ar</sup> Also at Yeditepe University, Physics Department, Istanbul; Türkiye.
- \* Deceased